Appendix PA

Attachment SOTERM

This page intentionally left blank

Table of Contents

List of Figures

List of Tables

ACRONYMS *AND ABBREVIATIONS*

An	***actinide(s)***
atm	***atmosphere (a unit of pressure)***
aq	***aqueous***
ASTP	***Actinide Source Term Program***
BNL	Brookhaven National Laboratory
brucite	$Mg(OH)_2$
calcite	$CaCO_3$
CFR	Code of Federal Regulations
CPR	***cellulosics, plastics, and rubber***
DOE	(U.S.) Department of Energy
DRZ	disturbed rock zone
EDTA	ethylene-diaminetetra acetate
EPA	***(U.S.) Environmental Protection Agency***
eq	***equivalent(s)***
ERDA	(U.S.) Energy Research and Development Administration
FA-Suw	***fulvic acid isolated from the Suwannee River acquired from the International Humic Substances Society, Golden, Colorado***
FMT	***Fracture-Matrix Transport***
f_{CO_2}	***the fugacity of a gaseous species,*** f_i ***(similar to the partial pressures of that species,*** p_i***)***
g	***gaseous or gram(s)***
gal	***gallon(s)***
GWB	***Generic Weep Brine***
HAal-Ald	***aliphatic humic acid purchased from Aldrich Chemical Co., purified by Florida State University***
HAal-LBr	***aliphatic humic acid isolated from sediments collected from Lake Bradford, Florida, prepared by Florida State University***
HAar-Gor	***aromatic humic acid isolated from groundwaters near Gorleben, Germany, obtained from Professor J.-I. Kim, Institut für Radiochemie, München***
HAar-Suw	***aromatic humic acid isolated from the Suwannee River acquired from the International Humic Substances Society, Golden, Colorado***
HMW/FW	Harvie-Møller-Weare/Felmy and Weare
hydromagnesite	$Mg_4(CO_3)_3(OH)_2 \cdot 3H_2O$ ***or*** $Mg_5(CO_3)_4(OH)_2 \cdot 4H_2O$
L	***Liter(s)***
LANL	Los Alamos National Laboratory
LLNL	Lawrence Livermore National Laboratory
m	***molal***
M	***molar***
meq	***milliequivalent(s)***
mL	***milliliter(s)***
mol	***mole(s)***
~~NIST~~	~~National Institute of Standards and Technology~~
PA	***performance assessment***

periclase	***MgO***
pH	***the negative logarithm of the activity of hydrogen ion (H^+)***
redox	***oxidation-reduction***
s	***second***
SIT	Specific-~~i~~***I***on Interaction Theory
SPC	Salado Primary Constituent
STTP	***(WIPP) Actinide Source Term Waste Test Program***
SWCF	Sandia National Laboratories WIPP Central File
TRU	transuranic
TWBIR	Transuranic Waste Baseline Inventory Report
UV	***ultraviolet***
WIPP	Waste Isolation Pilot Plant

~~APPENDIX SOTERM~~

SOTERM-1***.0*** INTRODUCTION

The actinide source term ~~at~~***used in the performance assessment (PA) calculations for*** the ***Waste Isolation Pilot Plant (***WIPP***)*** represents the ~~mobile~~***aqueous*** concentration***s*** of ~~select actinide elements~~***thorium (Th), uranium (U), plutonium (Pu), and americium (Am)*** in the ~~WIPP~~ repository. The source term is the sum of ~~contributions from~~***the*** dissolved ~~actinide~~ species ***(solubilities)*** and ***the*** mobile ***suspended (***colloidal***)*** ~~actinide~~ species ~~existing in the repository~~***of these radioelements***. The actinide source term establishes the mobile concentration***s*** of ~~actinides~~***Th, U, Pu, and Am*** that may ~~move~~***be released from*** the repository in brine. ***Brine*** ~~R~~***r***elease***s*** to the accessible environment ~~in brine~~ may ~~follow a pathway up~~***occur through*** the sealed ~~operational~~ shafts, ~~out through~~***up*** possible intrusion boreholes, and/or out laterally through ~~Salado~~ ***Salado*** Formation interbeds. ***(***For a discussion of release scenarios and pathways, see ***Chapter 6.0,*** Section 6.3***)***. Quantification of the impact of these releases contributes directly to assessing compliance with Title 40 Code of Federal Regulations (CFR) Part 191. Direct release***s of particulate actinides*** to the surface ~~of actinides entrained as particulates~~***associated*** with solid waste ~~stemming~~***resulting*** from drilling~~,~~ ***(***cuttings, ***cavings,*** and spallings~~,~~***)*** ~~is~~***are*** not ~~part of~~***included in*** the actinide source term***.***~~ as described herein.~~

The actinide source term is limited to those radionuclides that ~~may~~ ***could*** significantly impact the ***long-term*** performance of the WIPP. ~~Consequently, the actinide source term provides a quantification of mobile concentrations~~***These radionuclides are all isotopes*** of ~~thorium~~***Th***, ~~uranium~~***U***, ~~plutonium~~***Pu***, ***and*** ~~americium~~***Am.*** ~~and curium.~~ ***From the standpoint of their potential effects on the long-term performance of the repository, the order of importance of these actinides is Pu ≈ Am >> U > Th (Helton et al. 1998). Other actinides, especially neptunium (Np), have been included in the laboratory and modeling studies used to develop the actinide source term because it was not known at the outset which actinides could significantly affect the long-term performance of the repository.*** Other radio~~nuclides~~***elements***, such as strontium ***(Sr)***, cesium ***(Cs)***, and radium ***(Ra)***, are not included in the actinide source term because of their relatively short half-lives or limited waste inventory ~~(Appendix WCA, Sections WCA.3.2 and WCA.8.3)~~.

~~Appendix~~ ***Attachment*** SOTERM (SOurce TERM) focuses on the development of ~~actinide~~ ***actinide-***~~source~~***source-***term parameter values and the implementation of th~~o~~***e***se ~~values~~***parameters*** in ~~performance assessment~~***PA*** calculations. In Section ~~SOTERM-~~2***.0***, an overview of ~~the repository system~~***near-field chemical processes and conditions*** is presented***.***~~, including a review of relevant geochemical and chemical constraints on the repository system, the conceptual framework on which the actinide source term is based, simplifications required to develop parameter values, and assumptions made.~~ Sections ~~SOTERM-~~3***.0*** and ~~SOTERM-~~4***.0*** focus on the development of the ~~dissolved~~ ***dissolved-***actinide solubility parameters and ~~oxidation~~ ***oxidation-***state distribution, respectively. Section ~~SOTERM-~~5***.0*** focuses on the impact of organic ligands on dissolved actinide concentration***s***. The ~~mobile~~ colloidal actinide source term is described in Section ~~SOTERM-~~6***.0***. In Section ~~SOTERM-~~7***.0*** the ~~performance assessment~~***PA*** implementation of the dissolved ~~actinide~~ and colloidal ~~actinide~~ components of the ~~actinide~~ source term is described.

~~Appendix SOTERM~~ ***This attachment*** is a supplement to information presented in ***Chapter 6,*** Sections ***6.4.3.3,*** 6.4.3.4, 6.4.3.5, and 6.4.3.6 of this application.

SOTERM-2.***0*** ~~CONCEPTUAL FRAMEWORK OF CHEMICAL CONDITIONS~~ ***OVERVIEW OF NEAR-FIELD PROCESSES AND CONDITIONS***

~~In this section, an overview of the chemistry of the repository system is presented.~~***This section presents an overview of near-field processes and conditions that will affect actinide solubilities in the WIPP.*** ~~The a~~***A***mbient geochemical conditions are described first. The effects of human intrusion and waste are then described. Emphasis is placed on how various components and processes within the repository will affect the dissolution and colloidal suspension of actinides. Excess ***magnesium oxide (***MgO***)*** will be added to the repository for assurance purposes, so the effect of MgO is included in this discussion. Simplifications and assumptions used to model the components and processes are discussed in each section.

SOTERM-2.1 Ambient Geochemical Conditions

The Salado is predominantly ***nearly pure*** halite (NaCl), ***with interbeds ("marker beds") consisting mainly of anhydrite (***$CaSO_4$***).*** ~~but also contains~~***The nearly pure halite contains*** accessory evaporite minerals such as ***anhydrite (***$CaSo_4$***)***, gypsum ($CaSO_4 \bullet 2H_2O$), polyhalite ($K_2MgCa_2(SO_4)_4 \bullet 2H_2O$), ~~and~~ magnesite ($MgCO_3$)***, and clays***. Small quantities of intergranular ***(grain-boundary) brines*** and intragranular brines ***(fluid inclusions)*** are associated with the salt at the repository horizon. These brines are highly concentrated solutions (up to 8 ~~molar~~***M***) of predominantly ***sodium (***Na^+***),*** Mg^{2+}***, potassium (***K^+***), chloride (***Cl^-***), and sulfate (***SO_4^{2-}***)*** with smaller amounts of Ca^{2+}, CO_3^{2-}, and B. These brines have been in contact with the ***Salado*** evaporite ~~salts~~***minerals*** for ~~geologic time~~ ***about 250 million years*** and are saturated with respect to the***se*** ~~evaporite~~ minerals.

Underlying the Salado is the Castile ***Formation***, composed of ~~bedded anhydrite~~***alternating units of interlaminated carbonate and anhydrite, and nearly pure halite***. The Castile in the vicinity of the WIPP site is known to contain localized brine reservoirs under sufficient pressure to force brine to the land surface if penetrated by a borehole. Castile brines are predominantly saturated ~~sodium chloride~~***NaCl*** solutions containing ~~calcium~~***Ca^{2+}*** and ~~sulfate~~***SO_4^{2-}***, and small concentrations of other elements, and are about eight times more concentrated than seawater. Overlying the Salado in the vicinity of the WIPP site is the Culebra ***Member of the Rustler Formation***, a fractured dolomite ($CaMg(CO_3)_2$) layer. It is significant because it is expected to be the most transmissive geologic pathway to the accessible environment. Culebra brines are generally more dilute than the Salado and Castile brines, and are predominantly ~~sodium chloride~~***NaCl*** with ~~potassium~~***K^+***, ~~magnesium~~***Mg^{2+}***, ~~calcium~~***Ca^{2+}***, ~~sulfate~~***SO_4^{2-}***, and ~~carbonate~~***CO_3^{2-}***. ***(***See Chapter 2.0***,*** ~~(~~Section 2.4.2***.1***~~)~~ of this application for information on the distribution of Culebra brine salinity.***)***

SOTERM-2.2 Repository Chemical Conditions

Three aspects of the repository chemical environment can have a major impact on the dissolution and colloidal suspension of actinides. These are***:***

- brine composition~~,~~***;***
- ~~the~~ microbial ~~degradation~~***consumption*** of ~~organic waste~~***cellulosic, plastic, and rubber (CPR) materials and concomitant production of carbon dioxide (CO_2);*** and
- ***anoxic*** corrosion of ~~metallic~~***steels and other iron-base (Fe-base) alloys in the waste containers and the*** waste ***and concomitant production of hydrogen (H_2)***.

For each of these, the effect, the range of possible behavior, and the simplifications used in modeling are discussed ***below***.

SOTERM-2.2.1 Brine

The compositions of ~~B~~***b***rine***s*** required for mobilization of actinides ~~and its composition~~ will affect the quantit~~y~~***ies*** of actinid~~e~~***ies*** that may be dissolved or suspended. For example, ~~high~~ ***high-***~~ionic~~ ***ionic-***strength brines have been shown to increase the solubilit~~y~~***ies*** of actinides and ~~also~~ to increase the coagulation and settling rate of ~~mineral~~ ***mineral-***fragment colloids.

In ~~human~~ ***human-***intrusion scenarios, Salado and/or Castile brine will enter the repository, depending on whether the intrusion penetrates a brine reservoir in the Castile. However, in addition to Salado and Castile brines, brines from the Rustler and Dewey Lake ***Formation*** ~~can~~***could*** flow down the borehole to the repository, mix with the waste, and then be forced back up a borehole. Rustler and ~~Dewey~~ ***Dewey-***Lake brines are considerably less concentrated than Salado and Castile brines. ~~As~~***If*** the Rustler and ~~Dewey~~ ***Dewey-***Lake brines flow into the repository, they would dissolve Salado halite until they attain compositions between ~~that~~***those*** of Salado and Castile brines (see Section ~~SOTERM.~~7.1.2). Under any intrusion scenario, therefore, the ~~brine~~ ***brine*** dissolving actinides would have the composition of Salado, Castile, or a mixture of Salado and Castile brines.

The Salado and Castile brine compositions bracket the range of possibilities within the repository, so experiment~~s~~***al*** and modeling ***studies*** of repository ***and actinide*** chemistry ~~were~~ ***have been*** performed using the ~~end~~ ***end-***member brines only. ~~Modeling~~***Inclusion*** of brine mixing ~~within the~~***in*** ~~performance assessment~~***PA*** ~~was~~***has been*** considered and rejected because it ~~was~~***would*** not ***be*** sufficiently accurate to reduce the uncertainty associated with brine mixing and related brine chemistry compared to bracketing this uncertainty with end-member brines. Brine mixing is addressed in Section ~~SOTERM.~~7.1.2.

~~Several synthetic brines that simulate brines collected from the Salado, the Castile, and the Culebra were used in the experimental program. Brine A is a synthetic brine often used to simulate the upper range in Salado brine, magnesium concentration and ionic strength, as is SPC (Salado Primary Constituent) Brine, a version of Brine A with the trace elements removed. Synthetic U.S. Energy Research and Development Administration (ERDA)-6 brine represents Castile brine. The primary chemical components of these brines are given in Table SOTERM-1 (from Brush 1990, pp. 20-22). As is evident in Table SOTERM-1, Salado brine contains high concentrations of magnesium chloride, whereas Castile brine is dominated by sodium chloride and contains bicarbonate.~~

The two synthetic solutions that best represent the end-member brines that could be present in the repository are: (1) Generic Weep Brine (GWB), which simulates intergranular (grain-boundary) brines from the Salado at or near the stratigraphic horizon of the repository (Snider 2003a); and (2) Energy Research and Development Administration-6 (ERDA-6), typical of fluids in Castile brine reservoirs (Popielak et al. 1983). Through the time of the CCA, Brine A (Molecke 1983) and Salado Primary Constituents (SPC) Brine, a version of Brine A from which trace elements had been removed, were used to simulate Salado brines for laboratory and modeling studies. Since the CCA, however, GWB has been shown to be more representative of intergranular Salado brines than either Brine A or SPC Brine (Brush and Xiong 2003a; Snider 2003a). In particular, the Mg^{2+} concentration of GWB (1.0 M) simulates the average concentration of this element in Salado brines more closely than Brine A (1.44 M). Table SOTERM-1 provides the compositions of GWB and ERDA-6.

In addition to using the ~~end~~ ***end***-member brines, ~~several~~ other simplifying assumptions ~~were~~***have been*** made, including the following:

- ***Any*** ~~B~~***b***rine ~~that may be~~***present*** in the repository is well-mixed with waste.
- Equilibri~~um~~***a*** with ~~the more available minerals (~~***halite and anhydrite***, ~~magnesite)~~ ***the most abundant Salado minerals at or near the stratigraphic horizon of the repository,*** ~~is~~***are*** established. ~~(Reduction-o~~***O***xidation-***reduction (redox)*** equilibri~~um~~***a*** with waste materials ~~is~~***ha***ve not ***been*** assumed.~~)~~
- For modeling purposes, brine composition***s attained after equilibration of GWB or ERDA-6 with the MgO engineered barrier*** ~~is constant in time~~***are assumed for the entire 10,000-year regulatory period***.

~~Table SOTERM-1. Some Chemical Components of WIPP Brines (from Brush 1990).~~

~~Ion or Chemical Property~~	**~~Brine A~~**	**~~ERDA-6~~**
~~Alkalinity (HCO$_3^-$ equivalent, mM)~~	~~–~~	~~43~~
~~B^{3+} (mM)~~	~~20~~	~~63~~
~~Br$^-$ (mM)~~	~~10~~	~~11~~
~~Ca^{2+} (mM)~~	~~20~~	~~12~~
~~Cl- (mM)~~	~~5,350~~	~~4,800~~
~~K$^+$ (mM)~~	~~770~~	~~97~~
~~Mg^{2+} (mM)~~	~~1,440~~	~~19~~
~~Na$^+$ (mM)~~	~~1,830~~	~~4,870~~
~~pH~~	~~6.5~~	~~6.17~~
~~SO$_4^{2-}$ (mM)~~	~~40~~	~~170~~
~~TDS (mg/liter)~~	~~306,000~~	~~330,000~~

Table SOTERM-1. Compositions of GWB and ERDA-6 Prior to Equilibration with MgO

Element or Property	***GWB***[2]	***ERDA-6***[3]
$B(OH)_3$	***155 mM***	***63 mM***
Na^+	***3.48 M***	***4.87 M***
Mg^{2+}	***1.00 M***	***19 mM***
K^+	***458 mM***	***97 mM***
Ca^{2+}	***14 mM***	***12 mM***
SO_4^{2-}	***175 mM***	***170 mM***
Cl^-	***5.51 M***	***4.8 M***
Br^-	***26 mM***	***11 mM***
Total inorganic C (as HCO_3^-)	***Not reported***	***16 mM***
pH	***Not reported***	***6.17***
Specific gravity	***1.2***	***1.216***
TDS	***Not reported***	***330,000 mg/l***

[1] From Molecke (1983).
[2] From Snider (2003a).
[3] From Popielak et al. (1983).
[4] Reported by Molecke (1983) as BO_3^{3-}.

SOTERM-2.2.2 Microbial ~~Degradation~~ Consumption of ~~Organic Materials~~ Cellulosic, Plastic, and Rubber Materials

A large quantity of ~~organic materials, including cellulosics, plastics, and rubber,~~***CPR materials*** will be emplaced in the WIPP, and ~~will potentially~~***could*** be ~~degraded~~***consumed*** by ~~microbes~~***microorganisms. There are large uncertainties as to whether significant microbial consumption of CPR materials will occur during the 10,000-year WIPP regulatory period. Therefore, it is assumed that significant microbial consumption of CPR materials is possible, but by no means certain. To incorporate these uncertainties in PA, Wang and Brush (1996a, 1996b) developed a conceptual model for microbial activity in the repository. According to this model, there is a probability of 0.50 for significant microbial activity. In the event of significant microbial activity, microbes would consume 100 percent of the cellulosic materials in the repository. Furthermore, there is a conditional probability of 0.50 that microbes would consume all of the plastic and rubber materials after consumption of all of the cellulosic materials. Thus, there is microbial consumption of all of the cellulosic materials, but no plastic or rubber materials, in about 25 percent of the PA realizations (vectors); microbial consumption of all of the CPR materials in 25 percent of the vectors; and no microbial activity in the remaining 50 percent of the vectors.***

~~There is considerable uncertainty whether significant microbial colonies will be viable in the WIPP for 10,000 years. As discussed in Appendix PAR, the U.S. Department of Energy (DOE) represents that uncertainty by assigning a 50 percent probability of significant microbial gas generation. It is further assumed that, in the event of significant microbial gas generation, there is a 50 percent chance that plastics and rubbers will be biodegraded (Wang and Brush 1996).~~

Microbial ~~degradation~~***consumption*** of ~~organic carbon~~***CPR materials*** ~~may influence~~***could affect the*** actinide ***source term*** ~~mobilization~~ in four ways:

- production ***of significant quantities of*** ~~carbon dioxide~~***CO_2, which could acidify any brine present and increase the solubilities of actinide elements;***
- ~~fast~~ reduction of oxidized actinide species, which in most cases are more soluble;
- consumption of solubilizing organic ligands***; and***
- production of humic and microbial colloids, thereby increasing the amount of actinide sorbed on colloidal surfaces~~, and~~**.**

~~(4) generation of CO2, which in the absence of added MgO, would increase acidity and carbonate concentrations in the brine and thereby increase actinide solubility.~~

The effect of CO_2 production is discussed in this section. The ~~first~~***remaining*** three ~~of these~~ ***effects*** are considered in the analyses that ***have*** studied the ~~oxidation~~ ***oxidation-***state distributions (Section ~~SOTERM.~~4***.0***), the effects of organic ligands (Section ~~SOTERM.~~5***.0***), and the effects of colloids (Section ~~SOTERM.~~6***.0***). ~~The effect of CO_2 production is discussed further in this section.~~ The simplifications used in ~~the performance assessment~~ ***PA*** calculations for all four of these effects are discussed at the end of this section.

~~The inventory of organic material, which includes cellulosics, plastics, and rubbers, is about 10^9 moles of carbon (DOE 1996, 3-13). At the maximum degradation rate of 0.3 mole carbon/kilogram of organic materials/year in the inundated repository (Wang and Brush 1996), this inventory will be entirely biodegraded within about 200 years after closure. It is expected that the maximum time for complete degradation would be about 2000 years in cases where significant microbial action occurs.~~

~~The primary reaction for CO_2 production from organic carbon biodegradation is expected to be~~

~~$C_6H_{10}O_5 + H_2O = 3CH_4 + 3CO_2$ (2-1)~~

~~Two other reactions can also contribute, although because of the limited amount of nitrate and sulfate relative to organic carbon in the waste (Wang and Brush 1996), the potential amount of CO_2 generated is much less:~~

~~$C_6H_{10}O_5 + 4.8\ HNO_3 = 7.4\ H_2O + 6\ CO_2 + 2.4\ N_2$ (2-2)~~

~~$C_6H_{10}O_5 + 3\ H_2SO_4 = 5\ H_2O + 6\ CO_2 + 3\ H_2S$ (2-3)~~

~~The pmH ($-\log_{10}$ of the hydrogen ion molality) of the brine in the repository is a function of the amount of CO_2 dissolved in the brine (in high ionic strength solutions, the pmH is a better indication of acidity than pH, $-\log_{10}$ of the hydrogen ion activity). Figures SOTERM-1 and SOTERM-2 show the dependence of pmH on carbon dioxide fugacity [$f(CO_2)$] for Brine A (Salado brine) and ERDA-6 (Castile brine), respectively, calculated by Wang (1996a and 1996b)~~

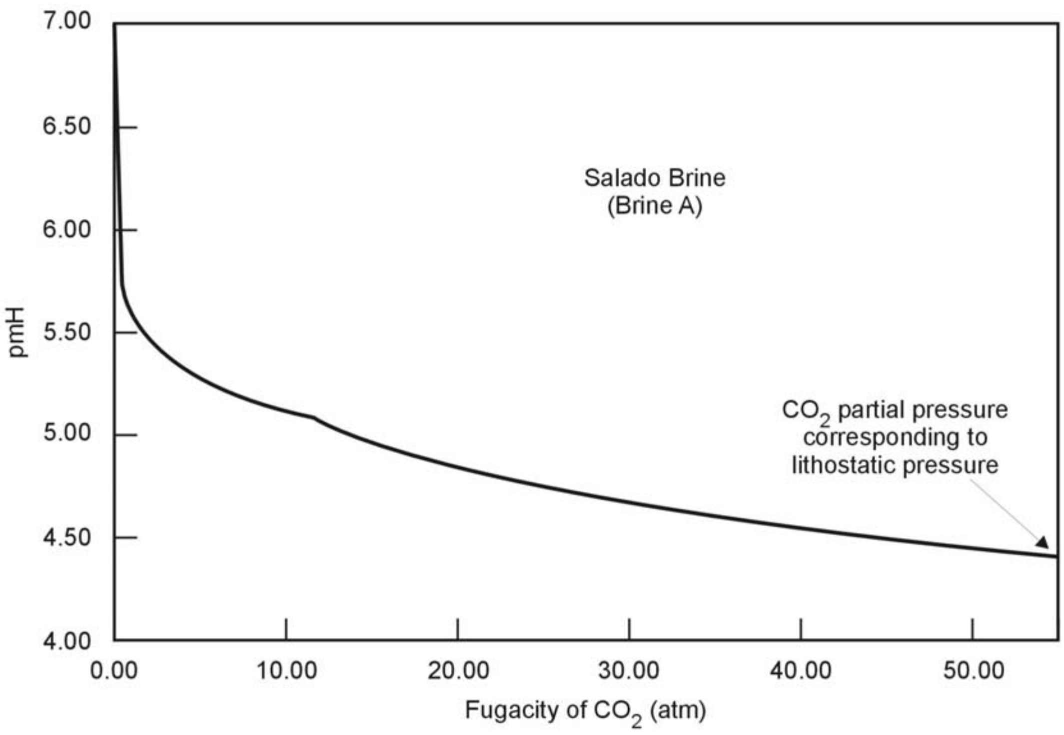

NOTE: It is assumed that CO_2 production by microbial reactions will be the dominant factor lowering brine pmH. Because of the difficulty in estimating the maximum CO_2 pressure in the repository, it is further assumed that the CO_2 pressure is limited by lithostatic pressure (approximately 150 atm), corresponding to approximately 55 atm CO_2 fugacity, according to a real-gas model developed by Duan et al. (1992) for a pure CO_2 system.

CCA-SOT002-0

~~Figure SOTERM-1. The pmH Changes of Salado Brine in the Absence of Added MgO as the Disposal Room is Pressurized with CO_2 Generated by Microbial Reactions.~~

~~using the code EQ3/6 (Wolery 1992; Wolery and Daveler 1992). The range shown in these figures is the range expected only when significant CO_2 generation takes place, and when MgO is not added to the repository. As can be seen in these figures, the pmH may approach 4.5 as the CO_2 fugacity exceeds 50 atm. At these pmH and f(CO_2) conditions, the solubilities of actinides are much higher than at neutral or slightly basic pmH and low f(CO_2). Excess MgO, however, will be emplaced with the waste for assurance purposes, and will buffer the pmH and f(CO_2) of the repository brine to values where the solubility of actinides is minimized. Figures SOTERM-3 and SOTERM-4 show the major minerals and pH obtained with titration of $Mg(OH)_2$ into each of the end member brines.~~

Microbial activity, if it occurs to a significant extent in the WIPP, would consume CPR materials by the following sequential reactions (Brush 1990; Francis and Gillow 1994; Brush 1995; Wang and Brush1996a; Francis and Gillow 1997):

$$C_6H_{10}O_5 + 4.8H^+ + 4.8NO_3^- \rightarrow 7.4H_2O + 6CO_2 + 2.4N_2; \quad (1)$$

$$C_6H_{10}O_5 + 6H^+ + 3SO_4^{2-} \rightarrow 5H_2O + 6CO_2 + 3H_2S; \quad (2)$$

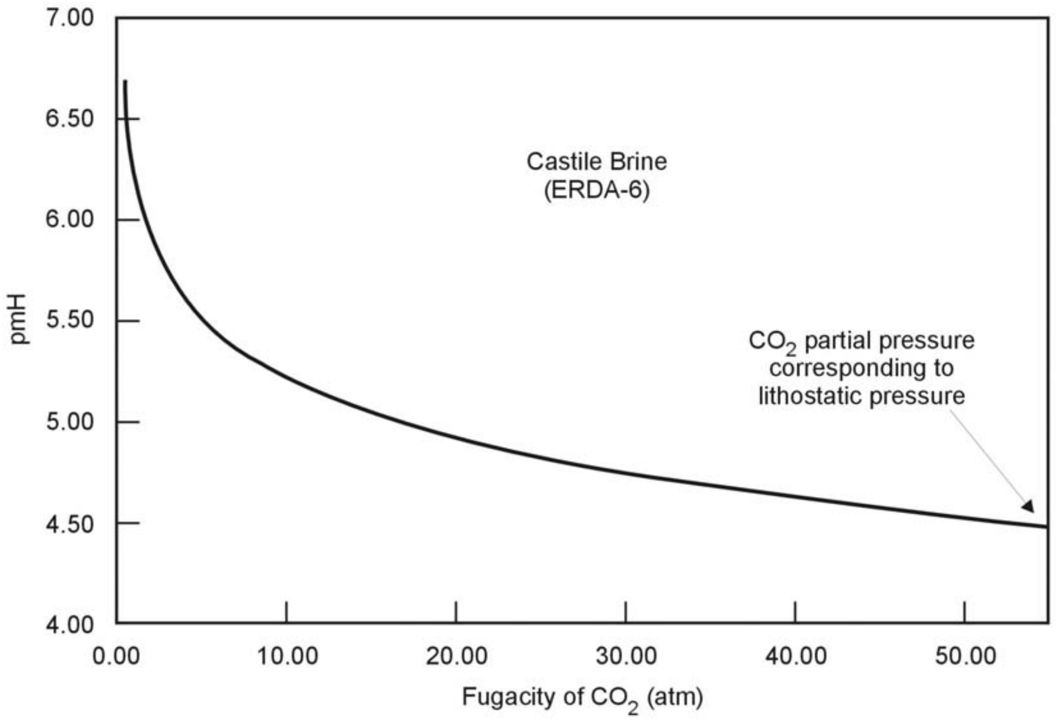

NOTE: It is assumed that CO_2 production by microbial reactions will be the dominant factor lowering brine pmH. Because of the difficulty in estimating the maximum CO_2 pressure in the repository, it is further assumed that the CO_2 pressure is limited by lithostatic pressure (approximately 150 atm), corresponding to approximately 55 atm CO_2 fugacity, according to a real-gas model developed by Duan et al. (1992) for a pure CO_2 system.

CCA-SOT003-0

~~Figure SOTERM-2. The pmH Changes of Castile Brine in the Absence of Added MgO as the Disposal Room Is Pressurized with CO_2 Generated by Microbial Reactions.~~

$$C_6H_{10}O_5 + H_2O \rightarrow 3CH_4 + 3CO_2. \qquad (3)$$

An analysis by Snider (2003b) based on the estimated quantities of CPR materials, nitrate (NO_3^-), and SO_4^{2-} (see Appendix Data, Attachment F) implies that, in the event all of the CPR materials are consumed, denitrification (Reaction (1)) would account for 4.72 mol percent, sulfate reduction (Reaction (2)) would account for 0.82 mol percent, and methanogenesis (Reaction (3)) would account for 94.46 percent of the consumption of CPR materials. (Appendix BARRIERS, Section BARRIERS-2.5, describes these calculations in detail.) Therefore, methanogenesis would be the primary microbial respiratory pathway in the repository.

Microbial consumption of CPR materials could produce significant quantities of CO_2, which could in turn acidify any brine present in the repository and increase the solubilities of the actinides relative to those predicted for neutral and mildly basic conditions. Therefore, the DOE is emplacing MgO in the repository to decrease actinide solubilities by consuming essentially all of the CO_2 that could be produced by microbial consumption of CPR materials,

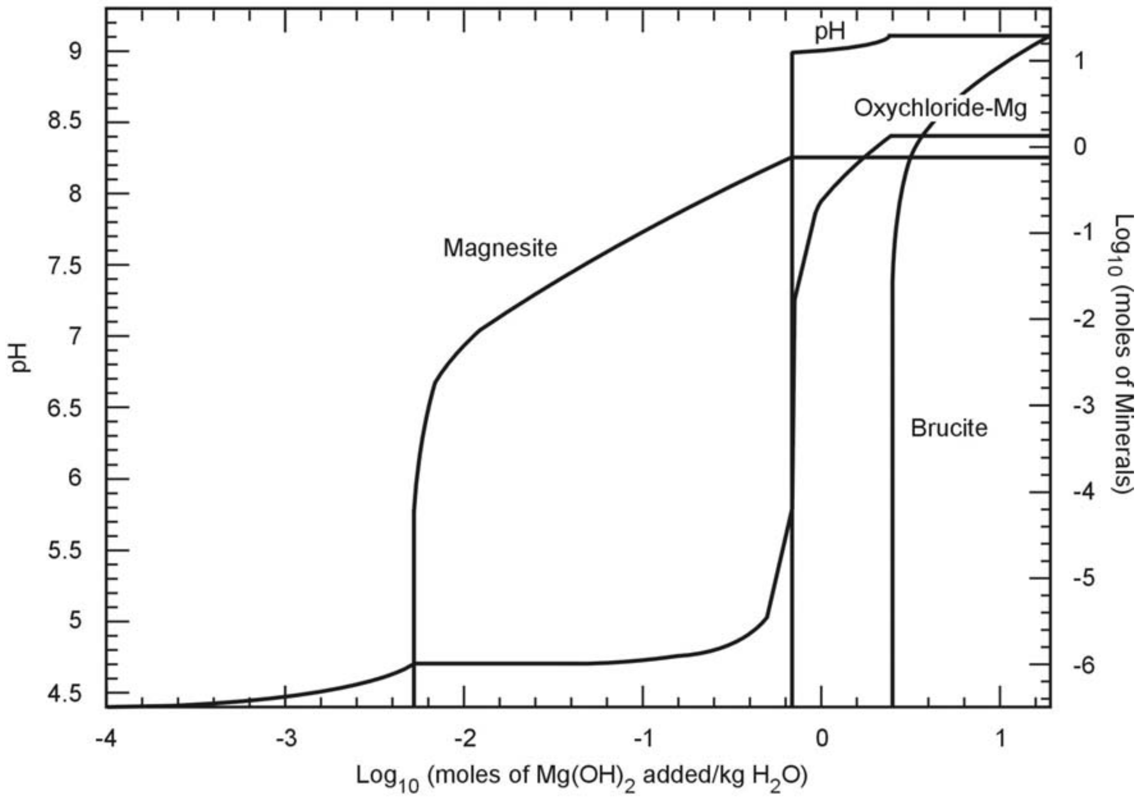

NOTE: The brine chemical composition used in the calculation is from Brush (1990, Table 2-2).

CCA-SOT004-0

~~Figure SOTERM-3. EQ3/6 Titration of Hydrated MgO into Salado Brine (Brine A).~~

and by buffering (controlling) the f_{CO_2} and pH within ranges that are favorable from the standpoint of actinide speciation and solubility (see Appendix BARRIERS, Section BARRIERS-2.0).

~~Hydrated MgO, $Mg(OH)_2$, will react with CO_2 by the reaction~~

~~$$Mg(OH)_2 + CO_2 = MgCO_3 + H_2O. \qquad (2\text{-}4)$$~~

~~This reaction will buffer the CO_2 fugacity at approximately 10^{-7} atm. However, CO_2 can also react with $Ca(OH)_2$ present as cementitious material in the waste by the reaction~~

~~$$Ca(OH)_2 + CO_2 = CaCO_3 + H_2O. \qquad (2\text{-}5)$$~~

~~If the reaction in Equation 2-5 buffered the hydrogen ion molality (pmH) of the repository, the pmH would be high. However, the effect of $Ca(OH)_2$ is minimal, because it will be quickly consumed by reactions 2.5 and 2.6 (reaction with $MgCl_2$ in Salado brine):~~

~~$$Ca(OH)_2 + MgCl_2 = CaCl_2 + Mg(OH)_2 \qquad (2\text{-}6)$$~~

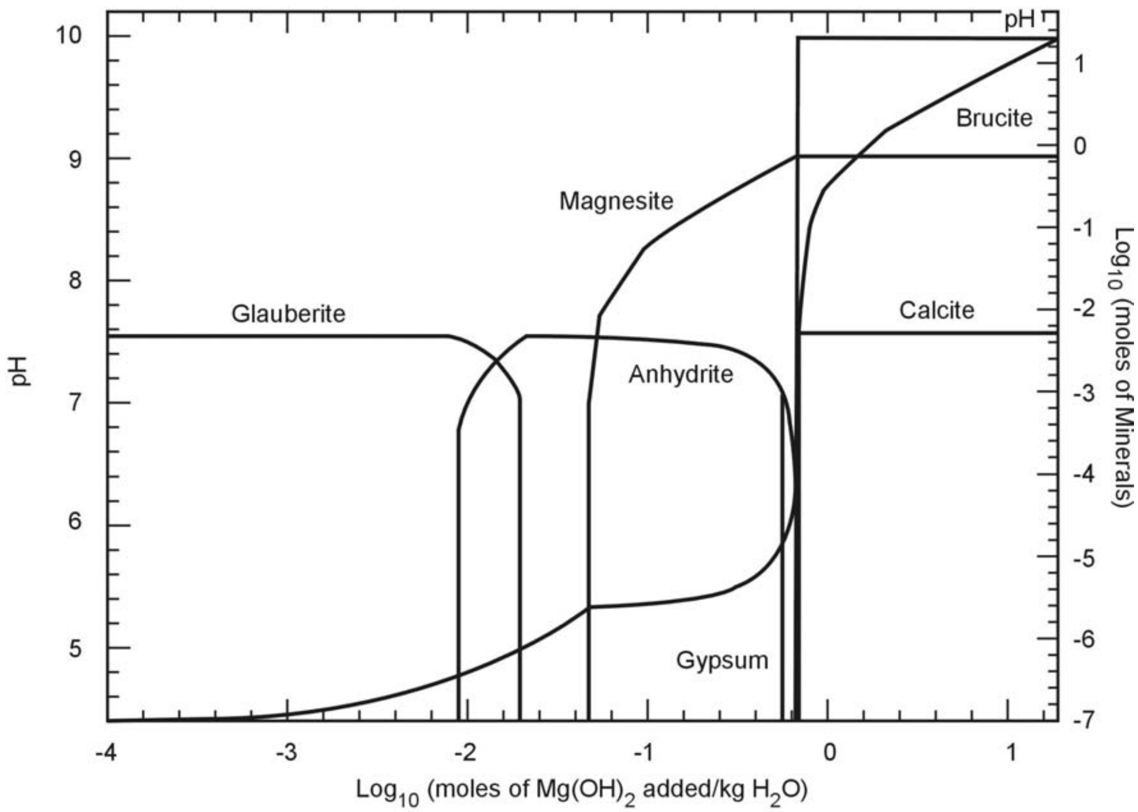

NOTE: The brine chemical composition used in the calculation is from Brush (1990, Table 2-3).

CCA-SOT005-0

~~**Figure SOTERM-4. Eq3/6 Titration of Hydrated MgO into Castile Brine (ERDA-6).**~~

~~Figures SOTERM-5a and 5b show the amounts of generated CO_2 , dissolved $Mg(OH)_2$ and $Ca(OH)_2$ that are expected within the repository and the corresponding buffers for each end member brine (Salado and Castile). It is estimated that $2x10^9$ moles of MgO will be added to the repository for assurance and $8x10^6$ moles of $Ca(OH)_2$ will be present as a cementious material in the waste (Storz 1996). Because the quantities of MgO and $Ca(OH)_2$ are fixed, the pH and $f(CO_2)$ will be a function only of the amount of CO_2 produced by microbial reaction, the volume of brine in the repository, and the type of brine. Figures 5a and 5b were constructed from the titration calculations with computer code EQ3/6 (Wolery 1992; Wolery and Daveler 1992). In the calculations, 0.004 moles $Ca(OH)_2$ were added for each mole of $Mg(OH)_2$. The figure indicates that, for Castile brine ERDA-6 (Figure SOTERM-5b), the transition from one buffer to another is very sharp whereas, for Salado brine Brine-A, a transition region (III) exists (Figure SOTERM-5a) (Wang 1996a, Figure 26). The existence of region (III) is due to the formation of Mg-oxychlorite. The transition region and region I have very similar pH values. Furthermore, the figure shows that the chemical conditions in the repository will be dominantly controlled by $Mg(OH_2)$ and carbonate minerals, because $Ca(OH)_2$ in the waste will be consumed easily by reaction with microbially-generated CO_2 or $MgCl_2$ in the Salado brine. (Note that even if there is no CO_2 generation, the Mg buffers will apply if more than 5000 cubic meters of Salado brine~~

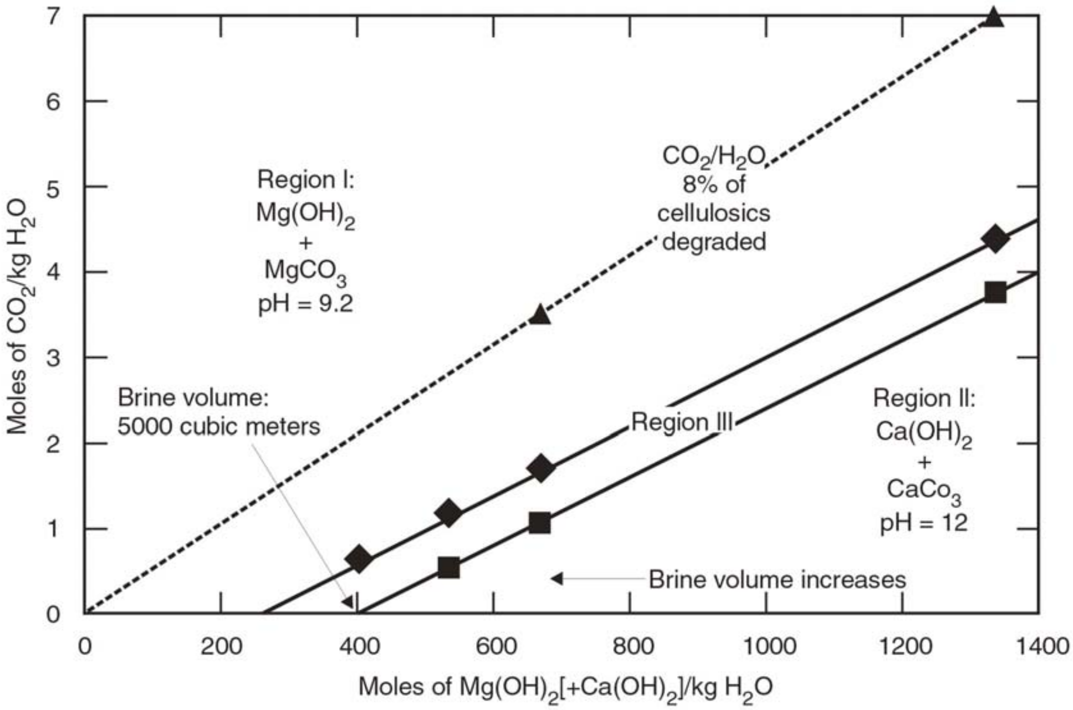

NOTE: Since MgO and $Ca(OH)_2$ are fixed, the ratio of $Mg(OH)_2/H_2O = 2 \times 10^9$ moles/kg of total water in the repository. The ratio of $Ca(OH)_2$/kg H_2O = 0.004*$Mg(OH)_2$/kg H_2O. The dashed line is the CO_2/H_2O ratio corresponding to 8% of cellulosics biodegraded. Region III can be combined into region I, because they have similar pH values.

CCA-SOT006-0

~~Figure SOTERM-5a. Chemical Buffer Distribution for Salado Brine (Brine A) as a Function of CO_2 Produced and $Mg(OH)_2[+Ca(OH)_2]$ Added per Kilogram of Water.~~

~~enter the repository. The amount of 5000 cubic meters is a small fraction of the repository pore volume.) The dashed line is included to show that the CO_2 produced from degradation of only 8 percent of the cellulosics is enough to react with all the $Ca(OH)_2$ in the waste.~~

~~Therefore, under all situations where repository performance may be affected, the brine pmH and $f(CO_2)$ will be controlled by the $Mg(OH)_2$ + $MgCO_3$ buffer.~~

Laboratory and modeling studies described in Appendix BARRIERS, Section BARRIERS-2.3 have shown that, in the event of significant microbial activity in the WIPP, the carbonation reaction

$$5Mg(OH)_2 + 4CO_2(aq\ or\ g) \rightleftharpoons Mg_5(CO_3)_4(OH)_2{\cdot}4H_2O \qquad (4)$$

will buffer f_{CO_2} at a value of $10^{-5.50}$ atm in both GWB and ERDA-6. In this reaction, $Mg(OH)_2$ is the mineral brucite (the main hydration product of the mineral periclase (MgO) expected in the WIPP); $Mg_5(CO_3)_4(OH)_2{\cdot}4H_2O$ is the form of the mineral hydromagnesite expected in the repository; and “aq” and “g” are the abbreviations for “aqueous” and “gaseous,” respectively. Furthermore, the brucite-dissolution reaction

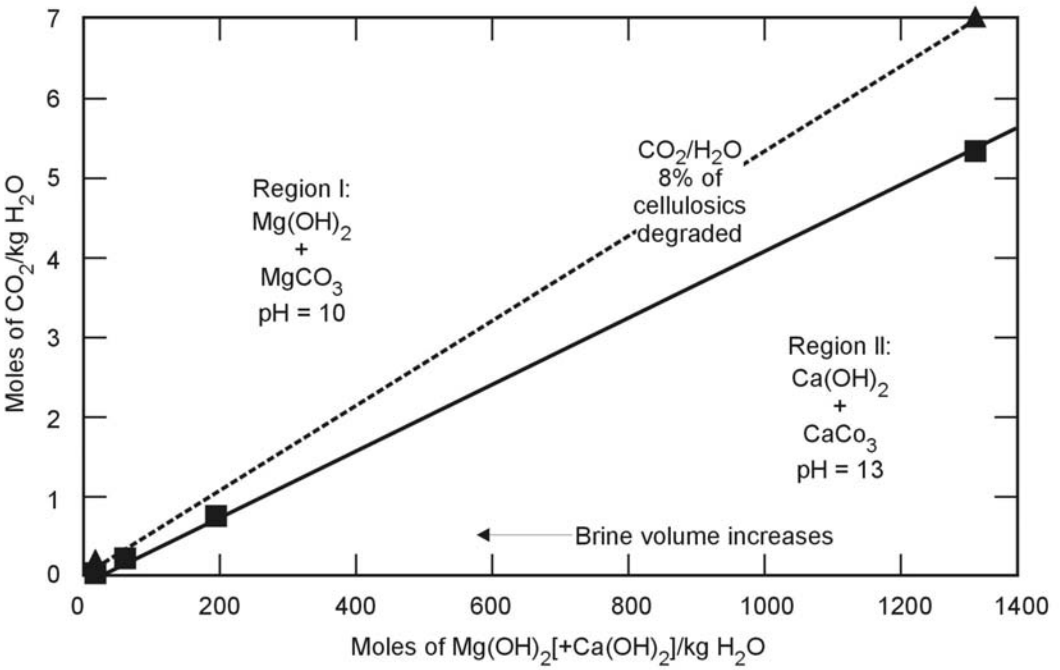

NOTE: Since MgO and $Ca(OH)_2$ are fixed, the ratio of $Mg(OH)_2/H_2O = 2 \times 10^9$ moles/kg of total water in the repository. The ratio of $Ca(OH)_2$/kg $H_2O = 0.004{*}Mg(OH)_2$/kg H_2O. The dashed line is the CO_2/H_2O ratio corresponding to 8% of cellulosics biodegraded.

CCA-SOT007-0

~~**Figure SOTERM-5b. Chemical Buffer Distribution for Salado Brine (ERDA-6) as a Function of CO_2 Produced and $Mg(OH)_2[+Ca(OH)_2]$ Added per Kilogram of Water.**~~

$$Mg(OH)_2 \rightleftharpoons Mg^{2+} + 2OH^- \qquad (5)$$

will buffer pH in the WIPP at a value of 8.69 in GWB and 9.02 in ERDA-6. These values of f_{CO_2} and pH were used for the actinide speciation and solubility calculations for the CRA-2004 PA vectors with significant microbial activity (see Section 3.5 below).

In the absence of significant microbial activity in the WIPP, the carbonation reaction

$$Mg(OH)_2 + Ca^{2+} + CO_2(aq\ or\ g) \rightleftharpoons CaCO_3 + Mg^{2+} + H_2O(aq\ or\ g) \qquad (6)$$

will buffer f_{CO_2} at a value of $10^{-5.48}$ atm in GWB and $10^{-6.15}$ atm in ERDA-6, and the brucite-dissolution reaction (Reaction (5)) will buffer pH at a value of 8.69 in GWB and 8.99 in ERDA-6 (see Appendix BARRIERS, Section BARRIERS 2.3). In this reaction, $CaCO_3$ is the mineral calcite. These values of f_{CO_2} and pH were used for the actinide speciation and solubility calculations for the CRA-2004 PA vectors without microbial activity (see Section 3.0 below).

Four effects of microbial ~~degradation~~***consumption*** of ~~organic materials~~***CPR materials*** are recognized in modeling system performance. A simplification has been made that the effects will be time independent after 100 years. The effects are~~:~~

- CO_2 ***production. With the addition of excess MgO, the effects of*** CO_2 ***production are minimized, and it is assumed that the system may be modeled using the*** ~~$Mg(OH_2)+$ $MgCO_3$-~~***brucite-hydromagnesite ($Mg_5(CO_3)_4(OH)_2\cdot 4H_2O$) buffer.***

- ~~Reduction-oxidation~~***Redox*** effects. After 100 years, the repository will have a reducing environment. Even though significant microbial action is only 50 percent likely, the corrosion of steel will also produce a reducing environment (Section ~~SOTERM.~~2.2.3).

~~NOTE: It is assumed that CO_2 production by microbial reactions will be the dominant factor lowering brine pmH. Because of the difficulty in estimating the maximum CO_2 pressure in the repository, it is further assumed that the CO_2 pressure is limited by lithostatic pressure (approximately 150 atm), corresponding to approximately 55 atm CO_2 fugacity, according to a real-gas model developed by Duan et al. (1992) for a pure CO_2 system.~~

- ***Possible*** ~~C~~***c***onsumption of organic ligands. While some microbes are known to consume some organic ligands, there is uncertainty as to the presence or viability of these particular microbes within the repository environment. Therefore, no credit has been taken for the microbial ~~degradation~~ ***consumption*** of organic ligands. Other mechanisms for reducing the effect of organic ligands are discussed in Section ~~SOTERM.~~5.**0**.

- Production of ~~humid~~***humic*** and microb~~e~~***ial*** colloids. ~~Even though microbes are modeled with only a 50 percent chance of significant growth, it is assumed that there are enough suspended microbes (viable or lysed) to increase the suspended actinide concentration. This is further discussed in Section SOTERM.6.~~

~~(4) CO_2 generation. With the addition of excess MgO backfill, the effects of CO_2 generation are minimized, and it is assumed that the system may be modeled using the $Mg(OH)_2$ + $MgCO_3$ buffer.~~

SOTERM-2.2.3 Anoxic Corrosion of Steels and Other Iron-Base Alloys

The corrosion of steels***, other Fe-base alloys,*** and other metals ~~with~~in the repository will have several effects on the ~~dissolution and suspension of~~ actinide~~s~~ ***source term***. Corrosion is expected to:

- reduce the oxidation states of some actinides, ~~affecting their solubility and binding constants~~ ***especially Pu, from relatively mobile oxidation states, such as Pu(V) and Pu(VI), to relatively immobile oxidation states, such as Pu(III) and Pu(IV)*** (Section ~~SOTERM.~~4.**0**)~~,~~***;***

- ~~release metal ions such as iron and nickel into solution. These metal ions can then bind organic ligands, thus reducing the ability of the ligands to increase actinide solubility (Section SOTERM.5),~~

- produce colloidal corrosion products on which actinides may sorb (***see*** Section ~~SOTERM.~~6***.0***).

It is expected that ~~the~~ oxic corrosion of steels and aerobic ***microbial*** ~~biodegradation~~***consumption*** of ~~organic materials~~***CPR materials*** will quickly consume the limited amount of ***oxygen (***O_2***)*** trapped within the repository at ~~emplacement~~ ***the time of closure***. After ~~the~~ O_2 is consumed, anoxic corrosion of ~~the~~ metals will occur (Brush 1990~~,~~***;*** ~~30 et seq.~~ ***Brush 1995; Wang and Brush 1996a***. ~~There will be about 2 x 10^9 moles of iron in the repository (DOE 1996, 2-5, 2-6) which is expected to corrode at a rate between 0.005 and 6.5 microns/year when inundated with brine but is immeasurably slow when in unsaturated conditions (Wang and Brush 1996). If the ferrous metals corroded at the maximum rate, they would be corroded within approximately 6,000 years after closure.~~ In ~~most cases, however, it is expected that~~ ***all of the vectors for the CRA-2004 PA, the EPA's 1997 Performance Assessment Verification Test (PAVT), and the CCA PA, there*** ~~will be~~***were significant amounts of uncorroded*** ~~metal~~***steels and other Fe-base alloys in the repository throughout the 10,000-year regulatory period.*** ~~In addition,~~ WIPP***-***specific experiments (***Telander and Westerman, 1993; 1997***~~Wang and Brush 1996~~) show***ed*** that ~~the~~ steels ***and other Fe-base alloys*** will corrode by the following reaction***s***:

~~$Fe(O) + H_2O = Fe(OH)_2 + H_2$. (2-7)~~

$$Fe + (x + 2)H_2O \Leftrightarrow Fe(OH)_2{\cdot}xH_2O + H_2; \tag{7}$$

$$3Fe + 4H_2O \Leftrightarrow Fe_3O_4 + 4H_2; \tag{8}$$

$$Fe + H_2O + CO_2 \Leftrightarrow FeCO_3 + H_2;\ \text{and} \tag{9}$$

$$Fe + H_2S \Leftrightarrow FeS + H_2. \tag{10}$$

Metal hydroxides such as ***Fe(II) hydroxide (***$Fe(OH)_2$***$\cdot xH_2O$)*** are more soluble in the WIPP ~~high~~ ***high-***~~ionic~~ ***ionic-***strength brines than in dilute ~~waters~~***solutions***, and significant amounts of Fe(II) may dissolve. Refait and Genin (1994) estimated Fe(II) solubilities between 10^{-4} and 10^{-6} M for pH between 8.5 and 10.5 ~~at~~ ***under*** ~~reduction-oxidation~~***redox*** conditions expected for the repository. Sagoe-Crentsil and Glasser (1993) observed even higher solubilities at pH 13 with electrolytic dissolution of ~~iron~~***Fe***.

Corrosion of metals will produce reducing conditions ~~with~~in the repository, but ~~the effective reduction-oxidation~~***redox conditions*** ~~state of the system is unknown~~ ***have not been predicted quantitatively***. The repository ~~system~~ is not described using Eh, because in ~~low~~ ***low-***temperature ***geochemical*** systems***,*** ~~reduction-oxidation~~ equilibri~~um~~***a*** ~~between~~***among*** the many ~~reduction-oxidation~~ ***redox*** couples ~~may not necessarily be~~ ***are generally not*** ~~ob~~***at***tained, and ~~no unique~~ Eh is ***generally poorly*** defined. For this reason***,*** the ~~reduction-~~oxidation states of the actinides have been determined experimentally***,*** as described in Section ~~SOTERM.~~4***.0***.

SOTERM-2.2.4 Other Effects

High pressure in the repository after closure ~~is expected to~~***will*** have an insignificant effect on actinide solubilit~~y~~***ies*** and the association of actinides with colloids and***,*** therefore***,*** its effect is ~~eliminated from~~***not included in*** ~~performance assessment~~ ***PA.*** ~~calculations.~~ Temperature within the repository is not expected to change by more than a few degrees from ambient ***(28 ºC)*** (***Munson et al. 1987;*** Sanchez and Trellue 1996; Wang and Brush 1996***a***). Because the effect on solubilit~~y~~***ies*** of a few degrees ***Celsius*** is insignificant compared to uncertainty of the measurements and modeling of solubilit~~y~~***ies***, temperature effects were also discounted (Section ~~SOTERM.~~3.3).

Radiolysis of brine may ~~change the effective reduction-oxidation state~~***affect redox conditions in the repository***. When energy from radioactive decay is absorbed by ~~water~~***H_2O***, the ~~water~~***H_2O molecule*** is broken into energetic fragments that reassemble into oxidized and reduced species. Depending on the chemical reactivity of these species, the system may be effectively more oxidizing or more reducing as a result of the radiolysis. For example, radiolysis often occurs by the following reaction:

$$2H_2O + \text{radiation} = H_2(g) + H_2O_2 \ .$$

(~~2-8~~***11***)

Hydrogen ~~P~~***p***eroxide (H_2O_2) is more reactive than ~~H_2~~ ***hydrogen (H_2)*** (g) at low temperature, and peroxide ~~reduction-oxidation~~***redox*** reactions will affect the system more than the slow H_2 reactions. If the system is initially very oxidized, ~~the~~ H_2O_2 will cause a reduction in the effective ~~reduction-oxidation~~***redox*** state, but if the system is initially very reduced, the peroxide will cause oxidation ~~in the effective reduction-oxidation state~~. In the WIPP, it is expected that the repository will be quite reducing due to the large amount of ~~iron metal~~***metallic Fe*** and dissolved Fe(II) species. Any oxidized species such as ~~peroxide~~ ***H_2O_2*** generated from radiolysis are expected to quickly react with the ***metallic Fe*** ~~iron metal~~ and Fe(II)***,*** thus negating any oxidizing effect of radiolysis. Therefore, radiolysis is not expected to affect the ~~reduction-oxidation~~***redox*** state of the repository ***significantly***.

Other components of the waste may ~~have a potential to~~ influence the concentration of dissolved actinides within the repository. These include, for example, organic ligands (Section ~~SOTERM.~~5***.0***); other salts such as ***calcium chloride (***$CaCl_2$***)***, which may raise the ionic strength of the brine; vermiculite, which may sorb actinides; and phosphate ***(PO_4^{3-})***, which may precipitate insoluble actinide phosphates. The effects of most of these components are assumed beneficial and ~~are unquantifiable~~***would be difficult to quantify***, so they were not included in ~~performance assessment modeling~~ ***PA***.

SOTERM-2.2.5 Summary

~~The c~~***C***hemical ~~environment~~***conditions*** in the ~~brine-inundated~~ repository ~~is a function of~~ ***will be affected by whether brine is present (humid or inundated conditions) and the type of*** brine ~~composition~~ (Salado or Castile); microbial ~~degradation~~***consumption*** of ~~organic materials~~***CPR materials***, which will produce ~~various gases~~***mainly methane (CH_4) and CO_2,*** and colloidal particles; ~~the~~ MgO ~~additive~~, which will control ~~the pmH and the CO_2 fugacity~~ ***f_{CO_2} and pH***; and corrosion of ~~the large quantity of~~***steels, other Fe-base alloys, and other*** metals in the repository, which will ~~cause~~***create*** reducing conditions***.*** ~~and release ions that will bind with and sequester organic ligands.~~

SOTERM-3*.0* PREDICTION OF DISSOLVED ACTINIDE SOLUBILIT~~Y~~*IES*

This section describes the basic approach ***used*** to predict~~ing dissolved~~ actinide solubilit~~y~~***ies*** for ~~this application~~ ***the CRA-2004 PA***. Surveys of different possible conceptual and mathematical descriptions of the system are presented, followed by a more detailed discussion of the method selected.

The material in this section is intended to provide an overview of the modeling methods. More detailed descriptions ~~of particular points or issues~~ can be found in the ~~indicated~~ references.

SOTERM-3.1 Previous Approaches to Estimating Actinide Solubilit~~y~~ies in the WIPP

Brine flow through the repository was not considered early in the WIPP ~~p~~**P**roject ~~history~~ because ~~none~~ ***brine*** was ***not*** expected ***to enter the repository (see CCA Appendix MASS, Section MASS.2)***. ~~As~~ ***When*** it was realized that brine***s from a variety of sources*** ~~may~~ ***might*** enter the ~~waste disposal region~~***repository*** ~~from a variety of sources~~, scenarios involving brine flow were developed. These scenarios ~~required~~ ***necessitated the*** investigation of potential mobilization ~~of actinides~~ ***mechanisms***, including ***dissolution of*** actinide***s*** ~~solubility~~ in ~~brine~~ ***high-ionic-strength aqueous solutions applicable to WIPP brines***.

The solubilit~~y~~***ies*** of actinides in ~~the~~ WIPP ***brines*** ~~was~~ ***were*** initially estimated by an expert panel that reviewed the existing literature on actinide solubilities (Trauth et al. 1992). The range of solubilities obtained was about 14 orders of magnitude because the chemical conditions surveyed included extremes of acidity and other conditions. With the addition of MgO and the demonstrat~~ed~~***ion of*** reducing conditions, ***it was realized that*** these extreme~~s~~ ***conditions*** ~~will~~ ***would*** not occur in the WIPP. The expert panel also estimated the effect of high ~~carbonate~~ CO_3^{2-} concentrations***,*** ~~(~~which are known to increase actinide solubilit~~y~~***ies*** significantly~~)~~***,*** ~~on the actinide solubility~~ despite the paucity of data for ~~carbonate~~ CO_3^{2-}***-bearing*** solutions. Median solubilities developed by the panel were Th***:*** 10^{-10} M; U***:*** 10^{-3} M; Np***:*** 10^{-7} M; Pu***:*** 10^{-9} M; and Am and Cm***:*** 10^{-9} M (Trauth et al. 1992, p. 4-5; Hobart et al. 1996). Published studies of actinides under environmental conditions ~~(that is, neutral or basic pH)~~ have focused on actinides in surface waters and groundwaters that are considerably more dilute than WIPP brines, which contributed to the wide range of ~~concentration~~ ***solubility*** estimates because more pertinent data were unavailable.

Experimental investigations for other radioactive waste projects (for example, Nitsche 1987) have ~~approached the question of potential actinide solubility by~~ measur~~ing~~***ed*** the solubilit~~y~~***ies*** of ~~the~~ actinides ~~in the waste~~ directly. Although this is possible for well-characterized and homogeneous waste and groundwaters, the waste intended for the WIPP is heterogeneous, and a relatively wide range of chemical conditions would be possible in the repository without ~~the~~ MgO ~~backfill~~. Measuring solubilit~~y~~***ies*** directly in experiments using transuranic (TRU) waste and ensuring that the measurements reflect steady-state WIPP conditions would entail an extremely large number of measurements and considerable uncertainty. This approach was determined to be neither practical nor feasible. The DOE therefore decided to estimate actinide solubilities by using a~~n~~ ~~equilibrium~~ thermodynamic~~s~~ model based on experimental parameterization.

SOTERM-3.2 Selection of the Pitzer ~~Activity~~ ***Activity-***Coefficient Model

The thermodynamic activity of a dissolved species ~~in solution~~ is ~~expressed as~~ ***the product of its actual concentration and*** an activity coefficient***.*** ~~multiplier of its analytical concentration.~~ In dilute aqueous solutions, the activity coefficient is close to unity, but in ~~high~~ ***high-*** ~~ionic~~ ***ionic-***strength ~~brines~~ ***solutions*** such as ~~encountered in the~~ WIPP ***brines***, the activity coefficient may ~~be quite different~~ ***deviate significantly*** ~~than~~ ***from*** unity.

The calculation of activity coefficients is the central feature of thermodynamic models in concentrated electrolyte systems. Activity coefficients represent the deviation from the nearly ideal behavior ~~that is~~ observed or assumed in dilute ~~electrolyte systems~~ ***solutions***. ~~Aqueous~~ ***Aqueous-***electrolyte ~~activity~~ ***activity-***coefficient models generally include the Debye-Hückel limiting law (see, for example, Pitzer 1991, 59 et seq.) to describe behavior in the dilute region (<0.1 m~~olal~~), and often include one or more adjustable parameters to reproduce measured behavior in more concentrated solutions.

Numerous ~~activity~~ ***activity-***coefficient models for concentrated electrolytes have been proposed, including the Pitzer ~~formalism~~ ***model*** (Pitzer 1991, Chapter 3), ~~the~~ Harned's Rule ~~approach~~ (Wood 1975), and the Specific-~~i~~***I***on Interaction Theory (SIT) ~~approach~~ (Grenthe and Wanner 1992), given in order of approximately decreasing mathematical complexity. The Pitzer ~~formalism~~ ***activity-coefficient model*** contains parameters that explicitly represent the contributions to the excess free energy from every two-moiety and three-moiety interaction, where a moiety is a cationic, anionic, or neutral aqueous species. The ~~Harned's~~ ***Harned's-***Rule ~~approach~~ ***model*** asserts that the "logarithm of the activity coefficient of one electrolyte in a mixture of constant total molality is directly proportional to the molality of the other component" (Robinson and Stokes 1959, 438), and thus by extension to multicomponent systems containing parameters for two-moiety interactions. The SIT ~~formalism~~ ***model*** contains parameters for two-moiety cation-anion interactions.

A primary consideration for selecting an ~~activity~~ ***activity-***coefficient model ~~for the WIPP~~ ***to predict*** actinide solubilit~~y~~***ies in the WIPP*** ~~data base~~ was the demonstrated applicability of existing models and databases to the brine***s*** and evaporite ~~systems~~ ***minerals*** at ~~the~~ WIPP~~ site~~. The Pitzer ~~formalism~~ ***model***, especially as parameterized by Harvie et al. (1980a), Harvie et al. (1984), and Felmy and Weare (1986), includes an established database describing solubilit~~y~~***ies*** in ~~the Na-K-Mg-Ca-H-Cl-SO_4-OH-HCO_3-CO_3-CO_2-B-H_2O~~***the hydrogen-ion- (H^+)-B-Na^+-Mg^{2+}-K^+-Ca^{2+}-OH^--bicarbonate-(HCO_3^-) CO_3^{2-}-SO_4^{2-}-Cl^- H_2O-CO_2*** system. ~~t~~***T***his system includes the significant ~~inorganic~~ ***nonradioactive*** constituents of WIPP brines. The ~~Harned's~~ ***Harned's-***Rule ~~approach~~ ***model*** has been parameterized for the ~~NaCl-KCl-$MgCl_2$-CaCl2~~ ***Na^+-Mg^{2+}-K^+-Ca^{2+}-Cl^-*** and ~~NaCl-$MgSO_4$-~~***Na^+-Mg^{2+}-$SO_4^{2-}$$Cl^-$*** systems (Wood 1975)***,*** but does not include ~~the carbonate ion~~ ***CO_3^{2-}***, ~~which is~~ one of the most important ***actinide*** complexants ~~for actinides~~ in aqueous systems. The SIT ~~formalism~~ ***model*** (Grenthe and Wanner 1992) is most commonly used for extrapolating apparent stability constants to zero ionic strength. No demonstrations that the SIT ~~formalism~~ ***model*** has been applied to multicomponent***,*** concentrated electrolytes such as brine-evaporite***-mineral*** systems have been identified in the literature.

The chemical behavior of the concentrated ~~electrolytes~~ ***brines*** that occur in evaporites like those at ~~the~~ WIPP ~~site~~ has been extensively studied and documented. The applications of the Harvie et al. (1980a), Harvie et al. (1984), and Felmy and Weare (1986) parameterization of the Pitzer ~~formalism~~ ***model*** include: prediction of the ~~mineral~~ ***mineral-***precipitation sequence accompanying ~~sea water~~ ***seawater*** evaporation (Eugster et al. 1980; Harvie et al. 1980b); the formation of borate minerals in Searles Lake, CA (Felmy and Weare 1986); and an analysis of Permian ~~sea water~~ ***seawater*** composition~~s~~ based in part on fluid***-***inclusion data from the Salado (Horita et al. 1991). Additional applications are given in Pitzer (1991, Chapters 6 and 7).

~~Brines in the~~ WIPP ~~system~~ ***brines*** range from about 0.8 m~~olal~~ to 8 m~~olal~~ ***in*** ionic strength. The Pitzer model is developed for and has been shown to work for electrolytes as concentrated as those ~~in the~~ ***at*** WIPP~~-system~~, and has been applied successfully to ~~evaporite systems~~ ***brines*** with concentrations greater than 10 m~~olal~~ (Felmy and Weare 1986). Rather than develop a new description of the chemical behavior of the ~~nonactinide~~ ***nonradioactive*** ~~chemical~~ constituents ~~in~~ ***of*** WIPP brines, it was decided to use the Harvie et al. (1984)/Felmy and Weare (1986) (HMW/FW) parameterization of the Pitzer model as the reference ~~activity~~ ***activity-***coefficient ~~formalism~~ ***model*** and thermodynamic database for ~~further~~ ***the*** WIPP ~~application~~ ***actinide source term***. ~~The~~ ***Additional research for the*** WIPP ~~actinide solubility research~~ focused on extending the database to include the actinides ~~of interest to~~ ***that could affect the long-term performance of*** the WIPP and the organic ~~waste constituents~~ ***ligands*** that ~~may~~ ***could*** ~~impact~~ ***affect the solubilities of these*** actinide***s*** ~~dissolved concentrations~~***(see Section 5.0)***.

SOTERM-3.3 The ~~FMT~~ ***Fracture-Matrix Transport*** Computer Code

The ***solubility and speciation code Fracture-Matrix Transport (***FMT***)*** ~~code (Novak 1995; WIPP Performance Assessment 1995~~ ***(Babb and Nowak 1997 and addenda***) ~~implements~~ ***uses*** the Pitzer ~~formalism~~ ***activity-coefficient model***~~, and is used~~ to calculate the solubilit~~y~~***ies*** of the actinide elements in equilibrium with the appropriate solubility-controlling solid~~(s)~~ in WIPP brines ***by*** ~~through the~~ minimiz~~ation~~***ing*** ~~of~~ the Gibbs free energy of the system. Where appropriate parameters already existed in the HMW/FW database, they have been used in FMT calculations for the WIPP. Additional parameters, most notably those for ~~the~~ ***dissolved*** actinide ~~ions~~ ***species***, have been ~~taken~~ ***obtained*** from the literature or determined from experimental data (see Section ~~SOTERM-~~3.4) using the NONLIN code (Novak 1995; WIPP Performance Assessment ***Department*** 1996). NONLIN calculates the Pitzer parameters using a nonlinear ~~least~~ ***least-***squares fitting program.

The FMT calculations were done for three actinides: Am(III), Th(IV), and Np(V) that are ~~chemical~~ ***oxidation-state*** analogs for ~~the~~ actinide***s in the*** ***+***III, ***+***IV, and ***+***V oxidation states, respectively. Because actinides in the same oxidation state exhibit similar chemical behavior, these FMT model calculations ~~are applied~~ ***apply*** to all actinides in ~~that particular~~ ***the same*** oxidation state; for example, the Am(III) ~~FMT~~ ***speciation and solubility*** model applies to Pu(III) ~~and Cm(III),~~***; the Th(IV) model applies to U(IV), Np(IV), and Pu(IV);*** and the Np(V) model applies to Pu(V). ***However, Pu will not persist to a significant extent in the +V oxidation state (or the +VI oxidation state) in the WIPP (see Section 4.6.)***

The dissolved concentrations of the actinides ~~Am, Cm, Np, Pu, Th, and U~~ ***Th, U, Np, Pu, and Am*** will be limited by solubility-controlling solid~~s~~ for each of the***se*** actinides in ~~the~~ ***WIPP*** brines. The important ions in WIPP brines are ~~H^+, Na^+, K^+, Mg^{2+}, OH^-, Cl^-, CO_3^{2-} SO_4^{2-}, and Ca^{2+}~~ ***H^+, Na^+, Mg^{2+}, K^+, Ca^{2+}, OH^-, CO_3^{2-}, SO_4^{2-}, and Cl^-***. Other ions***,*** ~~(~~for example, ~~PO_4^{3-}, F^-, Al^{3+}, and Fe^{2+}/Fe^{3+},~~ ***fluoride (F^-), aluminum (Al^{3+}), PO_4^{3-}, Fe^{2+}, and Fe^{3+},*** may ~~be important at influencing dissolved~~ ***affect*** actinide ~~concentrations~~ ***solubilities significantly.*** ~~both by influencing solubility and by influencing reduction-oxidation reactions.~~ Pitzer parameters for these other ions ~~were~~ ***are*** not ~~quantitatively~~ included in the dissolved species ***and*** source term model, but ~~are qualitatively included in the~~ ***enhance*** understanding of the chemical environment. For example, phosphates are known to precipitate actinides (Cotton and Wilkinson 1988), but this effect has conservatively been ignored due to the uncertainty of the phosphate inventory in the WIPP and the lack of a complete set of Pitzer parameters for its inclusion. The existence of Fe(II) from the anoxic corrosion of ~~iron~~ ***steels and other Fe-base alloys*** is accounted for in the oxidation state distribution (see Section ~~SOTERM.~~4***.0***), but is expected to have an insignificant effect on the solubilit~~y~~***ies*** of ~~an~~ individual actinide oxidation state ***and distribution***.

The expected temperature of the WIPP disposal rooms during the ***10,000-year*** regulatory ~~time frame~~ ***period*** is not expected to change by more than a few degrees from ambient ***(28 ºC)*** (***Munson et al. 1987;*** Sanchez and Trellue 1996; Wang and Brush 1996). The small differences in thermodynamic properties caused by these changes are well within acceptable uncertainty for the WIPP system. For these reasons, the small differences in properties over this temperature range are not significant for the WIPP, and all information was developed for 25°C. Literature information taken at approximately 20°C was deemed acceptable for model parameterization as well.

The development of the ~~dissolved~~ ***+III, +IV, and +V*** actinide ~~concentration~~ ***solubility*** model***s*** ~~was~~ ***consisted*** largely ***of*** the development of a database that includes the standard chemical potentials of the aqueous and solid ~~chemical~~ ***actinide-bearing*** species ~~containing actinides~~, and the ~~specific ion~~ ***ion-***interaction parameters required to describe the interactions between these species and other constituents of ***WIPP*** brines ~~in WIPP scenarios~~. The following ~~sub~~sections describe briefly how ~~these~~ ***this*** database~~s~~ ~~were~~ ***was*** built and how the needed parameters were obtained. The development of the ~~oxidation~~ ***oxidation-***state distribution***s*** reflected in these sections is discussed in Section ~~SOTERM.~~4***.0***.

Section ~~SOTERM.~~3.4 provides a guide to the information that is needed ~~for~~ ***to*** predict~~ing~~ ~~dissolved~~ actinide ~~concentrations~~ ***solubilities***. The FMT database ***currently*** used ~~in this application~~ ***to predict the solubilities of the +III, +IV, and +V actinides*** is documented in ~~Novak and Moore (1996)~~ ***Giambalvo (2002a, 2002b, 2002c, 2002d, 2002e, 2003)***. ~~The user's manuals for the FMT and NONLIN codes are contained in Attachments 1 and 2 respectively to this appendix.~~

~~**SOTERM.3.4 Overview of the Experimental Data**~~

~~***SOTERM.3.4.1 The III Actinides: Am(III), Pu(III), Cm (III) and the Lathanide Analog Nd(III)***~~

~~The III actinides of interest to the WIPP are Am(III), Pu(III), and Cm(III). The lanthanide analog Nd(III) has been shown to exhibit the same chemical properties as the III actinides. The An(III)[*] model has been demonstrated to describe the chemical behavior of both Am(III) and Pu(III) accurately, by a combination of comparisons with existing literature information and comparisons with additional experiments designed specifically to perform this demonstration. For the III system, working with Nd(III) provides a particular advantage because Nd is not radioactive, which simplifies the laboratory work, and is stable in the III state.~~

~~The dissolved concentration model was used to predict the behavior of the III actinides in the WIPP system, as is shown for the simple example of the solubility of Am(III) in a closed system of SPC brine as a function of pmH (Appendix E of Novak 1995).~~

~~Data for the III actinides and lanthanides are the most extensive of all the oxidation states of interest. The An(III) model was developed simultaneously from individual data for the Pu(III), Am(III), Nd(III), and Cm(III) systems. Cm(III) may be presumed to behave virtually identically with Am(III) (see, for example, Katz et al. 1986, 1498). The An(III) model has been parameterized in the Pitzer formalism for the Na, Cl, SO_4, CO_3, and PO_4 systems; $Pu^{3+}-Na^{+}-Cl^{-}$ in Felmy et al. (1989); $Am^{3+}-Na^{+}-HCO_3^{-}-OH^{-}-H_2O$ in Felmy et al. (1990); $Am^{3+}-Na^{+}-SO_4^{2-}-PO_4^{3-}$ in Rai et al. (1995); and $Nd^{3+}-Na^{+}-CO_3^{2-}-HCO_3^{-}-H_2O$ in Rao et al. (1996). Some of the aqueous species required are Am^{3+}, $AmCO_3^{+}$, $Am(CO_3)_2^{-}$, $Am(CO_3)_3^{3-}$, and the solid species $AmOHCO_3$(s). These are represented by the following reactions, as written for Am(III):~~

~~$Am^{3+} + CO_3^{2-} = AmCO_3^{+}$~~

~~$Am^{3+} + 2\,CO_3^{2-} = Am(CO_3)_2^{-}$~~

~~$Am^{3+} + 3\,CO_3^{2-} = Am(CO_3)_3^{3-}$~~

~~$Am^{3+} + OH^{-} = AmOH^{2+}$~~

~~$Am^{3+} + 2OH^{-} = Am(OH)_2^{+}$~~

~~$Am^{3+} + 3OH^{-} = Am(OH)_3(s)$~~

~~$Am^{3+} + OH^{-} + CO_3^{2-} = AmOH\,CO_3(s)$~~

~~These reactions represent one set of orthogonal reactions for americium(III) species.~~

---

[*] ~~The symbol An is used to designate any actinide element.~~

~~The An(III) data base has been extended to mixed Na^+-Cl^--CO_3^{2-} media, and has been shown to reproduce the independently measured solubility of $NaAm(CO_3)_2(s)$ in 5.6 M NaCl (Runde and Kim 1994) and Nd^{3+} solubility in WIPP brines.~~

~~***SOTERM.3.4.2 The IV Actinides: Th (IV), U(IV), Pu(IV), Np(IV)***~~

~~The IV actinides important to WIPP performance are Th (IV), U(IV), Pu(IV), and Np(IV). The variation in charge to radius ratio for the tetravalent actinides is greater than for actinides in other oxidation states (Cotton and Wilkinson 1988), and larger differences in the chemical behavior among the IV actinides is expected. The application of the Th(IV) model to the other IV species is more uncertain, yet still conservative because Th(IV) is the most soluble among these elements under WIPP conditions. The model was evaluated against data for Pu(IV) and Np(IV) solubility, and demonstrated to predict the chemical behavior of these actinides conservatively.~~

~~The Th(IV) dissolved concentration model is parameterized in the Pitzer formalism for interactions in the Na^+-K^+-Mg^{2+}-Cl^--SO_4^{2-}-CO_3^{2-}-HCO_3^--OH^--H_2O system. This model requires the species Th^{4+}, $Th(OH)_2SO_4$ (s), $Th(SO_4)_3^{2-}$, $Th(SO_4)_2$ (aq), ThO_2, $Th(OH)_4$(aq), $Th(OH)_3CO_3^-$, and $Th(CO_3)_5^{6-}$ to describe the data pertinent to the WIPP (Felmy et al. 1991; Felmy and Rai 1992; Felmy et al. 1996). The principal reactions required are (as written for Th(IV)):~~

~~$ThO_2\ (am) + 2H_2O = Th(OH)_4(aq)$~~

~~$Th^{4+} + 4OH^- = Th(OH)_4\ (aq)$~~

~~$Th^{4+} + 3OH^- + CO_3^{2-} = Th(OH)_3CO_3^-$~~

~~$Th^{4+} + 5CO_3^{2-} = Th(CO_3)_5^{6-}$~~

~~$Th^{4+} + 2SO_4^{2-} = Th(SO_4)_2\ (aq)$~~

~~$Th^{4+} + 3SO_4^{2-} = Th(SO_4)_3^{2-}$~~

~~$Th^{4+} + 2OH^- + SO_4^{2-} = Th(OH)_2SO_4\ (s)$~~

~~These reactions represent one set of orthogonal reactions for actinide(IV) species.~~

~~The Th(IV) model has been extended to concentrated NaCl, $MgCl_2$, $NaHCO_3$ and Na_2CO_3 solutions. In addition, Th(IV) solubility has been measured in WIPP brines.~~

~~***SOTERM.3.4.3 The V Actinides: Np(V)***~~

~~The only V actinide of interest to the WIPP is Np(V), which exists as the neptunyl ion, NpO_2^+. The base model for Np(V) comes from Fanghänel et al. (1995), constructed for the German repository program. The Np(V) model was parameterized for the elements Na, Cl, CO_3, and ClO_4 (the last of which is not important for the WIPP but is invaluable for interpreting data in the literature). The model requires the aqueous species NpO_2^+, NpO_2OH(aq), $NpO_2(OH)_2^-$,~~

~~$NpO_2CO_3^-$, $NpO_2(CO_3)_2^{3-}$, and $NpO_2(CO_3)_3^{5-}$, and the solid species $NpO_2OH(am)$, $NpO_2OH(aged)$, $Na_3NpO_2(CO_3)_2(s)$, $KNpO_2CO_3 \cdot 2H_2O(s)$, $K_3NpO_2(CO_3)_2 \cdot 0.5H_2O(s)$ and $NaNpO_2CO_3 \cdot 3.5H_2O(s)$ to explain the available data. These are represented by the reactions~~

~~$NpO_2^+ + OH^- = NpO_2OH(aq)$~~

~~$NpO_2^+ + 2\,OH^- = NpO_2(OH)_2^-$~~

~~$NpO_2^+ + CO_3^{2-} = NpO_2CO_3^-$~~

~~$NpO_2^+ + 2CO_3^{2-} = NpO_2(CO_3)_2^{3-}$~~

~~$NpO_2^+ + 3CO_3^{2-} = NpO_2(CO_3)_3^{5-}$~~

~~$NpO_2OH(am) = NpO_2^+ + OH^-$~~

~~$NpO_2OH(s) = NpO_2^+ + OH^-$~~

~~$NaNpO_2CO_3 \cdot 3.5H_2O(s) = Na^+ + NpO_2^+ + CO_3^{2-} + 3.5H_2O$~~

~~$Na_3NpO_2(CO_3)_2(s) = 3Na^+ + NpO_2^+ + 2CO_3^{2-}$~~

~~$KNpO_2CO_3 \cdot 2H_2O(s) = K^+ + NpO_2^+ + CO_3^{2-} + 2H_2O$~~

~~$K_3NpO_2(CO_3)_2 \cdot 0.5H_2O(s) = 3K^+ + NpO_2^+ + 2CO_3^{2-} + 0.5H_2O$~~

~~These represent a set of orthogonal reactions for neptunium(V) species. The Np(V) solubility model is being extended to potassium systems, including $K_3NpO_2(CO_3)_2(s)$.~~

~~*SOTERM.3.4.4 The VI Actinides: U(VI)*~~

~~The An(VI) FMT model has not been developed sufficiently for reliable use in predicting concentrations of this oxidation state in WIPP brines under various solution conditions. Although uranyl carbonate can be successfully modeled, the hydrolysis behavior of U(VI) is quite complicated and no satisfactory predictive models applicable to WIPP-like conditions are yet available. Because the implementation of an MgO backfill limits the pmH and fCO_2 to discrete values, empirical measurement of the solubility of U(VI) in WIPP and/or WIPP like brines became practical. As documented in Hobart and Moore (1996), the solubility of U(VI) at pH 10, in the absence of carbonate, was determined to be 8.8×10^{-5} molal. The incorporation of U(VI) data into performance assessment is discussed in Section SOTERM.7.~~

SOTERM-3.4 Overview of the Experimental Data

Studies of the solubilities and speciation of actinides, especially Pu, are often conducted by employing the oxidation-state analogy, which states that lanthanides and actinides in the same oxidation state have similar chemical behavior. There are several important advantageous aspects of the use of oxidation-state analogs, such as Th(IV) for Pu(IV). Redox-inert analogs can considerably simplify experimental design and consequently improve reliability of experimental data, in contrast to Pu, which can be a very labile experimental component. Additionally, the lanthanide and actinide analogs possess physical and chemical

characteristics that allow them to be used as probes in examination of the chemical behavior of Pu. For example, the luminescence lifetime of europium(III) (Eu(III)) can be directly correlated to the number of H_2O molecules in the inner coordination sphere, which allows interpretation of the nature of complexation of the trivalent lanthanides and actinides with ligands.

The 4f orbitals of the lanthanides and 5f orbitals of the actinides constitute the valence shells of the cations. The f orbitals are more diffuse than the p and d orbitals, and, upon ionization of the atom, become lower in energy than the 5d, 6s, and 6p orbitals in the case of the lanthanides, and comparable or slightly lower than the 6d, 7s, and 7p orbitals in the case of the actinides. The contraction of the radial component of the wave function of the f orbitals upon ionization of the element usually causes these orbitals to be unavailable for overlap with orbitals on other atoms, one of the conditions necessary for the formation of molecular orbitals. As a result, the lanthanide and actinide ions exhibit very little tendency to form covalent bonds.

Formation of complexes of most ligands with f elements is due to the electrostatic attraction between the metal cation and the electron-donating functionality of the ligand molecule. The effect of polarizability and Lewis acidity or basicity on formation of Lewis-acid or Lewis-base pairs has been described by Pearson (1963). Lanthanide and actinide cations, which have high charge density and low polarizability, are classified as hard cations. Similarly, ligands featuring O-donor atoms, such as citrate and oxalate, exhibit low polarizability and strong Lewis basicity, and are referred to as hard bases. Hard-acid metals interact with hard bases through electrostatic attraction. The stability of f-element complexes with many ligands is a function of the charge density on the donor atom. For example, progressively weaker Brönsted-Lowry acids (in order of increasing pKa: trichloroacetic < dichloroacetic < monochloroacetic < acetic acids) have progressively stronger conjugate bases due to increased electron density located on the carboxylic O's. As a result, the electrostatic attraction between the O and protons increases, resulting in weaker acidic behavior and corresponding increases in pKa values. Likewise, the force of electrostatic attraction between the carboxylate group and a metal ion increases with increasing basicity of the ligand.

The magnitude of electrostatic attraction between the f-element cations and ligands is dependent upon the local effective dielectric constant of the solution, the charge on the metal ion, and the distance of separation between the metal atom and the ligating atoms on the complexing agent. The magnitude of the local dielectric constant of the solution depends upon the ordering effect created by the electric-field gradient established by the cation. The charge densities of lanthanides and actinides with the same charge are similar enough that the responses of solvent molecules are similar, yielding local dielectric constants that are nearly constant for lanthanide and actinide cations with the same charge. The local dielectric constant is primarily dependent upon the charge of the ion; the variation due to the effect of different-magnitude electric-field gradients that result from the differences in ionic radii are small enough to be overlooked to a first approximation in the oxidation-state-analogy approach.

The factors that exert a much more pronounced influence are the ionic radii, charge on the metal ion, and, to a lesser extent, degree of solvation of the metal ion. The Gibbs free energy

of complex formation is inversely proportional to the distance between the metal and ligand, and directly proportional to the product of the numerical value of the electrostatic charges on the cation and anion. There are variations in the ionic radii of lanthanide and actinide ions that have the same charge, with decreasing ionic radii corresponding to increasing atomic number within the 4f and 5f series. However, the ionic radii of some of the metal ions are very similar. For example, neodymium ion (Nd^{3+}) and Am^{3+} have nearly identical ionic radii. As a result, the behavior of Nd(III) and Am(III) are very similar, with small differences attributable to the fact that the 5f orbitals of Am are closer in energy to the 6d, 7s, and 7p orbitals than the 4f orbitals of Nd are to the 5d, 6s, and 6p orbitals. Discussions of applications to the +III, +IV, +V, and +VI actinide oxidation states follow.

SOTERM-3.4.1 The +III Lanthanides and Actinides

The actinides most likely to occur in the +III oxidation state in the WIPP are Pu, Am, and Cu. Nd(III), Eu(III), Pu(III), Am(III), and Cu(III) have been widely used in studies of trivalent f-element chemical behavior in brines. The respective ionic radii for coordination number (CN) = 8 are 111, 17, 100, 109, and 97 pm (Shannon 1976). Due to the similarity of ionic radii, the magnitude of the electrostatic attraction between the metal ions and corresponding ligands is similar, yielding comparable thermodynamic stabilities. Each of the analog elements offers noteworthy advantages in probing various aspects of trivalent f-element solution behavior. For example, Nd(III) features hypersensitive absorption bands that respond to changes in the complexation environment, allowing examination of the nature of the metal-ligand interaction. The luminescence lifetime of Eu(III) can be used to measure the number of residual waters of hydration associated with the metal ion after formation of a complex. ^{241}Am, which has a 433-year half-life, undergoes α decay that is accompanied by 59.5-keV γ ray with a 35.9-percent yield. As a result, ^{241}Am may be used at tracer concentrations by well-developed radiochemical techniques, such as solvent extraction and ion exchange, as a means to study the thermodynamic behavior of trivalent actinides. Study of the solution behavior of Am(III) is uncomplicated by redox ability, unlike the situation for Pu(III), which requires Eh and pH controls of the solution to maintain a single oxidation state. Like Nd and Eu, Cu luminescence studies are useful to examine the coordination environment of the metal ion. Pu(III) does not have useful luminescence properties, making it impossible to study its complexation behavior by methods that are effective with the analogs.

The thermodynamic database for the +III actinides currently used in FMT was described by Giambalvo (2002a). Due to the redox ability of Pu, much of the experimental work carried out to develop an understanding of the chemical behavior of the +III actinides, particularly Pu, has been performed with Nd, Am, and Cm due to the stability of the trivalent oxidation states of these three elements. Speciation and solubility data for the +III actinides were parameterized for use in the Pitzer activity-coefficient model by Felmy et al. (1989) for the Na^+- Pu^{3+}-Cl^--H_2O system; by Felmy et al. (1990) for the Na^+-Am^{3+}-OH^--HCO_3^--H_2O system; by Rai et al. (1995) for the Na^+-Am^{3+}-PO_4^{3-}-SO_4^{2-}-H_2O system; and by Rao et al. (1996) for the Na^+-Nd^{3+}-CO_3^{2-}-HCO_3^--H_2O system. The inorganic aqueous and solubility-limiting species featured in the model for Am(III) are:

$$Am^{3+} + CO_3^{2-} \rightleftharpoons AmCO_3^{+}; \qquad (12)$$

$$Am^{3+} + 2CO_3^{2-} \rightleftharpoons Am(CO_3)_2^{-}; \tag{13}$$

$$Am^{3+} + 3CO_3^{2-} \rightleftharpoons Am(CO_3)_3^{3-}; \tag{14}$$

$$Am^{3+} + 4CO_3^{2-} \rightleftharpoons Am(CO_3)_4^{5-}; \tag{15}$$

$$Am^{3+} + OH^{-} \rightleftharpoons AmOH^{2+}; \tag{16}$$

$$Am^{3+} + 2OH^{-} \rightleftharpoons Am(OH)_2^{+}; \tag{17}$$

$$Am^{3+} + 3OH^{-} \rightleftharpoons Am(OH)_3(aq); \tag{18}$$

$$Am^{3+} + Cl^{-} \rightleftharpoons AmCl^{2+}; \tag{19}$$

$$Am^{3+} + 2Cl^{-} \rightleftharpoons AmCl_2^{+}; \tag{20}$$

$$Am^{3+} + SO_4^{2-} \rightleftharpoons Am(SO_4)^{-}; \tag{21}$$

$$Am^{3+} + 2SO_4^{2-} \rightleftharpoons Am(SO_4)_2^{+}; \tag{22}$$

$$Am^{3+} + OH^{-} + CO_3^{2-} \rightleftharpoons AmOHCO_3(s); \tag{23}$$

$$Na^{+} + Am^{3+} + 2CO_3^{2-} + 6H_2O \rightleftharpoons NaAm(CO_3)_2 \bullet 6H_2O(s);\ \text{and} \tag{24}$$

$$Am^{3+} + PO_4^{3-} \rightleftharpoons AmPO_4(cryst). \tag{25}$$

In these equations, “aq,” “cryst,” and “s” are the abbreviations for “aqueous,” crystalline,” and “solid,” respectively. The actinide(III) database was extended to mixed Na^{+}-CO_3^{2-}-Cl^{-}-media, and was shown to reproduce the independently measured solubility of $NaAm(CO_3)_2(s)$ in 5.6 M NaCl (Runde and Kim 1994) and Nd(III) solubility in WIPP brines.

SOTERM-3.4.2 The +IV Actinides

The tetravalent actinides important to WIPP performance are Th(IV), U(IV), and Pu(IV). Np is not included in the WIPP actinide source term, but has been included in the WIPP Actinide Source Term Program (ASTP). The +IV oxidation state is the only stable one in aqueous solution for Th, whereas U(IV) and Np(IV) are both readily oxidized. As a result, Th is often used to represent the behavior of the +IV actinides. Th(IV) does not have spectroscopic characteristics that are valuable in its study, but does have both long-lived (^{232}Th, $t_{1/2}$ = 1.41 × 10^{10} year) and shorter-lived (^{228}Th and ^{230}Th $t_{1/2}$ = 1.913 and 7540 year, respectively) isotopes that are useful in thermodynamic studies. The 105-pm ionic radius of the Th(IV) cation (C. N. = 8) is greater than the 96 pm Pu(IV) cation (Shannon 1976), resulting in complexation properties that vary in a systematic and predictable manner. The larger ionic radius of Th(IV) causes it to have complexes with stability constants lower than the corresponding complexes with Pu(IV). For example, the Pu(IV) complexes with OH^-, resulting from hydrolysis, have higher stability constants than Th(IV)-OH^- complexes. The actinide(IV) hydrolysis products are sufficiently stable that organic ligands present within the WIPP, (see Section 5.0) will be unable to effectively compete with OH^-. The net effect is that actinide(IV) complexation is dominated by OH^-, which forms very insoluble tetrahydroxide ($An(OH)_4$) precipitates. Pu has a pronounced tendency to form insoluble hydrolysis products that are less soluble than the corresponding Th(IV) oxides and hydroxides. The greater solubility of Th(IV) makes it a very good analog for Pu(IV) in the context of modeling the behavior of tetravalent actinides in the WIPP because the solubility of Th(IV) establishes an upper limit for the solubility of Pu(IV). Due to the experimental difficulty working with Pu(IV), it is more straightforward and defensible to establish upper limits rather than attempting to measure the solubility of Pu(IV) directly.

The thermodynamic database for the +IV actinides currently used in FMT was described by Giambalvo (2002c). Speciation and solubility data for Th(IV) were parameterized for the Pitzer activity-coefficient model for the Na^+-K^+ -Mg^{2+}-Cl^-- SO_4^{2-}-CO_3^{2-}-HCO_3^- -OH^--H_2O system. The inorganic aqueous and solubility-limiting species featured in the model are:

$$ThO_2(am) + 2H_2O \rightleftharpoons Th(OH)_4(aq); \tag{26}$$

$$Th^{4+} + 4OH^- \rightleftharpoons Th(OH)_4(aq); \tag{27}$$

$$Th^{4+} + 3OH^- + CO_3^{2-} \rightleftharpoons Th(OH)_3CO_3^-; \tag{28}$$

$$Th^{4+} + 5CO_3^{2-} \rightleftharpoons Th(CO_3)_5^{6-}; \tag{29}$$

$$Th^{4+} + 2SO_4^{2-} \rightleftharpoons Th(SO_4)_2(aq); \tag{30}$$

$$Th^{4+} + 3SO_4^{2-} \rightleftharpoons Th(SO_4)_3^{2-}; \tag{31}$$

$$Th^{4+} + 2SO_4^{2-} + 9H_2O \rightleftharpoons Th(SO_4)_2 \bullet 9H_2O(s); \tag{32}$$

$$Th^{4+} + 2SO_4^{2-} + 8H_2O \rightleftharpoons Th(SO_4)_2 \bullet 8H_2O(s); \tag{33}$$

$$Th^{4+} + 2Na^+ + 3SO_4^{2-} + 6H_2O \rightleftharpoons Th(SO_4)_2 \bullet Na_2SO_4 \bullet 6H_2O(s); \tag{34}$$

$$Th^{4+} + 2K^+ + 3SO_4^{2-} + 4H_2O \rightleftharpoons Th(SO_4)_2 \bullet K_2SO_4 \bullet 4H_2O(s); \tag{35}$$

$$Th^{4+} + 4K^+ + 4SO_4^{2-} + 6H_2O \rightleftharpoons Th(SO_4)_2 \bullet 2K_2SO_4 \bullet 2H_2O\ (s);\ \text{and} \tag{36}$$

$$Th^{4+} + 7K^{+} + 5.5SO_4^{2-} \rightleftharpoons Th(SO_4)_2\bullet 3.5K_2SO_4(s). \qquad (37)$$

SOTERM-3.4.3 The +V Actinides

Both Np and Pu have accessible +V oxidation states; however, Pu(V) is not expected to persist in significant quantities in the WIPP. The model for Np(V) was developed for the German repository program (Fanghänel et al. 1995). The speciation and solubility of Np(V) were parameterized for the Na^{+}-Cl^{-}-CO_3^{2-}-ClO_4^{-}-H_2O system.

The thermodynamic database for the +V actinides currently used in FMT is described by Giambalvo (2002d). Np(V) speciation and solubility were parameterized in the Pitzer activity-coefficient model for the Na^{+}-K^{+} -Mg^{2+}-Cl^{-}- SO_4^{2-}-CO_3^{2-}-HCO_3^{-} -OH^{-}-H_2O system. The inorganic aqueous and solubility limiting species used are:

$$NpO_2^{+} + OH^{-} \rightleftharpoons NpO_2OH(aq); \qquad (38)$$

$$NpO_2^{+} + OH^{-} \rightleftharpoons NpO_2OH(s, am); \qquad (39)$$

$$NpO_2^{+} + OH^{-} \rightleftharpoons NpO_2OH(s, aged); \qquad (40)$$

$$NpO_2^{+} + 2OH^{-} \rightleftharpoons NpO_2(OH)_2^{-}; \qquad (41)$$

$$NpO_2^{+} + CO_3^{2-} \rightleftharpoons NpO_2CO_3^{-}; \qquad (42)$$

$$NpO_2^{+} + 2CO_3^{2-} \rightleftharpoons NpO_2(CO_3)_2^{3-}; \qquad (43)$$

$$NpO_2^{+} + 3CO_3^{2-} \rightleftharpoons NpO_2(CO_3)_3^{5-}; \qquad (44)$$

$$Na^{+} + NpO_2^{+} + CO_3^{2-} + 3.5H_2O \rightleftharpoons NaNpO_2CO_3\bullet 3.5H_2O(s); \qquad (45)$$

$$3Na^{+} + NpO_2^{+} + 2CO_3^{2-} \rightleftharpoons Na_3NpO_2(CO_3)_2(s); \qquad (46)$$

$$K^{+} + NpO_2^{+} + CO_3^{2-} \rightleftharpoons KNpO_2CO_3(s);\ \text{and} \qquad (47)$$

$$3K^{+} + NpO_2^{+} + 2CO_3^{2-} + 0.5H_2O \rightleftharpoons K_3NpO_2(CO_3)_2\bullet 0.5H_2O(s). \qquad (48)$$

SOTERM-3.4.4 The +VI Actinides

The actinide(VI) speciation and solubility model for brines under basic conditions has not been developed sufficiently for use in FMT. The hydrolysis behavior of U(VI) is quite complicated and no satisfactory predictive models applicable to WIPP conditions are

available. As documented in Hobart and Moore (1996), the solubility of U(VI) at pH 10, in the absence of CO_3^{2-}, was estimated to be 8.8×10^{-5} m.

SOTERM-3.5 Calculations of Actinide Solubilit~~y~~*ies* Using the ~~FMT~~ *Fracture-Matrix Transport* Computer Code

Details of the ~~implementation of FMT and an early version of the CHEMDAT data base~~ ***solubility calculations for the +III, +IV, and +V actinides and the estimation of the solubility of +VI actinides for the CRA-2004 PA*** are given in ~~Appendix D of Novak (1995), and in the FMT User's Manual~~ ***Brush and Xiong (2003a, 2003b, 2003c) and Downes (2003a, 2003b)***. ~~FMT calculated chemical equilibrium for user-specified total element amounts for aqueous or aqueous/mineral geochemical systems.~~

The ~~set of~~ FMT calculations of actinide solubilit~~y~~**ies** ~~in the WIPP system performed~~ for the ~~performance assessment~~ ***CRA-2004 PA*** ~~included~~ ***featured the*** establish~~ing~~***ment of*** equilibrium ***of Salado brine (GWB) or Castile brine (ERDA-6)*** with halite, ***and*** anhydrite, ~~brucite, and magnesite (Novak et al. 1996), the minerals~~ ***minerals*** present in large quantities in the ***Salado at the*** repository ~~system~~ ***horizon***. The effects of ~~the~~ MgO ~~backfill are realized through~~ ***included*** ~~the establishment of~~ equilibri~~um~~***ation*** of ***Salado*** brine ***or Castile brine*** with brucite and ~~magnesite~~ ***hydromagnestie ($Mg_5(CO_3)_4(OH)_2{\cdot}4H_2O$) in the PA vectors with microbial activity, and with brucite and calcite in the vectors without microbial activity (see Reactions (4), (5), and (6) above; and Appendix BARRIERS, Section BARRIERS-2.3). For the CCA, it was assumed that Salado brine (Brine A) or Castile brine (ERDA-6) would be in equilibrium with brucite and magnesite ($MgCO_3$) in all of the PA vectors (both with and without microbial activity) (ERDA-6). For the 1997 PAVT, equilibria among Salado brine (Brine A) or Castile brine (CCA Appendix SOTERM; CCA Appendix BACK) and brucite and hydromagnesite ($(Mg_5(CO_3)4(O4)_2 \bullet 4H_2O)$) was assumed (EPA 1998a, 1998b).***

The FMT calculations for the CRA-2004 PA also included the effects of acetate, citrate, EDTA, and oxalate on the speciation and solubilities of the +III, +IV, and +V actinides (see Section 5.0 below).

Table SOTERM-2 provides the solubilities calculated for the +III, +IV, and +V actinides and estimated for the +VI oxidation state for the CRA-2004 PA, and compares them to the solubilities calculated or estimated for the CCA PA and the 1997 PAVT.

SOTERM-3.6 Use of ~~FMT~~ *Fracture-Matrix Transport* Results in Performance Assessment

~~Table SOTERM-2 gives the solubilities for each actinide oxidation state analog as calculated with the thermodynamic model and FMT.~~

~~Table SOTERM-2. Solubilities of the Oxidation State Analogs, in moles/liter, with MgO Backfill~~

~~Brine~~	~~PA Parameter Name~~	~~Solubilities for PA Material Name and Oxidation State~~			
		~~SOLMOD3 (III)~~	~~SOLMOD4 (IV)~~	~~SOLMOD5 (V)~~	~~SOLMOD6 (VI*)~~
~~Salado~~	~~SOLSIM~~	~~5.82 x 10^{-7}~~	~~4.4 x 10^{-6}~~	~~2.3 x 10^{-6}~~	~~8.7 x 10^{-6}~~
~~Castile~~	~~SOLCIM~~	~~6.52 x 10^{-8}~~	~~6.0 x 10^{-9}~~	~~2.2 x 10^{-6}~~	~~8.8 x 10^{-6}~~

~~*Not calculated with the FMT model~~

Table SOTERM-2. Actinide Solubilities (M) Calculated (+III, +IV, and +V) or Estimated (+VI) for the CRA-2004 PA, the 1997 PAVT, and the CCA PA

Actinide Oxidation State and Brine	***CRA Solubilities, Microbial Vectors[1]***	***CRA Solubilities, Nonmicrobial Vectors[1]***	***PAVT Solubilities[2]***	***CCA Solubilities[3]***
+III, Salado brine	3.07×10^{-7}	3.07×10^{-7}	1.2×10^{-7}	5.82×10^{-7}
+III, Castile brine	1.69×10^{-7}	1.77×10^{-7}	1.3×10^{-8}	1.3×10^{-8}
+IV, Salado brine	1.19×10^{-8}	1.24×10^{-8}	1.3×10^{-8}	4.4×10^{-6}
+IV, Castile brine	2.47×10^{-8}	5.84×10^{-9}	4.1×10^{-8}	6.0×10^{-9}
+V, Salado brine	1.02×10^{-6}	9.72×10^{-7}	2.4×10^{-7}	2.3×10^{-6}
+V, Castile brine	5.08×10^{-6}	2.13×10^{-5}	4.8×10^{-7}	2.2×10^{-6}
+VI, Salado brine[4]	8.7×10^{-6}	8.7×10^{-6}	8.7×10^{-6}	8.7×10^{-6}
+VI, Castile brine[4]	8.8×10^{-6}	8.8×10^{-6}	8.8×10^{-6}	8.8×10^{-6}

[1] Brush and Xiong (2003a, 2003b) and Downes (2003a, 2003b).

[2] Trovato (1997, Attachment 2), EPA (1998a, Table 5), EPA (1998b, Subsection 4.10.4, Tables 4.10-1, 4.10-3 and 4.10-4; and Subsection 12.4, Table 12.4-1), and EPA (1998c, Subsections 5.26–5.32 and Section 6.0, Table 6.4).

[3] CCA Appendix SOTERM, Table SOTERM-2; based on Novak et al. (1996, Table 1, columns entitled "@Mg"), except that Novak et al. (1996) used molal instead of molar units.

[4] Hobart and Moore (1996).

Uncertainties in the solubility data and ~~uncertainty in~~ the NONLIN least squares refinement result in uncertaint~~y~~***ies*** in the model predictions. This is ~~also~~ evident when the data of Runde and Kim (1994) are compared with FMT model results. A measure of ***these*** uncertaint~~y~~***ies*** was obtained by Bynum (1996) by examining the difference***s*** between the modeled solubilities for each ~~oxidation~~ ***oxidation-***state analog and comparing these to the experimental data used to generate the respective Pitzer parameters. The results of Bynum's analysis ~~is~~ ***are*** given in Figure SOTERM-~~6~~***1***. These results were combined as shown in Figure SOTERM-~~7~~***2*** for entry into the parameter database as a cumulative distribution. This distribution was sampled in ~~performance assessment~~ ***PA,*** as discussed in Section ~~SOTERM.~~7.1.3. Note that the median of this distribution is -0.09 and not zero, indicating that slightly more experimental values were below the model prediction***s*** than above. ~~Table 6-11 in Chapter 6.0 of this application reports the median values, which are 10^{-9} (0.8128) times the model values shown in Table SOTERM-2, for those actinides assigned a distribution of solubilities rather than a constant value.~~

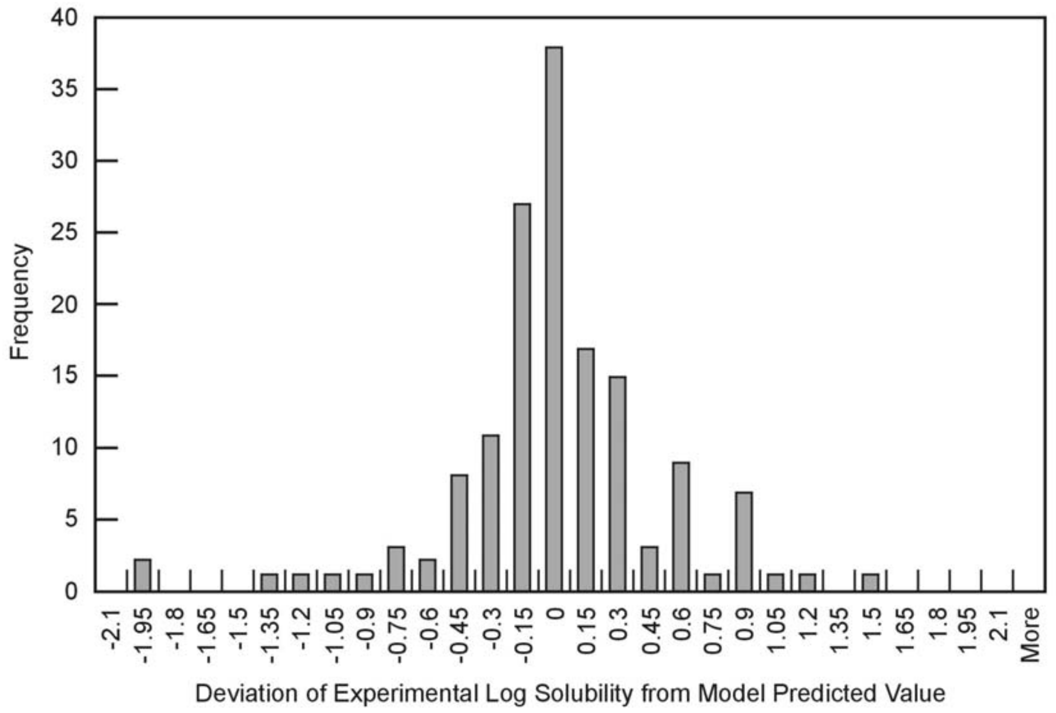

CCA-SOT008-0

Figure SOTERM-~~6~~*1*. Deviation of *the log of* 150 Experimental ~~Log~~ Solubilities from the ~~Model Predicted~~ Values *Predicted by the Model*.

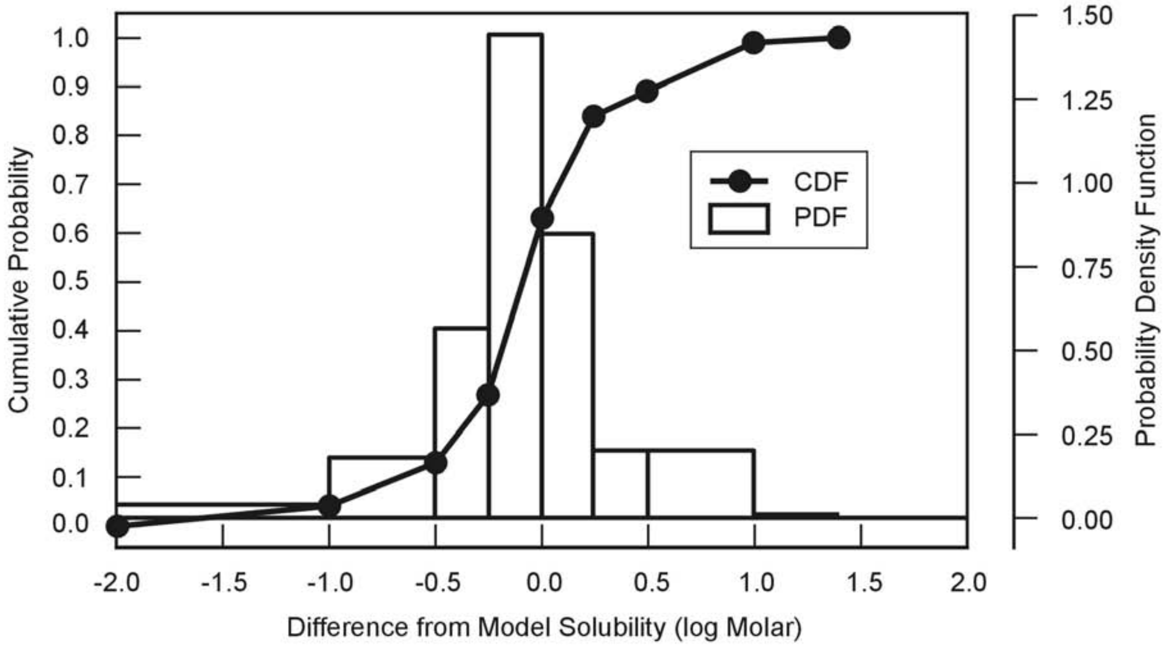

CCA-SOT009-0

Figure SOTERM-~~7~~*2*. Distribution of Actinide-Solubility Uncertainty Utilized ~~by~~ *in the CRA-2004* Performance Assessment.

~~SOTERM.4 Oxidation State Distribution of the Actinides in Solution~~

~~This section describes the literature investigation and experimental program that resulted in identification of the oxidation states of the actinides that may be stable under expected repository conditions. The large quantities of iron in the repository, which will corrode to produce hydrogen and dissolved iron, provide a chemically reducing environment, thereby stabilizing reduced valence states. Microbial metabolism and the presence of organic material will add to this reducing environment.~~

~~SOTERM.4.1 Thorium~~

~~Thorium is known to exist only in the IV oxidation state in the natural environment (Hobart 1990; Katz et al. 1986, 1135, and following; 1486). The standard reduction potential for the Th(IV)/Th(III) couple is very low at -3.8 V. (with the standard hydrogen electrode potential = 0). Therefore, conditions in the inundated WIPP are not expected to produce any other valence state of thorium, nor has one been observed in any of the experiments done in connection with the WIPP Project. Thorium will be stable in the WIPP in oxidation state IV.~~

~~SOTERM.4.2 Uranium~~

~~Uranium can exist in aqueous solution in the III, IV, V, and VI oxidation states (Hobart 1990; Keller 1971; Clark et al. 1995). The dominant valence states for uranium in the natural environment are IV and VI. U(III) is metastable in aqueous solution but is easily oxidized (Katz et al. 1986, 1139, and following), and is difficult to isolate without traces of U(IV). In uranium, with open electronic shell structure~~ ~~$5f^3 6d7s^2$~~~~, the shielding of the 5f electrons is not sufficiently effective for the trivalent state to dominate as it does in the transamericium actinides (Hobart 1990).~~

~~U(V) disproportionates rapidly in aqueous solution by the reaction~~

$$\cancel{2U(V) = U(IV) + U(VI)\ ,} \qquad \cancel{(4\text{-}1)}$$

~~and the reduction-oxidation potential for the U(VI)/U(V) couple is only +0.16 V. U(V)~~ ~~(UO_2^+)~~ ~~is most stable in the pH region 2-4 (Katz et al. 1986, 1144), which is considerably more acidic than anticipated WIPP conditions. U(VI)~~ ~~(UO_2^{2+})~~~~, on the other hand, is quite stable and difficult to reduce. However, in the highly reducing conditions expected in the WIPP, U(VI) may be reduced to U(IV). In experiments in simulated WIPP brines, Reed et al. (1996) have found that at pH 10 under anoxic conditions, U(VI) as a carbonate complex is quite stable. The stable oxidation states of uranium in the WIPP are IV and VI.~~

~~SOTERM.4.3 Neptunium~~

~~In the natural environment, neptunium may exist in oxidation states IV, V, and VI (Hobart 1990; Keller 1971; Clark et al. 1995). In the WIPP environment, Np(IV) is expected to be present (Rai and Strickert 1980; Rai et al. 1982; Kim et al. 1985; Pryke and Rees 1986). Np(V) appears to be the dominant oxidation state in natural groundwater (Hobart 1990). Nitsche and Edelstein (1985) have observed that Np(V) is the most stable state in Yucca Mountain well water. Studies~~

~~of the solubility of NpO_2OH in 1 M and 5 M NaCl solutions at pH 6.5 suggest that Np(V) may be reduced to Np(IV) under these conditions (Kim et al. 1985; Neck et al. 1992). Np(VI) may be introduced into the WIPP or be produced by radiolysis, but its long-term stability is unlikely in the presence of the reducing agents that are expected to be present in the WIPP. The reduction-oxidation potential for the Np(VI)/Np(V) couple in basic solution is +0.6 V (Katz et al. 1986, 470); in neutral solution, +1.24V. (Martinot and Fuger 1985, 651 et seq.). Reed et al. (1996) have found spectroscopic evidence for reduction of Np(VI) to Np(V) in ERDA-6 (Castile) brine at pH 10, and have observed total reduction of Np(VI) to Np(V) in G-Seep (Salado) brine at pH 7. In the presence of oxalate, citrate, and ethylene diamine tetra-acetate (EDTA), Reed et al. (1996) have observed rapid and complete reduction of Np(VI) to Np(V). Neck et al. (1995) have shown Np(V) carbonate complexes to be stable in 5 M NaCl. The stable oxidation states of neptunium in the WIPP are IV and V.~~

~~SOTERM.4.4 Americium~~

~~The trivalent state of americium (AmIII) is the most stable aqueous oxidation state (Katz et al. 1986, 912), and it is quite difficult to oxidize in aqueous solution (Hobart et al. 1982). Am(IV) is unstable, but Am(V) and Am(VI) are accessible under highly oxidizing conditions. These higher oxidation states are not stable in natural waters and can be readily reduced by action of reductants naturally present in those waters. Reduction-oxidation potentials for americium couples (Martinot and Fuger 1985, 660 et seq.) are 2.62 V., 1.20 V. and 1.59 V. for the (IV)/(III), (V)/(IV), and (VI)/(V) couples, respectively.~~

~~As is evident from the relatively high values of the reduction-oxidation potentials, all of the americium oxidation states higher than III can oxidize water and are thermodynamically unstable. The report of Am(V) resulting from radiolytic oxidation of Am(III) in NaCl solution (Runde and Kim 1994) may occur in micro-environments within the WIPP disposal rooms, but would not be stable in the homogeneous mixture of waste and brine. Solubility studies carried out by Pryke and Rees (1986) and Felmy et al. (1990) indicate that Am(V) is unstable in brine above pH 9 and reduces to Am(III). These studies showed significant instability of Am(V) even at pH 7. The large quantities of iron in the repository, as well as the presence of microbes, will result in a highly reducing environment. The MgO backfill in the WIPP will keep the pH in brine that may be in the repository between 9 and 10 (Wang 1996a). The stable oxidation state of americium in brine that may be in the repository is III.~~

~~SOTERM.4.4 Curium~~

~~Curium is distinguished by the relatively great stability of the III oxidation state with respect to oxidation or reduction (Katz et al. 1986, 970). The stability of Cm(III) may be attributed to the half-filled f-shell electronic configuration ($5f^7$). The oxidation of Cm(III) is achieved only with the strongest oxidizing agents, and only one report claims evidence for an oxidation state higher than IV (Korpusov et al. 1975). The Cm(III) to Cm(IV) transition has not been successfully induced by ozone or electrochemically, and the Cm(IV) phosphotungstate produced by oxidizing with peroxysulfate is considerably less stable than the Am(IV) analog (Katz et al. 1986, 971). In the reducing environment of the WIPP repository, any Cm(IV) produced radiolytically would be unstable. The oxidation state of curium therefore expected to be stable in the repository brine is III.~~

~~SOTERM.4.6 Plutonium~~

~~Plutonium can exist in oxidation states III, IV, V, VI, and VII (Katz et al. 1986, 781). Pu(VII) is very unstable and exists only in extremely basic solutions (for example, 7 M NaOH). Thus, Pu(VII) will not be stable in the WIPP environment. Pu(VI) has been shown to form stable chloride complexes (albeit under oxic conditions) in high-ionic strength NaCl solutions (Clark and Tait 1996). However, Clark and Tait (1996) and Reed et al. (1996) have shown the complete reduction of Pu(VI) under expected WIPP repository conditions to Pu(IV), with a transient Pu(V) intermediate, by iron and other reductants.~~

~~Massive quantities of iron metal (approximately 10^9 moles), an effective reductant, will be placed within the repository. An estimate of the amount of iron with respect to the amount of plutonium, for example, can be made on the scale of an average drum; all repository solution chemistry is presumed to occur under average conditions and at equilibrium. Each drum contains on the average about 60 millimoles of Pu. Each drum contains about 170 moles of iron in the container alone – potentially about a 2800-fold excess of iron. The reaction rate of iron with the brine is very fast (Appendix PAR, Parameter 1). Therefore, as any brine moves into the repository it will react with the iron and establish a highly reducing environment, leading to the reduction of plutonium to one of the lower oxidation states.~~

~~As brine enters the repository, iron will undergo anoxic corrosion, producing Fe^{2+}. Both metallic iron (Fe^0) and Fe^{2+} have been shown to quantitatively reduce Pu(VI) in WIPP brines to either Pu(IV) or Pu(III). Clark and Tait (1996) and Felmy et al. (1996) have experimentally observed the reduction of Pu(VI) carbonates by either Fe^0 or Fe^{2+} to Pu(IV). In the absence of carbonates, a quantitative reduction of Pu(VI) is also observed but the determination of the oxidation state of the resulting species cannot be definitively determined due to its concentration being below the lower limit of detection of the oxidation state analytical process (about 10^{-9} molar). However, since the concentration should have been above the analytical detection limit if the plutonium had been in the V state, it is reasonably assumed that the plutonium must have been reduced to either the IV or III oxidation state. Neretnieks (1982) has shown that when dissolved actinides in moving groundwater came in contact with Fe(II), the actinides were reduced to a much less soluble oxidation state and precipitated.~~

~~Pu(III) is not very stable under expected WIPP conditions, but Felmy et al. (1989) have observed Pu(III) in PBB1 and PBB3 brines at neutral and slightly basic conditions. Under highly basic conditions, the plutonium concentration is below the lower limit of detection, and it cannot be conclusively demonstrated that the plutonium remains in the III oxidation state.~~

~~The DOE has determined (Weiner 1996) that Pu(IV) will be the dominant oxidation state under WIPP conditions. Because the existence of Pu (III) cannot be conclusively excluded, it too has been included in the performance assessment.~~

~~SOTERM.4.7 Summary of Oxidation State Distribution~~

~~Table SOTERM-3 presents the oxidation states of the actinides as they are used in performance assessment of the WIPP.~~

~~Table SOTERM.3. Oxidation States of the Actinides in the WIPP As Used in PA~~

~~Actinide Element~~	~~Oxidation States~~			
~~thorium~~		~~IV~~		
~~uranium~~		~~IV~~		~~VI~~
~~neptunium~~		~~IV~~	~~V~~	
~~plutonium~~	~~III~~	~~IV~~		
~~americium~~	~~III~~			
~~curium~~	~~III~~			

SOTERM-4.0 OXIDATION-STATE DISTRIBUTION OF DISSOLVED ACTINIDES

This section describes the literature investigation and experimental program that identified the actinide oxidation states most likely to be stable under expected WIPP conditions.

SOTERM-4.1 Thorium

Th is a very electropositive metal, and Th(IV) is the only stable oxidation state in aqueous solutions and in the natural environment (Hobart 1990; Katz et al. 1986). Conditions in the WIPP cannot produce any other oxidation state of Th.

SOTERM-4.2 Uranium

U can exist in aqueous solution in the +III, +IV, +V, and +VI oxidation states (Hobart 1990; Keller 1971; Clark et al. 1995). The predominant oxidation states for U in the natural environment are +IV and +VI. U(III) may be prepared in aqueous solution but is easily oxidized to U(IV) (Katz et al. 1986, 1139 and following).

The standard reduction potential of U favors reduction of U(V) to U(IV) in aqueous solution, and the pentavalent oxidation state is the least stable oxidation state in solution. U(V) disproportionates in acidic aqueous solution by the reaction:

$$2UO_2^+ + 4H^+ \rightarrow UO_2^{2+} + U^{4+} + 2H_2. \qquad (49)$$

However, the U(VI) species UO_2^{2+} is the most stable in low concentrations in the pH 2 to 4 range (Katz et al. 1986).

It is the disproportionation reaction of U(V) that limits it to trace level concentrations. U(VI) is a stable oxidation state, even under mildly reducing conditions, but may be reduced to U(IV) by a variety of reducing agents. In the chemically reducing environment expected in the WIPP, U(VI) will be reduced to U(IV). However, Reed et al. (1996) found that at pH 10 under anoxic conditions, U(VI) is stable as a CO_3^{2-} complex in simulated WIPP brines. U(IV) is the predominant oxidation state in half of the PA vectors, and U(VI) in the other half, due to uncertainty predicting the more stable oxidation state of U under WIPP conditions.

SOTERM-4.3 Neptunium

In the natural environment, Np may exist in the +IV, +V, and +VI oxidation states (Hobart 1990; Keller 1971; Clark et al. 1995). In the WIPP, Np(IV) is expected to be present (Rai and Strickert 1980; Rai et al. 1982; Kim et al. 1985; Pryke and Rees 1986). Np(V) appears to be the dominant oxidation state in natural groundwater (Hobart 1990). Nitsche and Edelstein (1985) observed that Np(V) is the most stable oxidation state in Yucca Mountain well water. Studies of the solubility of NpO_2OH in 1 M and 5 M NaCl at pH 6.5 suggest that Np(V) may be reduced to Np(IV) under these conditions (Kim et al. 1985; Neck et al. 1992). Np(VI) may be introduced into the WIPP or be produced by radiolysis, but it will not be stable in WIPP brines that contain or are in contact with reducing agents, such as metallic Fe or Fe(II) oxides and hydroxides. The reduction potential for the Np(VI)-Np(V) couple is +1.24 V in neutral solutions (Martinot and Fuger 1985, 651 et seq.) and +0.6 V in basic solutions (Katz et al. 1986, 470), suggesting that the potential for reduction of Np(VI) to Np(V) at a pH of about 9 will be about 1 V. Reed et al. (1996) found spectroscopic evidence for reduction of Np(VI) to Np(V) in ERDA-6 brine at pH 10, and observed total reduction of Np(VI) to Np(V) in G-Seep brine at pH 7. In the presence of organic ligands (see Section 5.0), Reed et al. (1996) observed rapid and complete reduction of Np(VI) to Np(V). Neck et al. (1995) showed Np(V)-CO_3^{2-} complexes to be stable in 5 M NaCl.

In order to capture the uncertainty in the redox speciation of Np, Np(IV) would be the dominant oxidation state in half of the PA vectors and Np(V) in the other half. However, Np is not transported in PA.

SOTERM-4.4 Plutonium

Pu can exist in the +III, +IV, +V, +VI, and +VII oxidation states (Katz et al. 1986, 781). Pu(III) is the favored oxidation state in acidic solutions, but oxidation of Pu(III) to Pu(IV) becomes progressively easier with increasing pH. This occurs because Pu(IV) features a very strong tendency to undergo hydrolysis, which has the effect of reducing the solution concentration of the free Pu(IV) ion Pu^{4+}. As the pH of a Pu solution is raised from acidic to neutral, Pu(IV) begins to precipitate, resulting in a shift of equilibrium concentrations of Pu(III) to Pu(IV). Consequently, Pu(III) is not a thermodynamically stable oxidation state in the basic environment that will be established by MgO in the WIPP (see Reaction (5) above). Although Pu(III) is unstable under expected WIPP conditions, Felmy et al. (1989) observed Pu(III) in PBB1 and PBB3 brines at neutral and slightly basic conditions.

Pu(V) and Pu(VI) can be produced from Pu(IV) under oxidizing conditions. It is not possible to produce Pu(V) by direct oxidation of Pu(IV) because the oxidation potential that must be applied exceeds the potential required for the oxidation of Pu(V) to Pu(VI). Therefore, in a solution with oxidizing conditions, any Pu(V) that arises from the oxidation of Pu(IV) will be immediately oxidized to Pu(VI). Pu(V) can be produced in solution only by first producing Pu(VI), followed by a carefully controlled reduction of Pu(VI) to Pu(V). Pu(V) may persist in neutral to basic solutions even when it is not the thermodynamically stable oxidation state, due to the reduction reaction's inverse fourth power dependence on the concentration of H^+, which can make the reduction of Pu(V) to Pu(IV) kinetically slow. Neither Pu(V) nor Pu(VI) will persist in significant quantities in the repository, since oxidizing conditions are required

to produce them. Pu(VI) was shown to form complexes with Cl^- under oxic conditions in high-ionic-strength NaCl solutions (Clark and Tait 1996). Clark and Tait (1996) and Reed et al. (1996) showed the reduction of Pu(VI) to Pu(IV) by Fe and other reductants under expected WIPP repository conditions. Metallic Fe and Fe^{2+} reduce Pu(VI) in WIPP brines to either Pu(IV) or Pu(III). Clark and Tait (1996) and Felmy et al. (1996) experimentally observed the reduction of Pu(VI)-CO_3^{2-} complexes to Pu(IV) by either metallic Fe or Fe^{2+}. Reduction of Pu(VI) was also observed in the absence of CO_3^{2-}, but the oxidation state of the resulting species was not determined because the concentration was below the analytical detection limit, ca. 10^{-9} M. Neretnieks (1982) showed that dissolved actinides are reduced to a less soluble oxidation state and precipitated from moving groundwater upon coming in contact with Fe(II).

Pu(VII) can be produced in concentrated OH^- solutions that are also highly oxidizing. Pu(VII) will not be formed in the WIPP.

The DOE determined (Weiner 1996) that Pu(IV) will be the dominant oxidation state under WIPP conditions, but the possibility of the existence of Pu(III) cannot be excluded. As a result, Pu is modeled as Pu(III) in half of the PA vectors, and as Pu(IV) in half of the vectors.

SOTERM-4.5 Americium

Am(III) is the most stable aqueous oxidation state of Am (Katz et al. 1986, 912), and will be the only oxidation state of Am in the WIPP. Am(III) is not easily oxidized in aqueous solution (Hobart et al. 1982); however, Am(V) and Am(VI) are accessible at high pH under highly oxidizing conditions. Am(V) and Am(VI) are not stable in natural waters and are readily reduced. Am(V) and Am(VI) can oxidize H_2O, and as a result, they are thermodynamically unstable in aqueous solutions. Am(V) may be formed by oxidation of Am(III) by radiolysis products in NaCl solutions (Runde and Kim 1994), which may occur in microenvironments within WIPP disposal rooms, but Am(V) would not be stable in the homogeneous mixture of waste and brine. Solubility studies carried out by Pryke and Rees (1986) and Felmy et al. (1990) indicated that Am(V) is unstable in brine above pH 9 and reduces to Am(III). These studies also showed significant instability of Am(V) at pH 7. Due to the thermodynamic instability of Am(V) and Am(VI) in aqueous solution, and the lack of a credible mechanism for maintaining the highly oxidizing conditions necessary for persistence of these two oxidation states, Am(III) is the only oxidation state that is used in modeling the speciation and solubility of this element in the repository.

SOTERM-4.6 Curium

Cm is distinguished by the relatively great stability of the +III oxidation state with respect to oxidation or reduction (Katz et al. 1986, 970). The oxidation of Cm(III) is achieved only with the strongest oxidizing agents; one report claims evidence for an oxidation state higher than +IV (Korpusov et al. 1975). The Cm(III)-to-Cm(IV) transition has not been successfully induced by ozone or electrochemically, and the Cm(IV) phosphotungstate produced by oxidizing with peroxysulfate is considerably less stable than the Am(IV) analog (Katz et al. 1986, 971). Cm(III) is the only oxidation state expected to be stable in the WIPP. However, Cm is not transported in PA.

SOTERM-4.7 Summary of Oxidation-State Distributions

Table SOTERM-3 presents the oxidation-state distributions used in the CRA-2004 PA, the CCA PA, and the 1997 PAVT. Np would speciate entirely as Np(IV) in half of the PA vectors and as Np(V) in the other half, but Np is not transported in PA. Cm would speciate identically to Am, but Cm is not transported in PA.

Table SOTERM-3. Actinide Oxidation States Used for the CRA-2004 PA, the 1997 PAVT, and the CCA PA

Actinide Element	Oxidation States			
Th		+IV		
U		+IV		+VI
Pu	+III	+IV		
Am	+III			

SOTERM-4.8 Implications of the Source-Term Waste Test Program for Oxidation-State Distributions of Dissolved Actinides

The Actinide Source Term Waste Test Program (STTP) was an experimental program carried out at Los Alamos National Laboratory (LANL). The objective of the STTP was to examine the behavior of actinides in TRU wastes that will be present in the WIPP. The STTP was conducted by placing samples of various types of wastes from LANL in liter-scale (3-L) and drum-scale (65-gal) titanium (Ti) containers (Scherer and Villarreal 2000, 2001; Scherer et al. 2001a, 2001b, 2001c; Villarreal et al 2000; Villarreal et al. 2001a, 2001b, 2001c, 2001d; Villarreal et al. undated). This discussion focuses on the results from the liter-scale tests.

The samples were composed of process wastes solidified with Portland cement or Envirostone, and pyrochemical salts that resulted from Pu-refining processes. Metallic Fe and Nd, Th, U, Np, and Am were also added. Each waste sample was inundated with about 2 L of either Brine A or ERDA-6.

Pu(V) was identified in two of the liter-scale containers, and Pu(VI) was identified in three of these containers. The DOE's position is that the presence of Fe and other metals within the WIPP will create and sustain a chemically reducing environment in the event of brine intrusion into the waste-disposal areas. The DOE further concludes that Pu will be maintained in the +III or +IV oxidation state due to the reducing conditions. The observance of Pu(V) and Pu(VI) in the STTP tests was noted by the EPA and the New Mexico Environmental Evaluation Group, which led to reexamination of the DOE position that Pu(V) and Pu(VI) are not expected to persist. The LANL reports on the STTP project consist primarily of process descriptions and extensive compilations of experimental data. The reports do not include extensive discussion of the meaning of the data, or explanations based on thermodynamic or kinetic principles.

Oxidized Pu was never observed in 34 of 39 liter-scale containers or in any of the 15 drum-scale containers, strongly supporting the DOE position that Pu will exist in the +III or the +IV

oxidation state under the range of conditions that will exist within the repository. The data tables in the STTP final report are useful for plotting results on a container-by-container basis, to illustrate that in every case in which oxidized Pu was observed, the contents of the containers had not reached either a steady-state behavior or thermodynamic equilibrium. In many cases, first-order kinetic behavior was exhibited for both the solubilization and precipitation of solution components, including Pu. Solubilization of Pu due to oxidation as a consequence of build-up of radiolysis products is not supported by the data. A steady increase in radiolysis products, such as hypochlorite (OCl^-), would result in a steady-state condition of increased Pu(VI) concentrations. The presence of Pu(V) in two containers suggests that a reducing mechanism was available, which led to the reduction of Pu(VI) to Pu(V), followed by a kinetically slow reduction of Pu(V) to Pu(IV). LS-28 and LS-29 were the only two containers that exhibited Pu(VI) in large concentrations that did not decrease over time. However, LS-28 and LS-29 were pressurized with 60 bars of CO_2, and had pcH values about 5 (pH ≈ 4), conditions significantly different from those that will exist in the WIPP.

The STTP containers that were more nearly representative of WIPP conditions support the DOE position that oxidized Pu will not persist in the WIPP. The behavior of Nd, Th, U, Np, and Am in the STTP experiments also supports the DOE position that the solubilities of the actinides will be low in the event of brine influx into the repository.

SOTERM-5.*0* THE ROLE OF ORGANIC LIGANDS

Organic ligands ~~may be a~~ ***are*** ~~component~~ ***present*** ~~of~~ ***in*** the waste~~s~~ to be disposed of in the WIPP. Because organic ligands ~~may~~ ***form dissolved*** complex***es*** with ***the*** actinides***,*** ~~and~~ ***they could*** increase ~~dissolved actinide concentrations~~ ***actinide solubilities.***~~,~~ ***Therefore,*** the effect***s*** of ~~organic~~ ***these*** ~~liquids~~ ***ligands*** ~~was~~ ***have been*** ~~evaluated~~ ***included in the FMT calculations of actinide solubilities for the CRA-2004 PA***. Organic ligands also ***form*** complex***es*** ~~strongly~~ with ~~multivalent~~ ***dissolved, cationic species of several*** metal***s*** ~~cations~~ ***that will be present in the repository***~~.~~***, and thus metals compete*** ~~The multivalent metal cations thereby compete~~ with the actinides ***for the binding sites on these ligands***~~,~~***.*** ~~and an assessment of this~~ ***Therefore, the competitive*** effect***s of dissolved Mg^{2+} and Ca^{2+} have also been*** ~~was performed~~ ***included in the solubility calculations for the CRA-2004 PA***. ~~The analysis, summarized here, demonstrates that organic ligands will not be available to complex the actinides and thus will not impact dissolved actinide concentrations in the WIPP.~~

A number of organic ~~compounds~~ ***ligands*** are capable of forming strong complexes with actinide ions, thereby ~~stabilizing~~ ***increasing*** ~~the~~ ***actinide solubilities*** ~~actinide in solution~~. In general, the reactions that take place for one-to-one complexes are

$$An^{n+} + L^{m-} \rightleftharpoons AnL^{(n+m)} ,$$

~~(5-1)~~***(50)***

where An is a general symbol for an~~y~~ actinide, with charge n, and L is a general symbol for an organic ligand with charge m. The apparent stability constant for this reaction is

$$\beta = [AnL^{(n+m)}]/[An^{n+}][L^{m-}] .$$

~~(5-2)~~***(51)***

The square brackets indicate concentration***s***. Th~~is~~***e*** constant β is ~~sometimes~~ referred to as a~~n~~ ~~association constant~~ ***stoichiometric stability constant. If activities are used instead of concentrations,*** β ***is referred to as the thermodynamic stability constant.***

~~The TWBIR (DOE 1996, Appendix B4) initially identified about 60 organic compounds among the non-radioactive constituents of TRU waste to be emplaced in the WIPP (Drez 1991; Brush 1990). Ten of these compounds have the potential to increase radionuclide solubility (Choppin 1988). Screening studies of these compounds have been conducted by Florida State University. Deprotonation and complexation experiments have been performed with five of these: acetate, citrate, oxalate, lactate, and EDTA. Four of these (acetate, citrate, oxalate, and EDTA) were identified in the waste inventory of the WIPP (DOE 1996, 3-12) as the only water-soluble organic ligands present in significant quantities. Lactate was not included because none was identified in the initial inventory, and estimating its concentration resulting from both production and consumption by microbes is not possible. These organic ligands are capable of significantly enhancing dissolved actinide concentrations, are potentially present in the repository, and are generally representative of any organic ligand that could be present in the WIPP.~~

~~Ligand concentrations in the repository were estimated using inventory amounts of ligands and a brine volume of 29,841~~ ~~m^3~~~~, the smallest quantity of brine required to be in the repository which will support transport away from the repository (Larson 1996). As per the TWBIR, Rev. 2, Page 3-1, a scaling factor of 2.05 was applied to all values. The results are listed in Table SOTERM-4.~~

~~Table SOTERM-4. Organic Ligand Concentrations in Inundated Repository~~

~~Organic Ligand~~	~~Inventory Amount (g)~~	~~Organic Concentration (molality)~~	~~Organic Concentration (scaled)~~
~~acetate~~	~~1.3×10^6~~	~~5.2×10^{-4}~~	~~1.1×10^{-3}~~
~~oxalate~~	~~1.6×10^6~~	~~2.3×10^{-4}~~	~~4.7×10^{-4}~~
~~citrate~~	~~1.4×10^8~~	~~3.6×10^{-3}~~	~~7.4×10^{-3}~~
~~EDTA~~	~~2.3×10^4~~	~~2.0×10^{-6}~~	~~4.2×10^{-6}~~

Four organic ligands are included in FMT calculations of actinide solubilities: acetate $(CH_3CO_2^+)$***, citrate*** $(CH_2CO_2H)_2C(OH)(CO_2))^+$***, ethylenediaminetetraacetate (EDTA,*** $(CH_2CO_2H)_2N(CH_2)_2N(CH_2CO_2H)(CH_2CO_2)^+$***), and oxalate*** $((CO_2H)(CO_2)^+)$***. These ligands are included in the solubility calculations because: (1) approximately 60 organic compounds were identified among the nonradioactive constituents of the TRU waste to be emplaced in the WIPP (Brush 1990; Drez 1991; DOE 1996a, Appendix B); (2) 10 of these 60 organic compounds could, if present in the WIPP, increase actinide solubilities because they are soluble in aqueous solutions such as WIPP brines, and because they form complexes with dissolved actinides (Choppin 1988); and (3) 4 of these 10*** H_2O***-soluble organic ligands that form complexes with actinides (acetate, citrate, EDTA, and oxalate) were identified in the WIPP inventory (DOE 1996a).***

Brush and Xiong (2003d) calculated the current concentrations of acetate, citrate, EDTA, and oxalate in WIPP brines that could be present in the repository after filling and sealing. Brush

and Xiong (2003d) obtained the total masses of acetic acid, Na-acetate, citric acid, Na-citrate, Na-EDTA, oxalic acid, and Na-oxalate in the WIPP inventory (see Appendix Data, Attachment F). Brush and Xiong (2003d) then converted the total masses of each of these organic ligands to total moles, assumed that all these ligands will dissolve in any brine present in the repository after filling and sealing, and divided the total moles of each ligand by 29,841 m^3, "the smallest quantity of brine required to be in the repository [for] transport away from the repository" (Larson 1996). These calculations were carried out identically to those by Brush and Xiong (2003b) for the FMT calculations of actinide solubilities for the CRA-2004 PA, except that Brush and Xiong (2003b) used the masses of ligands reported by Crawford (2003, Table 2, column labeled "Scaled mass (kg)"), not the masses in Appendix Data, Attachment F.

Actinide solubilities were not recalculated using the corrected concentrations of organic ligands from Brush and Xiong (2003d) because the corrections decreased the ligand concentrations slightly. Because the concentrations of these ligands decreased, the actinide solubilities calculated using the uncorrected ligand concentrations of Brush and Xiong (2003b) are slightly higher than they would be if recalculated using the corrected ligand concentrations of Brush and Xiong (2003d).

Table SOTERM-4 provides: (1) the current, corrected concentrations of organic ligands calculated by Brush and Xiong (2003d) based on the masses in Appendix Data, Attachment F; (2) the ligand concentrations calculated by Brush and Xiong (2003b) based on the masses provided by Crawford (2003) (these concentrations were used for the actinide-solubility calculations for the CRA-2004 PA); and (3) the ligand concentrations calculated for the CCA (CCA Appendix SOTERM, Table SOTERM-4) based on the masses of organic ligands provided by DOE (1996a). Mistakes were apparently made in the calculation of the ligand concentrations for the CCA, the most significant of which was the likely transposition of citrate and oxalate in CCA Appendix SOTERM, Table SOTERM-4.

~~Apparent stability constants for organic ligand-actinide complexation and deprotonation constants for the organic acids were determined at Florida State University using potentiometric titration and a solvent extraction technique. The results of these studies are summarized in Table SOTERM-5.~~

~~Complexation constants for each organic-actinide binding reaction were determined using the Pitzer formalism. The NONLIN computer code was used to calculate Pitzer interaction parameters and standard chemical potentials (Moore 1996). The parameters were added to the existing FMT data base for inorganic compounds and equilibrium calculations were performed. In FMT modeling calculations including organic ligands, all four of the water-soluble organic ligands identified in the WIPP inventory were included together at the expected concentrations so that competition among complexing sites could be examined (Novak et al. 1996). Calculations were done separately for Salado and Castile brines, using the brine formulations given by Brush (1990, 17-28). Complexation constants for magnesium with the organic ligands were measured at Florida State University and the results are listed in Table SOTERM-6. These results were included in the calculations so that magnesium (backfill component) competition with the actinides for ligand complexation could be evaluated. The FMT output is the calculated equilibrium solubility of the actinide as a function of the repository conditions.~~

Table SOTERM-4. Concentrations of Organic Ligands in WIPP Brines That Could Be Present in the Repository after Closure

Organic Ligand	*Concentrations Based on Corrected CRA Inventory*[1]	*Concentrations Used in FMT for the CRA-2004 PA*[2]	*CCA*[3]
Acetate	3.56×10^{-3} M	5.05×10^{-3} M	1.1×10^{-3} m
Citrate	2.71×10^{-4} M	3.83×10^{-4} M	7.4×10^{-3} m
EDTA	2.73×10^{-6} M	3.87×10^{-6} M	4.2×10^{-6} m
Oxalate	1.53×10^{-2} M	2.16×10^{-2} M	4.7×10^{-4} m

[1] *Concentrations calculated by Brush and Xiong (2003d) based on the masses of organic ligands in Appendix Data, Attachment F.*

[2] *Concentrations calculated by Brush and Xiong (2003b) based on the masses of organic ligands provided by Crawford (2003).*

[3] *Concentrations calculated for the CCA (CCA Appendix SOTERM, Table SOTERM-4) based on the masses of organic ligands provided by DOE (1996a).*

~~Table SOTERM-5. Apparent Stability Constants for Organic Ligands and Actinides in NaCl Media~~

~~Organic Ligand~~	~~Actinide Ion~~	~~NaCl (molality)~~	~~$\log_{10}$ of Apparent Stability Constant (β)~~
~~Acetate~~	~~Am^{3+}~~	~~0.3 to 5~~	~~1.44 - 2.2~~
	~~Th^{4+}~~	~~0.3 to 5~~	~~3.68 - 4.18~~
	~~NpO_2^+~~	~~0.3 to 5~~	~~1.05 - 1.8~~
	~~UO_2^{2+}~~	~~0.3 to 4~~	~~2.23 - 3.09~~
~~Lactate~~	~~Am^{3+}~~	~~0.3 to 5~~	~~1.75 - 2.55~~
	~~Th^{4+}~~	~~0.3 to 5~~	~~3.83 - 4.28~~
	~~NpO_2^+~~	~~0.2 to 5~~	~~1.43- 1.95~~
	~~UO_2^{2+}~~	~~0.3 to 5~~	~~2.45 - 2.73~~
~~Oxalate~~	~~Am^{3+}~~	~~0.3 to 5~~	~~4.17 - 4.63~~
	~~Th^{4+}~~	~~0.3 to 5~~	~~7.04 - 7.47~~
	~~NpO_2^+~~	~~1.0 to 5.0~~	~~3.62 - 4.63~~
	~~UO_2^{2+}~~	~~0.3 to 5~~	~~5.82 - 6.7~~
~~Citrate~~	~~Am^{3+}~~	~~0.3 to 5~~	~~4.84 - 5.9~~
	~~Th^{4+}~~	~~0.1 to 5~~	~~9.31 - 10.18~~
	~~NpO_2^+~~	~~0.1 to 5~~	~~2.39 - 2.56~~
	~~UO_2^{2+}~~	~~0.3 to 5~~	~~7.07 - 7.32~~
~~EDTA~~	~~Am^{3+}~~	~~0.3 to 5~~	~~13.76 - 15.1~~
	~~Th^{4+}~~	~~0.3 to 5~~	~~15.56 - 16.94~~
	~~NpO_2^+~~	~~0.3 to 5~~	~~5.45 - 6.7~~
	~~UO_2^{2+}~~	~~0.3 to 4~~	~~10.75 - 12.16~~

~~Table SOTERM-6. Apparent Stability Constants for Magnesium Complexation with Organic Ligands at High Ionic Strength~~

~~Organic Ligand~~	~~NaCl (Molality)~~	~~$\log_{10}$ of Apparent Stability Constant~~
~~acetate~~	~~5~~	~~0.690~~
~~oxalate~~	~~5~~	~~2.20~~
~~citrate~~	~~3~~	~~2.02~~
~~EDTA~~	~~5~~	~~6.66~~

Stability constants for complexes between acetate, citrate, EDTA, lactate, and oxalate and the +III, +IV, +V, and +VI actinides (or oxidation-state analogs of these actinides) were determined to incorporate these complexes in the actinide-speciation-and-solubility models described above (see Section 3.4). Stability constants for complexes between these ligands and Mg^{2+} were also determined to include competition between Mg^{2+} and the actinides for the binding sites on these ligands. Choppin et al. (2001) provided the results of all of these experiments. Giambalvo (2002b, 2002e) incorporated these results in the FMT database used for the calculation of actinide solubilities for the CRA-2004 PA. Giambalvo (2003) described this database in detail.

Brush and Xiong (2003a) used FMT, the thermodynamic database described by Giambalvo (2003), and the concentrations of acetate, citrate, EDTA, and oxalate calculated by Brush and Xiong (2003b) to calculate the solubilities of the +III, +IV, and +V actinides for the CRA-2004 PA. (No lactate has ever been identified in the TRU waste to be emplaced in the WIPP.) In the FMT calculations with ligands, all four ligands (acetate, citrate, EDTA, and oxalate) were present simultaneously in Salado or Castile brine at the concentrations calculated by Brush and Xiong (2003b). In these calculations, the stability constants for the complexes formed by these ligands and Ca^{2+} were assigned the same values as the stability complexes formed by these ligands and Mg^{2+} (Giambalvo 2003). However, these calculations did not include competition from dissolved metals such as vanadium (V), chromium (Cr), nickel (Ni), copper (Cu), and lead (Pb), all of which could be present at significant concentrations due to dissolution of steels and other metallic constituents of TRU waste (CCA Appendix SOTERM, SOTERM.5). The results of the FMT calculations for the CRA-2004 PA demonstrate that acetate, citrate, EDTA, and oxalate will not form complexes with the +III and +IV actinides to a significant extent under expected WIPP conditions, and thus will not affect the +III and +IV actinide solubilities significantly (Brush and Xiong 2003d; Downes 2003a, 2003b).

~~As the iron and steel in the repository corrode, additional transition metal ions will dissolve. These ionic species include iron (Fe), nickel (Ni), chromium (Cr), vanadium (V), and manganese (Mn), because the steels used for the waste drums contain on average at least 0.001 weight percent of Ni, Cr, V, and Mn as minor constituents (National Institute of Standards and Technology 1995). Because at least $1.9x10^9$ moles of steels will be disposed of in the WIPP, there should be at least $1x10^4$ moles of Ni, Cr, V, and Mn in the repository. There are also expected to be > $6x10^7$ moles of Pb. Additionally, these and other metals will be present in some of the waste forms; however, these additional quantities in the waste were not considered in this evaluation because insufficient data were available.~~

~~The complexation constants for the various metals cited above with the four representative organic ligands are listed in Table SOTERM-7. To assess the ability of these metals to complex with the organic ligands, competition calculations with EDTA (selected because it is the most strongly complexing of the four organic ligands under consideration) in low ionic strength NaCl solution saturated with iron hydroxide, nickel hydroxide and magnesium oxide (backfill) were performed. The calculations showed that under these conditions 99.8 percent of the EDTA was complexed by Ni, thus effectively rendering the EDTA unavailable for complexation with the actinides and rendering complexation of actinides by organic ligands inconsequential. Although~~

~~these results are approximate because complexation constants for low ionic strength media were used, the fact that a single metal cation could bind more than 99 percent of the EDTA strongly suggests that the full range of metals that will be present will readily overwhelm the complexation sites of the organic ligands. Additionally, at higher ionic strength, iron and nickel have much higher solubility than in dilute solutions. Variation in ionic strength is not expected to change the complexation constants sufficiently to reduce this effect on the organics.~~

~~In addition to the calculations using the HYDRAQL code, simple scoping type equilibrium calculations were performed including several of the expected transition metals. The following equations were solved simultaneously:~~

~~$\beta_{Fe(II)} = [EDTA\text{-}Fe^{2-}] / [EDTA^{4-}] [Fe^{2+}]$~~

~~$\beta_{Ni(II)} = [EDTA\text{-}Ni^{2-}] / [EDTA^{4-}] [Ni^{2+}]$~~

~~$\beta_{Mg(II)} = [EDTA\text{-}Mg^{2-}] / [EDTA^{4-}] [Mg^{2+}]$~~

~~$\beta_{Th(IV)} = [EDTA\text{-}Th] / [EDTA^{4-}] [Th^{4+}]$~~

~~along with mass balance equations for each metal. The nickel concentration of 3.65×10^{-4} used in the calculations was determined by taking the minimum number of moles of nickel expected in the repository, dividing by the available repository volume reported by Weiner (1996) and converting the value to molality. An approximation of 1×10^{-4} molal was chosen for the iron concentration. All other values for component concentrations and apparent stability constants are reported above. To approximate the effect of ionic strength on the apparent stability constants for nickel and iron the values used were an order of magnitude lower than those reported in Table WCA-10. These calculations do not include all possible metal ions expected under repository conditions, for example calcium and chromium are not included. Therefore, these results are considered conservative. The results indicate more than 97 percent of the total EDTA is complexed by the transition metals. Thus the excess of nonradioactive metals present in the repository will overwhelm the complexation sites of the organic ligands and complexation of the organic ligands with actinides will be negligible.~~

~~Table SOTERM-7. Apparent Stability Constants for Organic Ligand with Metals (Martell and Smith 1982, 75, 284, 307, 328).~~

~~Organic Ligand~~	~~Metal~~	~~Ionic Strength (molality)~~	~~log$_{10}$ of Apparent Stability Constant~~
~~EDTA~~	~~Fe^{2+}~~	~~0.1~~	~~14.3~~
	~~Ni^{2+}~~	~~0.1~~	~~13.6~~
	~~Cr^{2+}~~	~~0.1~~	~~18.4~~
	~~Mn^{2+}~~	~~0.1~~	~~13.9~~
	~~V^{2+}~~	~~0.1~~	~~12.7~~
	~~Cu^{2+}~~	~~0.1~~	~~18.9~~
	~~Pb^{2+}~~	~~0.1~~	~~18~~
~~Citrate~~	~~Fe^{2+}~~	~~0.1~~	~~4.4~~
	~~Ni^{2+}~~	~~0.1~~	~~5.4~~
	~~Mn^{2+}~~	~~0.1~~	~~4.15~~
	~~Cu^{2+}~~	~~0.1~~	~~5.9~~
	~~Pb^{2+}~~	~~0.1~~	~~4.08~~
~~Oxalate~~	~~Fe^{2+}~~	~~1.0~~	~~3.05~~
	~~Ni^{2+}~~	~~0.0~~	~~5.16~~
	~~Cr^{2+}~~	~~0.1~~	~~3.85~~
	~~Cu^{2+}~~	~~0.1~~	~~4.84~~
	~~Pb^{2+}~~	~~0.16~~	~~4.00~~
~~Acetate~~	~~Fe^{2+}~~	~~0~~	~~1.4~~
	~~Ni^{2+}~~	~~0~~	~~1.43~~
	~~Cr^{2+}~~	~~0.3~~	~~1.25~~
	~~Mn^{2+}~~	~~0.16~~	~~0.8~~
	~~Cu^{2+}~~	~~0~~	~~2.22~~
	~~Pb^{2+}~~	~~0.1~~	~~2.15~~

SOTERM-6.*0* MOBILE COLLOIDAL ACTINIDE SOURCE TERM

Colloidal particles will be generated in the repository ~~environment~~ as a result of microbial ~~degradation~~ ***consumption*** of cellulosics, ***and*** corrosion of steel waste containers and waste constituents, by the hydrodynamic entrainment of colloidal-sized mineral fragments~~,~~ and several other mechanisms. Those colloidal particles may sorb dissolved actinides or the dissolved actinides themselves may form colloidal~~-sized~~ particles. In an intrusion scenario, actinide-bearing colloidal particles, together with dissolved actinides, may be transported to the Culebra by Castile or Salado brines ~~that are~~ present in the repository. Additional colloidal particles may be present in natural Culebra groundwater and could form additional actinide-bearing colloidal particles. After introduction to the Culebra, the dissolved actinides and actinide-bearing colloidal particles are transported by Culebra ground-waters. Colloidal actinides may also be transported through the fractured anhydrite interbeds of the Salado.

The actinide source term at the WIPP is defined as the sum of contributions from dissolved actinide species and mobile colloidal actinide species. Colloidal actinides that are not suspended in the aqueous phase (that is, not mobile) are not included in the colloidal actinide source term. Sorption of colloidal actinides onto fixed substrates will also reduce the mobile colloidal actinide source term, but no credit is currently being taken for reduction by that means.

In this section, the quantification of the mobile actinide-bearing colloid component of the actinide source term is described. The quantification of colloid-facilitated transport of actinides in the overlying Culebra, in the event of an intrusion into the repository, is described in Chapter 6.0 (Section 6.4.6.2.2) and ***Appendix PA, Attachment MASS, Section MASS-15.3.***

SOTERM-6.1 Introduction

Colloidal particles are generally defined as particles with at least one dimension between 1 nm and 1 µm, suspended in a liquid, and maintained in suspension for very long periods of time by Brownian (random thermal) motion (Hiemenz 1986; Buddemeier and Hunt 1988; Stumm 1992, 1993). Those size boundaries are approximately defined on the basis of physical phenomena. Particles larger than about 1 µm are too large for Brownian motion to overcome gravitational forces, and the particles will rather quickly settle by gravity. An exception is the case of microbes, which are considered to be colloidal, but may exceed 1 µm. The specific gravities of microbes are typically quite close to that of the dispersant, and so they may not settle by gravitational forces. Generally, particles smaller than approximately 1 nm behave in transport like dissolved ionic species.

SOTERM-6.1.1 Formation and Behavior of Colloidal Particles

Inorganic colloidal particles have been reported to form by a variety of processes. Colloidal particles may form by condensation or homogenous nucleation from dissolved species when a mineral phase is supersaturated or as hydrolyzed precipitates of mixed metal ions (Kim 1992). Colloidal particles may also form by release of particles from bulk material due to disruption of fragile aggregates by changes in ionic strength or hydrodynamic forces, dissolution of a more soluble surrounding matrix (Buddemeier and Hunt 1988; Kim 1994), mechanical grinding of mineral surfaces, or mechanical disruption of secondary minerals present at mineral surfaces (McCarthy and Zachara 1989).

Organic colloidal particles may form from microbial ~~degradation~~ ***consumption*** of ***CPR*** materials, condensation reactions of organic molecules to form humic substances, or microb~~e~~***ial*** activity. A variety of naturally occurring organic materials, such as viruses, microbes, and pollen, are colloidal-sized particles (McCarthy and Zachara 1989; Stumm 1992, 243).

Colloidal particles may interact with actinides to form radiocolloids in two ways (see, for example, Lieser et al. 1986a, ***1986***b, 1990; Kim et al. 1984a, ***1984***b; Buddemeier and Hunt 1988; Kim 1992, 1994). First, radiocolloids may form as a result of chemical reactions involving dissolved polyvalent actinide ions. Hydrolysis and condensation reactions have been shown to form actinide macromolecules in which the actinide ions are bridged with hydroxyl ions to form polymers. Those radiocolloids are termed “actinide intrinsic colloids,” “true colloids,” “real colloids,” “Eigenkolloide,” or “type I colloids.”

A second means to form radiocolloids is by sorption of actinides by ordinarily nonradioactive colloidal particles. In the actinide environmental geochemistry literature, the nonradioactive colloidal particle has been called a “groundwater colloid.” Once actinide sorption has occurred, the resulting radiocolloids may be called “pseudo colloids,” “carrier colloids,” “Fremdkolloide,” or “type II colloids.” The colloidal substrate for sorption may be a mineral fragment, a microbial cell, or a humic substance. Bates et al. (1992) recently described radiocolloids, which they called "primary colloids," forming in situ at the surfaces of vitrified radioactive waste as it reacts chemically with ~~water~~ H_2O. Considering that coprecipitation is a continuum with adsorption (see, for example, Comans and Middleburg 1987; Stumm 1992, 253 et seq.), the "primary colloid" can be included in the carrier-colloid category, and more specifically, a mineral-fragment-type colloidal particle. A similar sort of colloid would form by isomorphous lattice substitution of actinide ions during mineral precipitation (that is, coprecipitation) or precipitation of actinide minerals.

In the traditional colloid-chemistry literature, two types of colloidal particles are defined on the basis of how they interact with the dispersant (see, for example, Alexander and Johnson 1949, 114; Vold and Vold 1983; Hirtzel and Rajagopalan 1985; Hiemenz 1986; Ross and Morrison 1988; Hunter 1991-1992). Hydrophobic colloids are stabilized by electrostatic forces, whereas hydrophilic colloids are stabilized by solvation forces. In light of increased knowledge of aqueous surface chemistry gained over the past two decades, the terms hydrophilic and hydrophobic must be used cautiously, because even hydrophobic surfaces have hydrophilic surface functional groups. It is important, however, to make the distinction between how those two types of colloidal particles behave, because they exhibit different kinetic stability behaviors in electrolytes.

Kinetic stability differs from thermodynamic stability. Thermodynamic stability refers to the chemical equilibrium between the colloidal particles and the dispersant, whereas kinetic stability refers to the rate at which colloidal particles in a colloidal dispersion are removed from suspension due to agglomeration followed by gravitational settling. Thermodynamic stability may be most important for actinide intrinsic colloids, because that type of colloid forms directly from solution by chemical reactions. Kinetic stability is inversely related to the rate of particle aggregation, which is dependent on the frequency and efficiency (the fraction resulting in permanent joining) of collisions between colloidal particles. The behavior of colloidal particle types as a function of ionic strength is probably the single most important phenomenon affecting the importance of colloid-facilitated actinide transport at the WIPP.

Hydrophobic colloidal particles are kinetically stabilized and destabilized by electrostatic forces. In an aqueous dispersant, hydrophobic colloidal particles are attracted to one another by van der Waals forces. That electrostatic attraction is countered by repulsive forces generated by a cloud of counterions surrounding each particle (Lyklema 1978; Hiemenz 1986). In a kinetically- stable colloidal dispersion, colloidal particles are usually repelled from one another before they get close enough to become agglomerated. However, as the ionic strength of the dispersion is increased, the thickness of the cloud of counterions is compressed, allowing closer particle-particle interaction. The net effect is that as colloidal particles come into proximity with one another in the dispersion, a greater chance for sticking exists, and so the rate of agglomeration increases. That phenomenon is very effective at removing colloidal particles from suspension even at fairly low ionic strengths over periods of hours to days. Mineral fragments, which are a hydrophobic colloid type, are affected by ionic strength in this way.

Hydrophilic colloidal particles are stabilized by solvation forces, which are largely independent of the ionic strength of the dispersant (Alexander and Johnson 1949). This type of colloidal particle is essentially a dissolved macromolecule. Humic materials are an example of the traditional hydrophilic colloid type. Two major categories of hydrophilic colloidal particles are recognized. Micelles are aggregates of dissolved monomers, that are in thermodynamic equilibrium with those monomers. Polyelectrolytes are charged polymers that are not in thermodynamic equilibrium with a monomeric species (examples of polyelectrolytes include gum arabic, gelatin, pectin, and proteins). An important distinction, therefore, is that micelles require a minimum threshold concentration of monomers (the critical micellization concentration, or c.m.c.) to form. In contrast, the formation of polyelectrolytes is not dependent on monomer concentration. Polyelectrolytes may act as an association colloid by adsorbing on hydrophobic colloidal particles. The resulting dispersions may be extremely kinetically stable (Hiemenz 1986, 659).

The kinetic stability of hydrophobic colloidal particles may be modified by coatings of steric stabilizing compounds, which themselves are essentially hydrophilic materials (also referred to as protective or association colloids) which modify the surface behavior to inhibit close interaction of particles. Such colloidal systems are rendered kinetically stable. Particles stabilized by organic compounds in seawater are an example of a sterically stabilized colloidal system. Microbes can be considered as stabilized in a similar manner, except that the stability is imparted by molecules (for example, polysaccharides), attached to the surface of the microbe, which have hydrophilic parts extending into the dispersant.

Colloidal particles may have rigid or flexible structures, which may affect the way in which they interact with the host rock during transport. "Hard-sphere" colloidal particles, such as mineral fragments, have discrete well-defined boundaries at the particle-~~water~~H_2O interface, and are rigid. "Soft-sphere" colloidal particles, such as humic substances, have less distinct boundaries at the particle-~~water~~H_2O interface, are flexible and may undergo conformational changes in response to environmental variations. "Soft-sphere" colloids are essentially dissolved macromolecules and are closest in form and behavior to particles referred to as hydrophilic colloids in the traditional colloid-chemistry literature (Lyklema 1978; Hiemenz 1986).

SOTERM-6.1.2 Definition of Colloidal Particle Types

On the basis of the phenomena described in the previous section, several classification schemes have been proposed by various workers, and a large number of descriptive terms have evolved and been propagated in the literature. For actinide environmental geochemistry, most of the classification schemes are based on how the colloidal particle interacts with radionuclides. Colloidal particles are classified into the following four types for evaluation of the impact of colloidal particles at the WIPP site:

~~(1)~~. Mineral fragments are hydrophobic, hard-sphere particles, that are kinetically stabilized or destabilized by electrostatic forces, and may consist of crystalline or amorphous solids. Mineral fragments may be made kinetically stable by coatings with steric stabilizers that prevent close contact. Mineral fragments may act as substrates for sorption of actinides or they may consist of precipitated or coprecipitated actinide solids.

~~(2)~~***.*** Actinide intrinsic colloids are macromolecules of actinides that, at least in some cases, may mature into a ~~mineral~~ ***mineral-***~~fragment~~ ***fragment-***type ***of*** colloidal particle. When immature, they are hydrophilic; when mature, they become hydrophobic.

~~(3)~~***.*** Humic substances are hydrophilic, soft-sphere particles~~,~~ that are stabilized by solvation forces. They are often powerful substrates for uptake of metal cations and are relatively small (less than 100,000 atomic mass units).

~~(4)~~***.*** Microbes are relatively large colloidal particles that are stabilized by hydrophilic coatings on their surfaces, which behave as steric stabilizing compounds. They may act as substrates for extracellular actinide sorption or they may actively bioaccumulate actinides intracellularly.

SOTERM-6.2 Performance-Assessment Implementation

Results of the colloidal actinide investigation were used in ~~performance assessment~~ ***the CRA-2004 PA, the CCA PA, and the 1997 PAVT*** in three types of parameter values: (1) constant concentration values; (2) concentration values proportional to the dissolved actinide concentration; and (3) maximum concentration values. The parameter types are summarized below and are described in parameter record packages (Papenguth 1996a, ***1996***b, ***1996***c, ***1996***d).

For actinide intrinsic colloids and mineral-fragment colloids, actinide concentrations associated with them were described as constant values. Table SOTERM-~~8~~***5*** summarizes the material and parameter names and descriptions. ~~As discussed in Appendix PAR (Section PAR.3), IDMTRL is the material name in the INGRES database, and IDPRAM is the parameter name.~~

Experiments conducted to quantify actinide concentrations associated with humic substances and microbes provided the basis for a more sophisticated representation, in which colloidal actinide concent***r***ations were related to the dissolved actinide concentration by proportionality constants. For microbes, the proportionality relationship was made by element. For humic actinides, however, the relationship was made by oxidation state rather than by element. For microbes and humic substances, the experiments also provided a basis to define upper limits for the ~~concentration of~~ actinide ***concentration*** that could be associated with each of those colloid types. For both humic and microbial actinides, the ~~upper~~ ***upper-***limit parameter was defined by element rather than oxidation state, and is in units of molarity. The use of the two ~~upper~~ ***upper-***limit parameters is slightly different, and is described in the sections below discussing humic substances and microbes.

SOTERM-6.3 Development of Parameter Values

In this section, the experimental basis for the parameter values is described. For each of the four ~~colloidal particle~~ types ***of colloids***, the characteristics of the colloidal particle type are described, the experimental program is outlined, methods of interpretation are described, and results are summarized.

Table SOTERM-~~8~~*5*. Material and ~~Parameter~~ *Property* Names for ~~Colloids~~ *Colloidal Parameters*

~~IDMTRL~~*Material*	~~IDPRAM~~*Property*	Brief Description of Parameter
Th, U, Np, Pu, Am	CONCMIN	*C*~~c~~oncentration of actinide associated with mobile mineral fragment colloids
Th, U, Np, Pu, Am	CONCINT	*C*~~c~~oncentration of actinide associated with mobile actinide intrinsic colloids
Th, U, Np, Pu, Am	PROPMIC	*P*~~p~~roportionality constant for concentration of actinides associated with mobile microbes.
PHUMOX3~~[*]~~[1] PHUMOX4 PHUMOX5 PHUMOX6	PHUMCIM	*P*~~p~~roportionality constant for concentration of actinides associated with mobile humic colloids, in Castile brine, actinide solubilities are inorganic only (complexes with man-made organic ligands are not important), solubilities were calculated assuming equilibrium with Mg-bearing minerals (brucite and magnesite);
PHUMOX3~~[*]~~[1] PHUMOX4 PHUMOX5 PHUMOX6	PHUMSIM	*P*~~p~~roportionality constant for concentration of actinides associated with mobile humic colloids, in Salado brine, actinide solubilities are inorganic only (complexes with man-made organic ligands are not important), solubilities were calculated assuming equilibrium with Mg-bearing minerals (brucite and magnesite).
Th, U, Np, Pu , Am	CAPMIC	*M*~~m~~aximum (cap) concentration of actinide associated with mobile microbes;
Th, U, Np, Pu, Am	CAPHUM	*M*~~m~~aximum (cap) concentration of actinide associated with mobile humic colloids.

~~[*]~~[1] Proportionality constant for concentration of actinides associated with mobile humic substances, for PHUMOX3, for actinide elements with oxidation state +***III*** ~~[~~*(*that is, Pu(III) and Am(III)~~]~~*)*; PHUMOX4, oxidation state +***IV*** *(*~~[~~Th(IV), U(IV), Np(IV), and Pu(IV)~~]~~*)*; PHUMOX5, oxidation state +***V*** ~~[~~*(*Np(V)~~]~~*)*; and PHUMOX6, oxidation state +***VI*** ~~[~~*(*U(VI)~~]~~*)*.

SOTERM-6.3.1 ~~Mineral~~ Mineral-Fragment Colloids

~~Mineral~~ ***Mineral-***~~fragment~~ ***fragment-***type colloidal particles may be present in naturally occurring groundwaters, and they may be released from the host rock due to disruption of fragile aggregates by changes in ionic strength or hydrodynamic forces, dissolution of a more soluble surrounding matrix, mechanical grinding of mineral surfaces, or mechanical disruption of secondary minerals present at mineral surfaces. Under certain conditions, such as extreme changes in ionic strength of the groundwater or by physical disruption due to natural or human-induced events, ~~mineral~~ ***mineral-***~~fragment~~ ***fragment-***type colloidal particles could also be produced within the Culebra. In an intrusion scenario at the WIPP, mixing of repository brines with Culebra brines may result in mineral precipitation that may include coprecipitation of actinide-bearing ~~mineral~~ ***mineral-***~~fragment~~ ***fragment-***type colloidal particles. Within the repository, ~~mineral~~ ***mineral-***~~fragment~~ ***fragment-***type colloidal particles may form from corrosion of ~~iron~~***Fe-***bearing waste and the steel packaging materials. In addition, ~~Portland~~ ***Portland-***~~cement~~ ***cement-***based matrixes will be attacked and will produce ~~mineral~~ ***mineral-***~~fragment~~ ***fragment-***type colloidal particles. Bentonite, which may be a constituent of drilling mud is itself a potential source of ~~mineral~~ ***mineral-***~~fragment~~ ***fragment-***type colloidal material that should be considered for actinide transport.

In terms of colloidal actinide transport, ~~mineral~~ ***mineral-*** ~~fragment~~ ***fragment-***type colloids act as carriers, in that actinide ions sorb onto the surfaces of the colloids. Because each mineral substrate has a different affinity for actinides, quantification of actinide concentrations associated with the wide range of mineralogies likely to be present at the WIPP is insurmountable. Instead, a bounding approach was used based on residual concentrations of colloidal particles in WIPP-relevant brines coupled with estimates of reasonable maximum concentrations of actinides that could be sorbed onto the colloid surfaces. That approach requires three pieces of information: (1) the number of ~~mineral~~ ***mineral-*** ~~fragment~~ ***fragment-***type colloidal particles in the aqueous phase; (2) the geometric surface area of individual colloidal particles; and (3) the site-binding capacity of the mineral surface. In the remainder of this section, descriptions of the determination of items (1) through (3), the interpretation of that information, and the development of parameter values are provided.

SOTERM-6.3.1.1 Description of Experiments

Hydrophobic colloidal particles, such as mineral fragments, are kinetically stabilized and destabilized by electrostatic forces (refer to detailed discussion in Papenguth and Behl 1996, Sections 2.5.1 and 2.6). In an aqueous dispersant, hydrophobic colloidal particles are attracted to one another by van der Waals forces. That electrostatic attraction is countered by repulsive forces generated by a cloud of counterions surrounding each particle. In a kinetically stable colloidal dispersion, colloidal particles are usually repelled from one another before they get close enough to become agglomerated. However, as the ionic strength of the dispersion is increased, the thickness of the cloud of counterions is compressed, allowing closer particle-particle interaction. The net effect is that as colloidal particles come into proximity with one another in the dispersion, a greater chance for sticking exists, and so the rate of agglomeration increases. That phenomenon is very effective at removing colloidal particles from suspension even at fairly low ionic strengths over periods of hours to days.

The kinetic stability of the mineral-fragment-type colloids in WIPP-relevant brines was evaluated in ~~coagulation~~ ***coagulation-***series experiments. Colloidal dispersions of mineral fragments were prepared by mechanical disaggregation of representative mineral, rock samples, and other materials or by chemical precipitation from laboratory reagents. Brine simulants were prepared that covered the ranges of ionic strengths observed in WIPP brines. The brines were sequentially diluted with deionized ~~water~~ H_2O by factors of 10 and adjusted to acidic, neutral, and basic pH conditions to evaluate the effects of ionic strength and pH on kinetic stability. At the ionic strength referred to as the critical coagulation concentration (c.c.c.), colloidal particles will rapidly coagulate, forming agglomerates large enough to settle by gravitational forces. The number population of colloidal particles remaining in suspension in the various dispersions was measured over time to assess their stability as a function of solution ionic strength and time.

Colloidal dispersions were prepared for the following minerals or materials: bentonite, kaolinite, montmorillonite, vermiculite, illite, anhydrite, calcium carbonate, magnesite, hematite (mechanically disaggregated), hematite (chemical precipitate), limonite, goethite, magnetite, quartz, siderite, brucite, strontianite, diatomaceous earth, pyrite, and cellulosic materials (Masslinn paper towels and Scott paper towels). The brine solutions used included a Salado-like brine simulant (SPC brine) and a Culebra brine simulant (H-17). For c.c.c. experiments, sequential dilutions of those brines were made that spanned approximately five orders-of-magnitude. Brine simulants consisting of 0.5 M NaCl or $CaCl_2$ were also used. For the residual concentration measurements which were used as the basis for the ~~performance assessment~~ ***CRA-2004 PA, the CCA PA, and the 1997 PAVT*** ~~deliverables described herein~~, the one order-of-magnitude dilution (that is, 10 percent of original strength) of the Salado-like brine and the Culebra brine simulants were used. That reduction in ionic strength provides a degree of conservatism in the results.

The c.c.c. experiments for the various concentrations of WIPP brine simulants were conducted under acidic (observed pH generally ranging from 3 to 4), neutral (pH 6 to 8), and basic (pH 9 to 12) conditions. Following the introduction of an aliquot of dispersed colloidal particles to a series of test tubes containing the sequentially diluted brine, colloidal particle concentrations remaining near the top of the fluid columns (residual concentration) were measured as a function of time. The degree of coagulation and settling was quantified using an inductively coupled argon-plasma atomic emission spectrophotometer, nephelometry, and direct particle counting.

Most of the experiments conducted relating to the kinetic stability of ~~mineral~~ ***mineral-***fragment colloidal particles were qualitative to semiquantitative, and were focused on evaluating whether a c.c.c. existed. For the final experiments, however, a state-of-the-art particle spectrometer was used with significantly greater sensitivity. That device was designed for semiconductor fabrication plants, which require extremely pure processing ~~water~~***H_2O***, and use a similar instrument to ascertain purity. The final experiments were conducted over an extended period of time using the more sensitive analytical technique to determine the number and size of colloids in the brine suspensions. Those experiments were conducted in a similar fashion to previous experiments for bentonite (supplied by the Aldrich Chemical Co.), goethite, and hematite (mechanically disaggregated), but in a relatively dilute (and therefore conservative) brine simulant consisting of 0.1 M NaCl. Residual particle concentrations made with the particle spectrometer compared favorably with measurements made with spectroscopic techniques made at similar experiment times. Generally after the first day of the c.c.c. experiments, the majority (greater than 99 percent) of the colloidal particles had already settled out of suspension. With the more sensitive particle spectrometer, however, residual concentrations of colloidal particles were observed to continue to decrease. For experiments analyzed by spectroscopic or light-scattering techniques, final residual colloid number populations remaining suspended in the test vessels were determined by multiplying the initial colloid number populations determined at the start of the experiments by the fraction of suspended colloids remaining at the final reading. Using the particle spectrometer, final number populations were measured directly.

SOTERM-6.3.1.2 Interpretation and Discussion

Parameter values (CONCMIN) describing the amount of actinide element bound by ~~mineral~~ ***mineral-***~~fragment~~ ***fragment-***type colloidal particles were determined from the information described above, combined with estimates of adsorption**-**site densities.

Actinides sorbed to the surfaces of colloidal particles can be estimated using ranges of values for adsorption**-**site densities taken from published surface complexation modeling research. The actinide concentration contained by a single ~~mineral~~ ***mineral-***~~fragment~~ ***fragment-***type colloidal particle is calculated by considering the geometrical surface area of a spherical particle:

$$[\mathrm{An}]_p = \frac{\pi D^2 N_s}{N_A} , \tag{52}$$

where:

$[\mathrm{An}]_p$ = concentration of an adsorbed actinide element (mol~~es~~/particle)
D = spherical colloidal particle diameter (nm)
N_S = adsorption site density (sites/nm^2)
N_A = Avogadro***'s*** ~~constant~~ ***number.***

An adsorption**-**site density of 1 site/nm^2 was used for N_S in the above equation, a value which is realistic, but probably conservative. With that site density, ~~1~~ **1**-nm**-** and ~~1~~ ***1-***µ~~m -~~-diameter particles could have a maximum of about 10^{-24} and 10^{-18} mol~~es~~ actinide per particle, respectively. To obtain an estimate of the maximum actinide concentrations that could be associated with the colloids, the estimates of residual colloid number populations ~~(particles per liter of dispersion)~~ were multiplied by the estimated maximum actinide**-**transport capacity described by Equation ~~6-1~~ ***(52)***. The use of a uniform adsorption**-**site density is a conservative approach, because the actual sorption on mineral surfaces should be described by some kind of isotherm ~~which~~ ***that*** will result in less than 100 percent coverage. Further, if multivalent adsorbates are present ~~[~~***(***for example, U(VI)~~]~~***),*** multiple adsorption sites may be required for one adsorbate ion, reducing the net adsorption capacity of the surface.

Final residual colloid ~~number~~ populations quantified by spectrophotometry or nephelometry showed that ~~mineral~~ ***mineral-***~~fragment~~ ***fragment-***type colloidal particles are kinetically destabilized by brines similar in composition to those present at the WIPP site. Colloid number population values were, with a few exceptions, reduced to less than 5 percent of the initial values within ~~1~~ ***one*** day. Conservative estimates of maximum actinide concentrations associated with those residual colloid populations are on the order of 10^{-7} to 10^{-9} moles actinide per liter of dispersion.

The final experiments, which utilized the particle spectrometer to measure the quantity of colloids remaining in suspension offered the most sensitive estimates. Moreover, those experiments were conducted for substantially longer periods of time than the semiquantitative c.c.c. experiments. Those experimental results are shown in Table SOTERM-~~9~~***6***.

Table SOTERM-~~9~~*6*. Experimental Results for ~~Mineral~~ *Mineral-*Fragment Colloids

Mineral	Time of Final Reading (days)	Estimated Actinide Concentration (moles/liter dispersion)
~~hematite~~ ***Hematite***	12.8	1.6×10^{-8}
~~goethite~~ ***Goethite***	12.9	9.5×10^{-10}
~~bentonite~~ ***Bentonite***	12.8	1.6×10^{-10}
~~geometric~~ ***Geometric*** mean		1.3×10^{-9}

The DOE believes that the experimental results using the particle spectrometer with the three distinct colloids (hematite, goethite, and bentonite), are representative of other ~~mineral~~ ***mineral-***

~~fragment~~ ***fragment-***type colloidal particles in terms of their behavior in brine solutions. The geometric mean was assumed to be a more representative average of the final colloid concentrations than the arithmetic mean because of the very small final colloid concentrations (which, for this particular case, is also conservative).

~~Mineral~~ ***Mineral-*** ~~fragment~~ ***fragment-***type colloidal particles are unique among the four colloidal particle types addressed for the WIPP, because their concentrations are not generally linked to solubility, as are actinide intrinsic colloids and humic substances, or to a maximum supportable population in the case of microbes. Consequently, in an intrusion scenario at the WIPP, as dissolved actinide elements are introduced to the Culebra, it is possible that those dissolved actinides could sorb onto a separate population of indigenous mineral fragments, producing a supplemental source term. To account for that possibility, the geometric mean value listed above was multiplied by a factor of two, producing a final "most-likely value" of 2.6 ~~x~~***×***10^{-9} moles actinide per liter of dispersion.

To capture uncertainty, mainly stemming from knowledge of the adsorption***-***site density value, a triangular distribution with "minimum values" and "maximum values" spanning one order of magnitude about the geometric mean was provided for ***the*** ~~performance assessment~~ ***CRA-2004 PA, CCA PA, and 1997 PAVT*** calculations. Additional conservatism is incorporated into the mineral***-***fragment***-***parameter values in that the total concentration of actinides carried by mineral fragment colloidal particles have essentially been multiplied by a factor of five, because a separate population of colloidal particles has been assumed for each actinide element. No consideration of competition for sorption sites is incorporated into the calculation***s*** ~~approach~~. The value used for adsorption***-***site density is conservative, but reasonable. For the ~~performance assessment~~ ***PA*** calculations, however, the triangular distribution was not sampled. Instead, the maximum parameter values were used as constant values, which essentially results in a site density of 10 sites/nm^2. Parameter values for CONCMIN are summarized in ~~Section 6.3.5~~ ***Table SOTERM-11***. Section ~~SOTERM-~~7***.0 of this attachment*** discusses details on ~~performance assessement~~ ***PA*** implementation.

SOTERM-6.3.2 Actinide Intrinsic Colloids

Actinide intrinsic colloids (also known as true colloids, real colloids, type I colloids, and Eigenkolloide) form by condensation reactions of hydrolyzed actinide ions and consist solely of actinide cations linked by anions. There are several stages in the development of actinide intrinsic colloids at which they have significantly different behaviors. When immature, actinide intrinsic colloids display physi***c***ochemical properties that are similar to ionized humic substances. With age, they become more similar to mineral ~~fragment~~ ***fragment-***type colloidal particles.

The experimental approach used was strongly influenced by reviews of published literature on actinide intrinsic colloids. Pertinent literature is discussed below (see also Papenguth and Behl 1996).

SOTERM-6.3.2.1 Intrinsic Colloids of Plutonium

The most well-known and well-studied actinide intrinsic colloid is the Pu(IV) intrinsic colloid, which has been used as a basis of comparison for investigating intrinsic colloids of other actinides. Most of the knowledge about the Pu(IV) intrinsic colloid comes from research at high Pu concentrations in highly acidic solutions, which was conducted to help improve the efficiency of processing techniques. The Pu(IV) intrinsic colloid is notorious in its propensity to polymerize to form a gel-like material, which can even plug process lines.

A conclusive demonstration of the mechanisms of formation of the Pu(IV) intrinsic colloid has not yet been made, but there is a preponderance of evidence that suggests that polymerization is strongly linked to hydrolysis, and that the initial polymerization, or condensation, produces a macromolecule that becomes progressively more crystalline with time. The final mature colloid has a composition between $Pu(OH)_4$(am) and PuO_2(c), although the latter compound may be only partly crystalline and both may include interstitial ~~water~~ ***H_2O*** molecules.

The most convincing and consistent explanation for the chemistry of the Pu(IV) intrinsic colloid is presented by Johnson and Toth (1978). Those authors developed a conceptual model to explain the solution chemistry of a variety of metal cations and a variety of oxidation states. The conceptual model involves processes referred to as "olation" and "oxolation" in which metal cations become bridged with hydroxyl groups, which in turn undergo irreversible elimination of ~~water~~ ***H_2O*** and concurrent formation of ~~oxygen~~ ***O*** bridges. Johnson and Toth demonstrate that the model is consistent with the observed behavior of the Pu(IV) intrinsic colloid.

Hydrolysis reactions for metal cations such as Pu may be written as follows:

first: $$Pu^{4+} + H_2O \rightleftharpoons PuOH^{3+} + H^+$$ ~~(6-2)~~***(53)***

second: $$PuOH^{3+} + H_2O \rightleftharpoons Pu(OH)_2^{2+} + H^+$$ ~~(6-3)~~***(54)***

third: $$Pu(OH)_2^{2+} + H_2O \rightleftharpoons Pu(OH)_3^{+} + H^+$$ ~~(6-4)~~***(55)***

fourth: $$Pu(OH)_3^{+} + H_2O \rightleftharpoons Pu(OH)_4\,(aq) + H^+$$ ~~(6-5)~~***(56)***

Johnson and Toth (1978) point out, however, that in interpreting the formation of the Pu(IV) intrinsic colloid, it makes better sense to include the implied waters of hydration that surround metal cations in solution. Hydrolysis Equations ~~6-2~~ ***(53)*** through ~~6-5~~ ***(56)*** can be rewritten as follows, where n equals 4:

first: $$[Pu(H_2O)_m]^{n+} \rightleftharpoons [Pu(OH)(H_2O)_{m-1}]^{n-1} + H^+$$ ~~(6-6)~~***(57)***

second: $$[Pu(H_2O)_{m-1}]^{n-1} \rightleftharpoons [Pu(OH)(H_2O)_{m-2}]^{n-2} + H^+$$ ~~(6-7)~~***(58)***

third: $$[Pu(H_2O)_{m-2}]^{n-2} \rightleftharpoons [Pu(OH)(H_2O)_{m-3}]^{n-3} + H^+$$ ~~(6-8)~~***(59)***

fourth: $[Pu(H_2O)_{m-3}]^{n-3} \rightleftharpoons [Pu(OH)(H_2O)_{m-4}]^{n-4} + H^+$ ~~(6-9)~~***(60)***

From the literature, it is clear that polymerization occurs nearly immediately after the first hydrolysis (Equation ~~6-6~~ ***(57)***) occurs. Johnson and Toth (1978) suggest the following reaction involving polymerization of two hydrolyzed species by loss of ~~water~~ ***H_2O*** (oxolation):

$$2\{[(H_2O)_{d-2}Pu(OH)(H_2O)]^{+(y-1)}\} \rightleftharpoons [(H_2O)_{d-2}Pu(OH)(OH)Pu(H_2O)_{d-2}]^{+2(y-1)} + 2H_2O$$ ~~(6-10)~~***(61)***

Aging or maturation of polymer then occurs by loss of ~~water~~ ***H_2O*** (olation) as follows:

$$[Pu(OH)(OH)Pu(OH)(OH)Pu(OH)(OH)...] \rightleftharpoons [Pu(O)Pu(O)Pu(O)...]_n + 3nH_2$$ ~~(6-11)~~***(62)***

Maiti et al. (1989) and Laul et al. (1985) describe similar reactions, but it appears that they believe that the third hydrolysis reaction occurs, because they use the $Pu(OH)_3^+$ ion in their proposed polymerization reaction. Use of that ion does not appear to be consistent with observations by many workers that polymerization occurs immediately after the first hydrolysis reaction.

As the actinide polyelectrolytes mature through the olation process to become closer in composition to an actinide-oxide mineral, they will be kinetically destabilized by the high ionic strengths of the WIPP brines and will not be mobile. Further, the solubilities of the mature solid phase cannot be exceeded. In fairly long-term experiments, Nitsche et al. (1992, 1994) showed that the concentration of Pu(IV) intrinsic colloid stabilized at about 10^{-8} M. It is not known whether the form was Pu(IV) polyelectrolyte or Pu(IV) ~~mineral~~ ***mineral-*** ~~fragment~~ ***fragment-***type colloid.

SOTERM-6.3.2.2 Intrinsic Colloids of other Actinides

Reference is made to a variety of intrinsic colloids of other actinides, but no systematic investigations of their formation and behaviors appear to have been made. Pu is apparently unique in its propensity to form an intrinsic colloid. No mention is made in the literature of maturation of polyelectrolytes of other actinides to form ~~mineral~~ ***mineral-*** ~~fragment~~ ***fragment-***type colloidal particles as Pu does.

In general, the tendency of actinides to hydrolyze and to polymerize to form intrinsic colloids follows the order:

$$An^{4+} >> An(VI)O_2^{2+} > An^{3+} > An(V)O_2^{+}$$ ~~(6-12)~~***(63)***

(Cleveland 1979a, ***1979***b; Choppin 1983; Kim 1992; Lieser et al. 1991, 119). The order of oxidation states in the equation above results from the ~~ionic~~ ***ionic-*** ~~charge~~ ***charge-*** ~~to~~ ***to-*** ~~ionix~~ ***ionic-***radius ratios. The tendency for hydrolysis of $An(VI)O_2^{2+}$ is greater than for An^{3+} because the effective charge on the central cation on the linear $[O\text{-}An\text{-}O]^{2+}$ ion is 3.3 ± 0.1, slightly greater than 3. This trend generally holds true for the actinide elements~~ in general~~, because of the very small changes in ionic radii among the actinide ~~elements~~ (this is the ~~oxidation~~

oxidation-state analogy; refer to Novak et al. 1996). There are differences in the behaviors of the actinides from element to element that stem from very subtle changes in the ~~charge~~ ***charge-***~~to~~ ***to-***radius ratio and the nature of the configuration of the f molecular orbital.

Considering Pu as an example, hydrolysis becomes significant for Pu^{4+}, $Pu(VI)O_2^{2+}$, Pu^{3+}, and $Pu(V)O_2^{+}$ at pH values of <1, 4-5, 6-8, and 9-10, respectively (Choppin 1983). On the basis of the hydrolysis trend, it is not likely that An(III) and An(V) ~~actinides~~ ***species*** will form actinide intrinsic colloids. There are suggestions in the literature, however, that Am^{3+} may form an intrinsic colloid, which is surprising because it does not undergo hydrolysis until relatively high pH. Th does not follow the trend described by Equation ~~6-12~~ ***(63)*** because its large size makes it resistant to hydrolysis (Cotton and Wilkinson 1988). Nevertheless, thermodynamic data suggest that in almost all environments (near neutral or higher pH) Th exists as $Th(OH)_4(aq)$. Moreover, ~~thorium~~ ***Th*** has been reported to form a polymer (Kraus 1956; Johnson and Toth 1978), although as discussed below, this species should be referred to as an oligomer.

Examples can be found in the literature of polymeric species of many of the actinides of importance to the WIPP (see, for example, Baes and Mesmer 1976; Kim 1992). It is important, however, to note the sizes of polymers described in the literature. It is well known that as polyvalent metals, the actinides can form polynuclear species, but they are largely lower polymers (that is, oligomers) such as dimers, trimers, tetramers, and hexamers (see, for example, Choppin 1983, 46). However, in terms of physical-transport behavior, lower polymers will behave no differently than dissolved monomeric species. In contrast, the higher polymers, such as the Pu(IV)-polymer, may reach colloidal sizes (1 nm to 1 µm) and will have different hydrodynamic properties than the subcolloidal-sized dissolved species. Johnson and Toth (1978) reported a molecular weight of 4000 for a Th polymer. Assuming that it consisted of $Th(OH)_4$, that polymer would consist of about 13 ~~thorium~~ ***Th*** ~~metal~~ ions (that is, the degree of polymerization number, N). That observation is consistent with Kraus (1956), in which he quotes an N value of about 9 for Th polyelectrolyte.

Empirical evidence published in the literature does not always support the suggestion that Am, as a trivalent cation, will form an intrinsic colloidal particle. Avogadro and de Marsily (1984) suggested that, like Pu, Am is a likely candidate to form an insoluble hydroxide. Buckau et al. (1986) reported the formation of Am(III) intrinsic colloids at near neutral pH conditions, with a particle size greater than 1 nm. In their study of the hydrolysis of Am(III) over a pH range from 3 to 13.5, however, Kim et al. (1984a) found only monomers of Am. Regardless of whether Am(III) intrinsic colloids will form under highly idealized laboratory environments, it would be highly unlikely that they would form in a geologic system, because of the tremendously strong sorption properties of the Am(III) ion.

SOTERM-6.3.2.3 Experimental

The ~~focus~~ ***objective*** of experiments, conducted at Lawrence Livermore National Laboratory (LLNL), ~~were~~ ***was*** to test phenomena described in the published literature, under WIPP-relevant conditions:

- critical coagulation concentration for mature Pu(IV) mineral-fragment-type colloid (refer to description of experiment AIC-1 in Papenguth and Behl ~~[~~***(***1996~~]~~***)***)~~,~~***;***

- formation of Pu(IV) colloid, from oversaturation and undersaturation in the absence of CO_2 (AIC-8 and AIC-9, respectively)~~,~~***;***
- inhibition of Pu(IV) polymerization due to organic complexants (AIC-2)~~,~~***;***
- depolymerization of Pu colloid due to organic complexants (AIC-2b)~~,~~***;***
- polyelectrolyte chain termination by nonactinide metal cations (AIC-4)~~,~~***;*** and
- sorption effects of WIPP repository substrates on Pu(IV) colloid (AIC-5).

The last four experiments listed above provide evidence that, under some conditions at the WIPP, the Pu(IV) colloid is less likely to form or is sorbed. To parameterize the ~~WIPP performance assessment~~ ***CRA-2004 PA, CCA PA, and 1997 PAVT*** ~~calculations~~, however, the first two experiments listed above were used. Both sets of experiments (AIC-1, AIC-8/9) can essentially be viewed as solubility experiments. The critical coagulation***-***experiments are solubility experiments conducted from undersaturation conditions, in which the in-growth of free Pu(IV) is observed (and are therefore equivalent to AIC-9). In both sets of experiments (AIC-1, AIC-8/9), the Pu solution concentration is measured as a function of time for as long as five weeks, as steady-state concentration is being reached. The two sets of experiments were anticipated to provide information to resolve the question of kinetic versus thermodynamic stability control on the formation and development of the Pu(IV) colloid. That question was not resolved, but the data still provide the necessary information for parameterizing the ~~WIPP performance assessment~~ ***PA*** calculations. The values for the parameters submitted for calculations were derived from the experiments listed in Table SOTERM-~~10~~*7*.

Table SOTERM-~~10~~*7*. ~~Plutonium~~*Pu* ~~Intrinsic~~ *Intrinsic-*Colloid Experiments

Number	Experiment	Starting Material	pcH approx.	NaCl (~~molality~~)	Duration
AIC-1	c.c.c. (equivalent to undersaturation experiment AIC-9)	Pu(IV) colloid: aged 1 month: about 2 ~~x~~*×* 10^{-4} M	4 7 10	0.001 0.01 0.1 0.8 3.0 5.0	3 to 5 weeks
AIC-8	~~o~~*O*versaturation	Pu(IV) aquo ion: about 1 ~~x~~*×* 10^{-4} M	3 7 10	0.05 0.5 1.0 5.0	4 weeks

The data from those experiments are plotted in Figure SOTERM-~~8~~***3*** along with regression lines for data collected by Rai et al. (1980) for $Pu(OH)_4$(am) and PuO_2 and Rai and Swanson (1981) for Pu(IV) polymer under acidic ~~pH~~ conditions. With MgO ~~backfill~~, the ~~pcH~~ ***pH*** of the

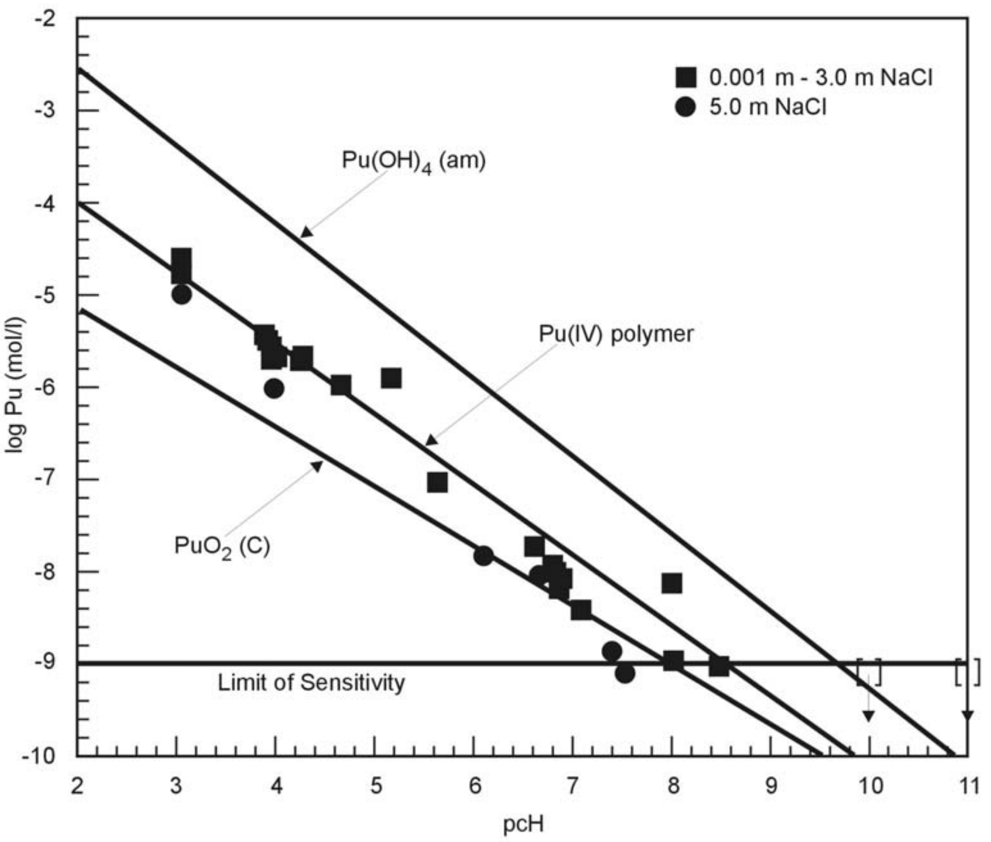

NOTE 1: Open brackets with arrows pointing down indicate Pu concentration is below the minimum analytical detection limit. Solubility lines for Pu(OH)$_{4\text{amorphous}}$ and PuO$_{2\text{crystalline}}$ are extrapolated from Rai et al. (1980). The solubility line for Pu(IV)-polymer is extrapolated from Rai and Swanson (1981). Plotted values were collected at LLNL as part of the WIPP colloid research program.

NOTE 2: Note that under basic pH conditions fixed by MgO, the solubility of the Pu(IV)-polymer is below the minimum analytical detection limit of 10^{-9} M.

CCA-SOT010-0

Figure SOTERM-~~8~~*3*. Solubility of Pu(IV) Polymer in NaCl Media as a Function of pcH.

repository brine is expected to be ***between*** ~~about 9.3~~ ***8.69 and 9.02*** ~~(refer to Wang 1996a; also see Novak and Moore 1996; Siegel 1996)~~ ***(see Section 2.0), equivalent to a pcH of 9.40 to 9.72***. As shown in Figure SOTERM-~~8~~*3*, the regression line calculated from the LLNL data suggests that at a pcH of ~~9.3~~ ***9.40 to 9.72,*** the solubility of Pu(IV)-polymer is ~~approximately 5 x 10^{-10} M. Because the extrapolated solubility is~~ less than the minimum analytical detection limit of 1 x 10^{-9} M~~,~~***. Therefore,*** the ~~minimum analytical~~ detection limit ~~value~~ was selected for use in ~~WIPP performance assessment~~ ***PA*** ~~calculations~~. The LLNL results are consistent with the extrapolated relationships based on published results of Rai et al. (1980) and Rai and Swanson (1981).

SOTERM-6.3.2.4 Interpretation and Discussion

Parameter values (CONCINT) describing the amount of actinide element bound by actinide intrinsic colloidal particles were determined from the information described above. For the Pu(IV) polymer, the minimum analytical detection limit was selected. In the absence of conclusive evidence that intrinsic colloids of other actinides form, or form polymers rather than oligomers, the concentration of Th, U, Np, and Am intrinsic colloids was set to zero.

Geochemical conditions in the Culebra are not conducive to the formation of a new supplementary population of actinide intrinsic colloids. In particular, the concentration of actinide ions is reduced. Therefore, the source term for actinide intrinsic colloids reflects what would form in the WIPP repository, under most favorable conditions for the formation of the Pu(IV) polymer.

Parameter values for CONCINT are summarized in ~~Section SOTERM.6.3.5~~ ***Appendix PA, Attachment SOTERM, Table SOTERM-11***.

SOTERM-6.3.3 Humic Substances

Humic substances are defined as high-molecular-weight organic compounds generally present as anions in natural waters. Humic substances may consist of humic acids, which may be aliphatic or aromatic, or fulvic acids. The difference between humic acids and fulvic acids is largely an operational distinction; humic acids can be precipitated at pH values below about 2, whereas fulvic acids are soluble over the entire pH range. Fulvic acids generally have lower molecular weights than humic acids. The dominant functional group that may react with dissolved actinides are carboxyl groups, but phenolic hydroxyl and alcoholic hydroxyl groups also contribute to complexation. At the WIPP, humic substances may be introduced to the repository as a constituent of soil-bearing waste or may be a constituent of the ~~organic~~ ***organic***-carbon ***(C)*** component of Castile, Salado, or Culebra groundwaters. Probably more importantly, humic substances may form from condensation reactions between microbial metabolites (for example, carboxylic acids), ~~cellulosic degradation products~~ ***byproducts of the consumption of cellulosic materials***, and the extracellular polymers associated with microbes. Because of the general lack of knowledge in the scientific community regarding the formation of humic substances, as well as very slow kinetics of formation, a direct attempt has not been made to quantify the amounts of humic substances that would form in situ. Instead, the contribution of humic-bound actinides was bounded through quantification of humic-actinide complexation behavior coupled with quantification of solubilities of humic substances in WIPP-relevant brines. Regardless of the source of humic substances, the total concentration of humic substance available to mobilize actinides is limited by the solubility of humic substances in WIPP brines. The chemical nature of humic substances generated in situ cannot be predicted either, but can be bounded by the three types of humic substances.

To determine the concentration of actinides associated with humic substances, four pieces of information are required: (1) the concentration of reactive humic substance in the aqueous phase (humic solubility); (2) the binding capacity of the humic substance; (3) actinide uptake (that is, actinide complexation constants); and (4) ~~concentrations of actinide ions in the aqueous phase (that is,~~ actinide solubilit~~y~~***ies***~~)~~. The quantification of actinide solubilities ~~(4)~~ is described in Novak and Moore (1996) and results are summarized in Siegel (1996). In the remainder of this document, the focus is on the determination of items ~~(1)~~ through ~~(3)~~, the interpretation of that information, and the development of parameter values suitable for ~~performance assessment~~ ***the CRA-2004 PA, CCA PA, and 1997 PAVT*** calculations.

SOTERM-6.3.3.1 Experimental

In general, humic substances encompass a broad variety of high-molecular-weight organic compounds. The range of their chemical behaviors, however, is covered by consideration of three types: aliphatic humic acid (generally terrestrial); aromatic humic acid (generally marine); and fulvic acid. The following humic substances were used:

- FA-Suw: fulvic acid isolated from the Suwannee River acquired from the International Humic Substances Society, Golden, Colorado;
- HAal-LBr: aliphatic humic acid isolated from sediments collected from Lake Bradford, Florida, prepared by Florida State University;
- HAal-Ald: aliphatic humic acid purchased from Aldrich Chemical Co., purified by Florida State University;
- HAar-Gor: aromatic humic acid isolated from groundwaters near Gorleben, Germany, obtained from Professor J.-I. Kim, ~~Institut für Radiochemie~~ ***Institute for Radiochemistry***, ~~München~~ ***Munich***; and
- HAar-Suw: aromatic humic acid isolated from the Suwannee River acquired from the International Humic Substances Society, Golden, Colorado.

Solubilities were measured in experiments ~~that were~~ conducted over periods of several weeks. The solubilities of humic substances remaining in the fluid column were determined using a scanning fluorometer, ~~carbon~~ ***C*** coulometer, and UV/Visible light spectrophotometer, in WIPP-relevant brine simulants with FA-Suw, HAal-LBr, HAal-Ald, and HAar-Suw. In addition to spectroscopic data, visible inspection proved valuable. In oversaturation experiments, humic substances were dissolved in deionized ~~water~~ H_2O under basic ~~pH~~ conditions to enhance dissolution and then added as a spike to a brine ~~solution~~. In undersaturation experiments, humic substances were added directly to brine***s*** ~~solutions~~ and allowed to dissolve until ~~an~~ equilibrium was reached. In either case, ~~an~~ equilibrium was reached between dissolved (that is, ionic) and precipitated humic substances. The precipitated humic substances coagulated and settled ~~by gravity~~. The kinetics of precipitation were sufficiently slow that several weeks were required for equilibrium to be reached. Brine***s*** ~~solutions~~ consisted of a NaCl matrix with various concentrations of ~~Ca^{2+} and Mg^{2+}~~ ***Mg^{2+} and Ca^{2+}***. The concentration of Na^+ in the brine had little effect on solubility except at very high concentrations, but the concentration of the divalent cations had a significant impact on humic-substance solubilities. Consequently, experiments were conducted with a NaCl background electrolyte concentration with concentrations of ~~Ca and Mg~~ ***Mg^{2+} and Ca^{2+}*** ranging from 10 mM each (representative of natural WIPP brines) to 500 mM each (representative of ~~a~~ MgO ~~backfill scenario~~). At Sandia National Laboratories ***(SNL)***, solubilities between approximately 1.5 mg/L and 2.0 mg/L were observed in systems containing 10 mM or greater ~~Ca^{2+} and Mg^{2+}~~ ***Mg^{2+} and Ca^{2+}***. For the calculations described below, the higher solubility value of 2.0 mg/L was used.

Site-~~binding~~ ***binding-***capacity values were determined by titration at Florida State University for two humic substances (HAal-LBr and HAal-Ald). Those values were supplemented with values for a variety of humic substances compiled from published literature. In general, site-binding capacities for humic substances are between 3 and 6 meq OH^-/g, but in isolated cases are as low as about 1.5 and as high as about 9.5 meq OH^-/g. For the calculations described below, values of 4.65, 5.38, and 5.56 meq OH^-/g were used for aliphatic humic acid, aromatic humic acid, and fulvic acid, respectively. The aliphatic humic acid value was determined from HAal-LBr at Florida State University. The aromatic humic acid value was from Gorleben (Gohy-573). The fulvic acid value represents the mean of 11 published values for fulvic acids collected in Europe (Ephraim et al. 1995).

Actinide complexation factors for ~~Am(III) and~~ U(VI) ***and Am(III)*** binding on three humic substances (FA-Suw, HAal-LBr, and HAar-Gor) were measured at Florida State University. Complexation measurements were made at measured pH_{obs} values of approximately 4.8 and 6, conditions at which the humic substances are highly deprotonated, and ~~actinides~~ U and Am have not undergone extensive hydrolysis ~~reactions~~. Those conditions were chosen to maximize complexation between the humic substances and those actinide elements. Measurements were made in NaCl media with ionic strengths of approximately 3 and 6 m. These experiments were completed prior to the DOE establishing the position that MgO ~~backfill~~ would be emplaced to sequester CO_2 and fix ~~pcH~~ ***pH*** at about ~~9.3~~ ***9***. The experiments conducted at Florida State University represent conservative conditions designed to provide high-end estimates of actinide uptake by humic substances. Actinide complexation by humic substances generally decreases at basic pH values because of the reduction in actinide-complex charges due to hydrolysis ~~reactions~~. In addition, the high concentrations of Mg^{2+} in solution due to the presence of MgO ~~backfill~~ will compete with actinides for binding sites on humic substances and reduce the actinide uptake. Florida State University reported the first and second stability constants defined as follows (square brackets represent concentration):

$$An + HS \rightleftharpoons AnHS;\ \beta_{1;An} = [AnHS]/[An][HS] \qquad \cancel{(6\text{-}13)}\,\mathbf{(64)}$$

$$An + 2(HS) \rightleftharpoons An(HS)_2;\beta_{2;An} = [An(HS)_2]/[An][HS]^2 \qquad \cancel{(6\text{-}14)}\,\mathbf{(65)}$$

where:

HS = humic substance (eq OH-/L, that is, site-binding capacity incorporated)
An = actinide element
$\beta_{1;An}$ = first stability constant, for 1:1 An:humic binding
$\beta_{2;An}$ = second stability constant, for 1:2 An:humic binding

For the calculations described below, complexation constants were selected from the most relevant experimental conditions, which were pH_{obs} 6 and 6 m~~olal~~ NaCl. The following stability constants reported by Florida State University were used (reported as log values), as shown in Table SOTERM-~~11~~***8***.

Table SOTERM-~~11~~***8***. Humic Substances Experimental Results

Humic Substance	Am^{3+} : β_1	Am^{3+} : β_2	U(VI)O$_2$$^{2+}$: β_1	U(VI)O$_2$$^{2+}$: β_2
HAal-LBr	6.09 +/- 0.05	10.46 +/- 0.12	5.91 +/- 0.16	10.43 +/- 0.19
HAal-Gor	6.02 +/- 0.04	10.40 +/- 0.10	5.35+/- 0.15	8.98 +/- 0.26
FA-Suw	4.6 +/-0.3	8.95 +/- 0.45	~~n~~*N*ot measured	~~not~~ *Not* measured

The Florida State University results show that there is little difference in ~~Am(III) and~~ U(VI)O$_2^{2+}$ ***and Am(III)*** uptake by aliphatic and aromatic humic acids, but that uptake by fulvic acid is significantly less. The Florida State University results also show that an increase of NaCl ionic strength from 3 to 6 has little effect on actinide uptake. Those observations aid in justifying the use of published stability constants for other actinide elements experimentally determined at lower ionic strengths and for other humic substances. On the basis of the similarities in stability constants for ~~Am(III) and~~ U(VI)O$_2^{2+}$ ***and Am(III)*** for the humic acids, ~~Sandia National Laboratories~~ ***SNL*** has used the Am(III) stability constant for FA-Suw for U(VI)O$_2^{2+}$ on FA-Suw.

Stability constants for Th(IV) with several humic and fulvic acids were reported by Nash and Choppin (1980). In NaCl media at pH values between 3.95 and 5.03, those authors reported log stability constants between 9.7 and 13.2. Under ***the mildly*** basic conditions expected in the WIPP repository, it is likely that complexation of Th(IV) will be markedly less, because the dominant Th(IV)-bearing aqueous species will be Th(OH)$_4$(aq) (Novak and Moore 1996). No reports of direct investigations of Th-complex binding on humic substances were found. For the calculations described herein, the published results from Baskaran et al. (1992) describing the distribution of Th(IV) in ~~sea water~~ ***seawater*** were used. From that work, a ratio of dissolved versus colloidal Th(IV) of 6.349 was calculated, assuming that the solubility of colloidal organic material in ~~sea water~~ ***seawater*** is equivalent to our measured value of humic substances in WIPP-relevant brines (that is, 2.0 mg/~~liter~~***L***). The nature of the humic substances is likely to be dominated by aromatic humic acid, but may also contain fulvic acid.

For the calculations described herein, a log stability constant for Np(V)O$_2^+$ of 3.67 measured at pH 9 for a Gorleben humic acid (Gohy-573; Kim and Sekine 1991) was used. Results presented in Rao and Choppin (1995) for Lake Bradford humic acid and a Gorleben humic acid (Gohy-573) show little effect of pH on Np(V) stability constants, presumably because of the ~~lack~~ ***absence*** of ~~hydrolysis of reactions for Np(V)~~ ***Np(V) hydrolosis*** over the pH range ~~those authors~~ studied. The Gorleben humic acid is aromatic in nature.

No published stability constants were found for ~~plutonium~~ ***Pu***. For the calculations described herein, an oxidation-state analogy was used for the ~~plutonium~~ ***Pu*** oxidation species, an approach that is conservative. Allard et al. (1980) have shown that at pH 9, Pu(IV) undergoes hydrolysis ~~reactions~~ to a greater extent than Th(IV), which should result in reduced complexation of Pu(IV).

An oxidation-state analogy was used to develop parameter values for elements expected to have multiple oxidation states in the WIPP repository. ~~Oxidation~~ ***Redox*** speciation of the actinide elements was evaluated as part of the dissolved ~~actinide source term program~~ ***ASTP***. Weiner (1996) ~~has~~ concluded that in the WIPP~~ repository~~, the following species will be present: Th(IV);

U(IV) and U(VI); Np(IV) and Np(V); Pu(III) and Pu(IV); and Am(III). The relative concentrations of ***the*** oxidation ~~species~~ ***states*** of a particular element are designated by their respective solubility values. The substitutions made following the ~~oxidation~~ ***oxidation-***state analogy are summarized in Table SOTERM-~~12~~***9***.

Table SOTERM-~~12~~*9*. Oxidation State Analogy Substitutions

Required Binding Constant	Substitute	Source of Data
Th(IV)	~~n~~*N*one required	Baskaran et al. (1992)
U(IV)	Th(IV)	Baskaran et al. (1992)
U(VI)	~~n~~*N*one required	WIPP-specific data, Florida State University
Np(IV)	Th(IV)	Baskaran et al. (1992)
Np(V)	~~n~~*N*one required	Kim and Sekine (1991)
Pu(III)	Am(III)	WIPP-specific data, Florida State University
Pu(IV)	Th(IV)	Baskaran et al. (1992)
Am(III)	~~n~~*N*one required	WIPP-specific data, Florida State University

To compensate for the effects of competition for actinide complexation by the high concentrations of ~~calcium and magnesium~~ ***Mg^{2+} and Ca^{2+}*** in repository brines in the presence of MgO~~ backfill~~, stability constants for ~~Ca^{2+} and Mg^{2+}~~ ***Mg^{2+} and Ca^{2+}*** were used in simultaneously solved equations (described below). Stability constants for ~~Ca^{2+} and Mg^{2+}~~ ***Mg^{2+} and Ca^{2+}*** at basic pH values are not available, but several published reports provide values in the acidic range. Choppin and Shanbhag (1981) reported log stability constants of 2.25 to 3.32 for Ca^{+} in 0.1 M ***sodium perchlorate (***NaClO$_4$***)*** at pH 3.9 and 5.0 for an aliphatic humic acid (Aldrich humic acid). Schnitzer and Skinner (1967) reported log binding constants ranging from 2.2 to 3.72 for Ca^{2+} in low***-***ionic strength solutions over a pH range of 3.5 to 5.0 for fulvic acid. For Mg^{2+}, Schnitzer and Skinner (1967) reported log stability constants ranging from 1.23 to approximately 2.0 under the same experimental conditions. For the calculations, a log stability constant of 2.0 for the sum of ~~Ca^{2+} and Mg^{2+}~~ ***Mg^{2+} and Ca^{2+}*** concentrations was used, which is a conservative value.

Binding of ~~Ca^{2+} and Mg^{2+}~~ ***Mg^{2+} and Ca^{2+}*** to humic substances is described in the same way as Equation ~~6-13~~ ***(64)*** above:

$$(\cancel{\mathrm{Ca+}}\mathrm{Mg} + \mathit{Ca}) + \mathrm{HS} \rightleftharpoons (\cancel{\mathrm{Ca}}\mathrm{Mg},\mathit{Ca})\mathrm{HS};\ \beta_{1;\cancel{\mathrm{Ca,}}\mathrm{Mg},\mathit{Ca}} = [(\cancel{\mathrm{Ca}}\mathrm{Mg},\mathit{Ca})\mathrm{HS}]/[\cancel{\mathrm{Ca+}}\mathrm{Mg} + \mathit{Ca}][\mathrm{HS}] \qquad \cancel{(6\text{-}15)}(66)$$

where:

$\beta_{1;\cancel{\mathrm{Ca}}\mathrm{Mg},\mathit{Ca}}$ = first stability constant, for 1:1 (~~Ca+~~Mg ***+ Ca***):humic binding (note that no second stability constants exist for ~~divalent~~ ***divalent-***cation binding)***.***

SOTERM-6.3.3.2 Interpretation and Discussion

Proportionality constants (PHUMCIM and PHUMSIM) describing the amount of actinide element bound to humic substances were determined from the data listed above, coupled with dissolved actinide concentrations. In addition, maximum theoretical concentrations of actinides that could be associated with humic substances (CAPHUM) were calculated from the data above.

The concentration of an actinide element of a given oxidation state was calculated by simultaneous solution of Equations ~~6-13~~ ***(64)*** and ~~6-15~~ ***(66)***, combined with a mass-balance expression:

$$[\mathrm{HS_{tot}}] = [\mathrm{AnHS}] + [(\cancel{\mathrm{Ca}}\mathrm{Mg}\boldsymbol{,Ca})\mathrm{HS}] + [\mathrm{HS}] \qquad \cancel{(6\text{-}16)}\boldsymbol{(67)}$$

where:

[HS$_{tot}$] = total concentration of humic substance
[HS] = concentration of uncomplexed humic substance
[AnHS] = concentration of humic complexed with an actinide element
[(CaMg)HS] = concentration of humic complexed with divalent cations.

Equation ~~6-13~~ ***(67)*** describ~~ing~~***es*** the effect of two humic substances binding with one actinide ion was disregarded for these calculations, because its contribution to the total humic-bound actinide concentrations was negligible.

Rearranging Equations ~~6-13~~ ***(64)*** and ~~6-15~~ ***(66)*** provides:

$$[\mathrm{AnHS}] = \beta_{1;\mathrm{An}}\,[\mathrm{An}]\,[\mathrm{HS}]\,, \qquad \cancel{(6\text{-}17)}\boldsymbol{(68)}$$

$$[(\cancel{\mathrm{Ca}}\mathrm{Mg}\boldsymbol{,Ca})\mathrm{HS}] = \beta_{1;\cancel{\mathrm{Ca}}\mathrm{Mg},\boldsymbol{Ca}}\,[\cancel{\mathrm{Ca+}}\mathrm{Mg}\;\boldsymbol{+\;Ca}]\,[\mathrm{HS}]\,. \qquad \cancel{(6\text{-}18)}\boldsymbol{(69)}$$

Substituting Equations ~~6-17~~ ***(68)*** and ~~6-18~~ ***(69)*** into Equation ~~6-16~~ ***(67)*** results in:

$$[\mathrm{HS_{tot}}] = \beta_{1;\mathrm{An}}\,[\mathrm{An}]\,[\mathrm{HS}] + \beta_{1;\,\cancel{\mathrm{Ca}}\mathrm{Mg},\boldsymbol{Ca}}\,[\cancel{\mathrm{Ca+}}\mathrm{Mg}\;\boldsymbol{+\;Ca}]\,[\mathrm{HS}] + [\mathrm{HS}]\,. \qquad \cancel{(6\text{-}19)}\boldsymbol{(70)}$$

Rearranging Equation ~~6-19~~***(70)*** provides:

$$[\mathrm{HS}] = \frac{[\mathrm{HS_{tot}}]}{\beta_{1;\mathrm{An}}[\mathrm{An}] + \beta_{1;\mathrm{CaMg}}[\mathrm{Ca+Mg}] + 1}\,. \qquad \boldsymbol{(71)}$$

Equations ~~6-17, 6-18, and 6-20~~ ***(68), (69), (70), and (71)*** were used to calculate humic-bound actinide concentrations ([AnHS]). The resulting AnHS concentration values were then summed for actinide elements with multiple oxidation states, and then divided by the dissolved concentration of the respective actinide element. The final forms of the parameter values PHUMCIM and PHUMSIM are proportionality constants in units of ~~“~~moles humic-bound colloidal actinide per mole of dissolved actinide.~~”~~ The proportionality values may be multiplied by the dissolved actinide concentration expressed in molarity or molality, depending on the desired final unit.

Depending on the intrusion scenario, the WIPP repository may be dominated by Castile brine or by intergranular Salado brine, resulting in different actinide solubilities, but also different solubilities of ~~Ca^{2+} and Mg^{2+}~~ ***Mg^{2+} and Ca^{2+}***. Under ~~MgO backfill~~ conditions ***characteristic of equilibrium with MgO***, solubility parameters calculated for a system buffered by brucite and magnesite were used (Siegel 1996).

Equations ~~6-17~~ ***(68)***, ~~6-18~~ ***(69)***, and ~~6-20~~ ***(71)*** were used to determine humic-bound actinide concentrations ([AnHS]) for one or more humic substance types for ~~Am(III),~~ Th(IV), ~~Np(V), and~~ U(VI)***, Np(V), and Am(III)***. The ~~oxidation~~ ***oxidation-***state analogy is most heavily utilized for ~~plutonium~~ ***Pu***, because stability constants for Pu(III) or Pu(IV) are not available. Concentrations of ~~Ca^{2+} and Mg^{2+}~~ ***Mg^{2+} and Ca^{2+}*** in Salado and Castile brines ***in equilibrium*** with MgO ~~backfill~~ were obtained from Novak and Moore (1996***)***. In the ~~performance assessment~~ ***PA*** calculations, the humic-bound actinide concentration in the **+**III oxidation state in Castile brine was sampled. All other humic-bound actinide concentrations were held constant.

The PHUMCIM and PHUMSIM parameters, used in conjunction with materials (idmtrls) PHUMOX3, PHUMOX4, PHUMOX5, or PHUMOX6, provide the means to calculate actinide-humic concentrations by actinide oxidation state and for intrusion scenarios involving different brines. For example, in an E1 scenario under ~~"more~~ ***strongly*** reducing~~"~~ conditions in the WIPP repository, PHUMCIM would be used with the following materials (idmtrls) to determine actinide-humic concentrations: ~~thorium~~ ***Th*** = PHUMOX4; ~~uranium~~ ***U*** = PHUMOX4; ~~neptunium~~ ***Np*** = PHUMOX4; ~~plutonium~~ ***Pu*** = PHUMOX3; and ~~americium~~ ***Am*** = PHUMOX3. For an E2 scenario under ***relatively*** less reducing conditions in the WIPP repository, PHUMSIM would be used with the following idmtrls to determine actinide-humic concentrations: ~~thorium~~ ***Th*** = PHUMOX4; ~~uranium~~ ***U*** = PHUMOX6; ~~neptunium~~ **Np** = PHUMOX5; ~~plutonium~~ ***Pu*** = PHUMOX4; and ~~americium~~ ***Am*** = PHUMOX3.

Uncertainties due to analytical precision are small compared to uncertainties in knowledge of the dominant humic substance type, site-binding densities, and actinide solubilities. The proportionality-factor approach coupled with the ~~actinide~~ ***actinide-*** ~~solubility~~ ***solubility-***model uncertainty results in an adequate representation of the uncertainty in the concentration of actinides bound by mobile humic substances.

The CAPHUM parameter simply represents the theoretical maximum concentration of actinides that can be bound by a humic substance. Based on a ~~solubility~~ ***solubility-***limit concentration of humic substances of 2.0 mg/~~liter~~ ***L***, and the highest site-binding capacity (for fulvic acids) of 5.56 meq OH$^-$/g, the theoretical maximum is 1.1 ~~x~~ $\times 10^{-5}$ eq/~~liter~~ ***L***. Assuming the conservative case in which actinide species are monovalent, the maximum theoretical concentration of actinides that can be bound by humic substances is 1.1 ~~x~~ $\times 10^{-5}$ ~~molar~~ ***M***. That number is conservative, because it assumes a pool of humic substances is available for each actinide element, when in reality, actinide elements will compete for the same pool of humic substances. CAPHUM is used in an expression such as the following:

[AnHS] = MIN(AnHS value calculated with proportionality constant, 1.1 ~~x~~ $\times 10^{-5}$) ~~(6-21)~~ ***(72)***

in which the calculated concentration of a particular actinide is compared to the upper-limit value. Parameter values for PHUMCIM, PHUMSIM, and CAPHUM are ~~found in Appendix PAR (Table PAR-39) and Section SOTERM.6.3.5~~ ***summarized in Table SOTERM-11***.

SOTERM-6.3.4 Microbes

Potentially important colloidal-sized microorganisms include bacteria, fungi, yeast, and protozoa. For the WIPP site, the focus is on the halophilic and halotolerant microbes ~~that have been~~ identified at the site (Brush 1990; Francis and Gillow 1994). Microbes are important to consider in ~~performance assessment~~ ***PA***s ~~of the WIPP~~ because they may significantly affect the characteristics of the waste stored at the WIPP, and also participate in transport of actinides. Microbes are known to actively bioaccumulate actinides intracellularly as well as act as substrates for passive extracellular sorption.

At the WIPP site, concentrations of naturally occurring microbes are on the order of 10^4 to 10^7 cells per ~~milliliter~~ ***mL*** (Francis and Gillow 1994, Table 1). In the presence of nutrients provided by WIPP waste constituents, including nitrates, sulfates, and cellulosic***s*** ~~materials~~ such as protective clothing and wood, the population of microbes is likely to increase. Lysis, a natural phenomenon whereby cells die and release their ~~cell~~ constituents to the solution, also provides a source of nutrients to microbes.

When introduced to nutrient***s***, microbes typically follow a predictable growth curve (defined by the population number of microbes plotted as a function of time), consisting of an initial period of inactivity (very early log phase) ranging up to several days, followed by a sharp increase in growth (early log phase). That level of growth is sustained for one or more days (log phase) during which time microbial metabolites, including carboxylic acids, enzymes, and exocellular polymers, are generated. The growth rate eventually begins to decline (late log phase) due to the effects of those metabolites, limitations in nutrients or substrates, or population dynamics, and reaches a steady-state population (stationary phase). Viable microbes may aggregate to form clusters.

SOTERM-6.3.4.1 Description of Experiments

Several types of experiments were conducted to evaluate the impact of microbes in support of the WIPP colloid research program (refer to descriptions in Papenguth and Behl 1996): (1) evaluation of indigenous concentrations of microbes; (2) quantification of mobile concentrations under nutrient- and substrate-rich conditions; (3) quantification and characterization of actinide bioaccumulation by microbes; and (4) evaluation of toxicity effects of actinide elements on microbe growth.

Experiments were conducted at Brookhaven National Laboratory (BNL) and as a collaborative effort between BNL and ~~Los Alamos National Laboratory (~~LANL~~)~~. Evaluation of indigenous concentrations was a collaborative effort between BNL and LANL. Quantification of mobile concentrations was conducted at BNL. The bioaccumulation and toxicity work was conducted at BNL or LANL depending on ***the*** actinide element. ~~Thorium~~ ***Th*** and ~~uranium~~ ***U*** were investigated at BNL. The other actinide elements of interest, ~~neptunium~~ ***Np***, ~~plutonium~~ ***Pu***, and ~~americium~~ ***Am***, were investigated at LANL under the guidance of BNL personnel.

Experiments to determine the mobile concentrations of microbes remaining suspended in the fluid column were conducted similarly to experiments previously conducted in support of the WIPP ~~g~~***G***as ~~g~~***G***eneration ~~p~~***P***rogram (Brush 1990; Francis and Gillow 1994). Bacterial cultures were introduced to a solution containing nutrient and substrate, and sealed. ***The*** ~~B~~***b***acteria***l*** population was monitored over periods of several weeks or more using measurements of optical density or by direct counting of aliquots of fixed cells. An important change in protocol from previous experiments, however, is that instead of filtering the entire contents of the vessels, only the mobile cells remaining suspended in the fluid column were counted. Results of the experiments showed that the mobile concentration of microbes was a couple ***of*** orders-of-magnitude less than the total concentration of microbes. The existence of indigenous microbes in Salado groundwaters has been demonstrated in previous work (Francis and Gillow 1994). As part of the WIPP ~~c~~***C***olloid ~~r~~***R***esearch ~~p~~***P***rogram, samples of Culebra groundwater were carefully collected from the H-19 hydropad, processed, and characterized for indigenous microbes. Concentrations of naturally occurring microbes were on the order of 10^5 cells per ~~milliliter~~ ***mL***, determined using direct counting methods.

The evaluation of indigenous concentrations of microbes and quantification of mobile concentrations provided important supporting evidence for quantifying the microbial actinide source term and for evaluating microbe-facilitated transport of actinides in the Culebra. However, the basis for developing the actual parameter values ~~to be~~ used in ~~performance assessment~~***the CRA-2004 PA, the CCA PA, and the 1997 PAVT*** calculations was established with bioaccumulation and toxicity experiments, referred to herein as filtration experiments. Those experiments were conducted by combining microbe cultures with various concentrations and complexes of ^{232}Th, ^{238}U, ^{237}Np, ^{239}Pu, or ^{243}Am. The actinide reagents used were Th(IV)-NO_3^-, Th(IV)-EDTA, U(VI)-NO_3^-, U(VI)-citrate, Np(V)-EDTA, Pu(V)-HClO4, Pu(V)-EDTA, and Am(III)-EDTA. For those experiments, a pure bacterial culture (WIPP-1A) and a mixed bacterial culture (BAB) were used. Most of the experiments were conducted with the WIPP-1A culture, because of the fast growth of that pure culture. The WIPP-1A mixed culture typically reaches steady-state concentration within several days, whereas the BAB mixed culture requires several weeks. Because of the rapid response of the WIPP-1A culture, most of the experiments were conducted with that culture to expedite the research program. A complementary set of experiments were repeated with the BAB mixed culture~~,~~ to evaluate the representativeness of the pure culture. Experiments were conducted over periods of 11 to 15 days for the WIPP-1A microbe culture, and up to 21 days for the BAB culture. Each experiment consisted of a subset of two or three replicate test vessels~~,~~ that were sampled during the overall test interval~~,~~ to provide ~~time~~ ***time-***sequence data. In addition, replicate test vessels that were not innoculated with microbes were included in each experiment to provide a control. Sequential filtration with 0.~~03~~ ***03-***µm, 0.~~4~~ ***4-***µm, and ~~10~~ ***10-***µm filter***s*** ~~pore sizes~~ was conducted on each vessel. The following size fractions were obtained as shown in Table SOTERM-~~13~~***10***.

Table SOTERM-~~13~~*10*. Microbe Experimental Results

Fluid Column Sample	Particle Size	Actinide Association with
~~n~~*N*ot filtered	all	~~a~~*A*ll forms listed below
0.~~22~~ ***22-µ***m syringe filter, filtrate	< 0.22 µm	~~d~~***D***issolved; lysed microbes
~~10~~ ***10-µ***m filter, filter retentate	> 10 µm	~~c~~***C***lumped microbes
~~10~~ ***10-µ***m filter, filtrate	< 10 µm	~~d~~***D***issolved; dispersed microbes; lysed microbes
0.~~4~~ ***4-µ***m filter, filter retentate	= 0.4 to 10 µm	~~d~~***D***ispersed microbes
0.~~4~~ ***4-µ***m filter, filtrate	< 0.4 µm	~~d~~***D***issolved; lysed microbes
0.~~03~~ ***03-µ***m filter, filter retentate	= 0.03 to 0.4 µm	~~l~~***L***ysed microbes
0.~~03~~ ***03-µ***m filter, filtrate	< 0.03 µm	~~d~~***D***issolved; lysed microbes

In addition to the potential actinide associations listed above, there was some evidence of the formation of inorganic precipitates in some of the experiments. The nutrient used in many experiments was phosphate ~~(1 g~~ PO_4^{3-} ***(1g***/~~liter~~ ***L***), which is known to coprecipitate actinide cations. The inoculated control samples provided the means to evaluate the extent of that experimental artifact. The control samples also provided the means to assess the extent of sorption of actinides onto test vessels, sampling, and filtration equipment. All sequential filters were composed of the same material, which simplifies assessment of sorption on the filtration equipment.

The toxicity experiments were conducted as a component of the filtration experiments described above, by varying the actinide concentration, and comparing growth curves measured by optical density and/or by direct cell counting. To increase the total concentration of actinides in solution, EDTA was added in some experiments in a one-to-one molar ratio with the actinide element. That approach was taken for ~~some Pu experiments, and~~ all of the ***experiments with*** Th, Np, and Am***, and for some of the*** experiments ***with*** Pu.

SOTERM-6.3.4.2 Interpretation and Discussion

Proportionality constants (PROPMIC) describing the amount of actinide element bound to mobile microbes were determined from the data listed above. In addition, maximum concentrations of actinides that could be associated with microbes (CAPMIC) were determined from the experimental data. Those two parameters are suitable for use in ~~performance assessment~~ ***the CRA-2004 PA, CCA PA, and 1997 PAVT*** calculations, when coupled with dissolved actinide solubilit~~y~~***ies*** ~~values~~ (refer to Section ~~SOTERM.~~7.2 for details).

The 0.~~4~~ ***4-***µ~~m~~ ***m-***filter retentate and 0.~~03~~ ***03-***µm filtrate (acquired from the inoculated vessels, not the uninoculated control vessels) were selected to represent the microbial actinide and dissolved actinide concentrations, respectively. The ratio between the microbial actinide and dissolved actinide, both expressed in molarity, represents the proportionality constant value used for the PROPMIC parameter. The 0.~~4~~ **4-**µ~~m~~ ***m-***filter retentate was selected to represent the microbial fraction because nearly all of the bacteria***l*** biomass was associated with that filter. A small concentration of actinides was associated with suspected biomass- trapped on the ~~10~~ ***10-***μm filter, as clumped microbes, and on the 0.~~03~~ ***03-***μm filter, as lysed microbes. The contribution of actinide~~s~~-associated biomass consisting of clumped and lysed microbes was typically at least one order-of-magnitude less than the actinide concentration associated with the dispersed microbes collected on the 0.~~4~~ ***4-***μm filter. The concentration of dissolved actinides measured from the 0.~~03~~ ***03-***~~μm~~ ***m-***filter filtrate was used in the ratio because it provides the best indication of final dissolved actinide concentration. Representative values for PROPMIC were developed on an element-by-element basis. Results of experiments using the BAB culture were disregarded, because of their lower uptake of actinides (especially ~~plutonium~~ ***Pu***), and because of the limited number of experiments conducted with that culture. For the WIPP-1A culture, the first sampling period (2 to 4 days, but generally 3 days) was disregarded in determining proportionality constants because steady state population had not yet been reached. The remaining values were averaged arithmetically.

The filtration experiments discussed above also provided the basis for determining CAPMIC values. Final cell population numbers in the test vessels were estimated using measurements of optical density at a wavelength of 600 nm or by direct counting with epifluorescent microscopy. The magnitude of the toxicity effects was estimated by comparing final cell numbers obtained from a series of test vessels with varying actinide concentration. The ~~direct~~ ***direct-***counting technique provided the most dependable measure of cell number and was used where available. The CAPMIC value is defined as the actinide concentration in molarity at which no growth was observed. For cases where growth clearly diminished as actinide concentration increased, but the actinide concentration was not great enough to stop growth, CAPMIC values were determined by linear extrapolation of population numbers, and then adding an order-of-magnitude to account for uncertainty. On the basis of WIPP experimental results (Papenguth 1996b), it appears that the toxicity effects are due to chemical toxicity rather than radiotoxicity. Because of the high radiation levels of Am and safety considerations in the laboratory facility used, the molar concentration could not be increased to the point at which toxicity effects could be observed. Consequently no CAPMIC value is currently available for Am. CAPMIC values are used similarly to the CAPHUM values (see Equation ~~6-21~~ ***(72)***), except that the upper limit for microbe concentration is due to toxicity rather than geometric limitations imposed by the colloid itself. Consequently, for microbes, the total concentration of mobile actinides in a ~~performance assessment~~ ***PA*** realization is used in the comparison, rather than the amount of actinides associated with the microbes.

The experiments conducted do not provide sufficient information ~~to enable us~~ to formulate a distribution of values for PROPMIC and CAPMIC. Therefore, single values for PROPMIC and CAPMIC ~~are~~ ***were*** used in ~~the performance assessment~~ ***the CRA-2004 PA, the CCA PA, and the 1997 PAVT***. Uncertainties due to analytical precision are small compared to uncertainties in knowledge of the microbe culture that might predominate in the WIPP repository or in the Culebra in an intrusion scenario. The proportionality**-**factor approach coupled with the ~~actinide~~ ***actinide-***~~solubility~~ ***solubility-***model uncertainty results in an adequate description of the uncertainty in the concentration of actinides bound by mobile microbes.

Parameter values for PROPMIC and CAPMIC are summarized in ~~Section SOTERM.6.3.5~~ ***Table SOTERM-11***.

SOTERM-6.3.5 Summary of Parameter Values

Parameter values for CONCMIN, CONCINT, PROPMIC, CAPMIC, PHUMSIM, PHUMCIM, and CAPHUM are summarized in Table SOTERM-~~14~~***11***.

SOTERM-6.4 Summary

Results of the colloidal actinide investigation ~~are~~ ***were*** used in ~~performance assessment~~ ***the 1996 PA, the CRA-2004 PA, and the 1997 PAVT*** in three types of parameter values: (1) ~~constant~~ ***constant-***concentration values for actinides associated with mineral fragment and actinide intrinsic colloids; (2) concentration values proportional to the dissolved actinide concentration for actinides associated with microbes and humic substances; and (3) maximum concentration values providing an upper limit for actinide concentrations associated with microbes and humic substances. The parameter values are summarized in Table SOTERM-~~14~~***11***. Given the actinide solubilities calculated for Salado and Castile brines in ~~the presence of~~ ***equilibrium with*** MgO ~~backfill material~~, the largest contributors to the mobile colloidal actinide source term are actinides associated with humic substances and microbes. The contribution from mineral fragment and actinide intrinsic colloids is comparatively small. More details can be found in the ***SNL WIPP Records Center (formerly referred to as the SNL WIPP Central File,*** SWCF***)*** parameter record packages describing the determination of the mobile colloidal actinide source term (Papenguth 1996a, ***1996***b, ***1996***c, ***1996***d).

Table SOTERM-~~14~~*11*. Colloid Concentration Factors

	CONCMIN Concentration on Mineral Fragments~~[a]~~[*1*]	CONCINT Concentration as Intrinsic Colloid~~[a]~~[*1*]	PROPMIC Proportion Sorbed on Microbes~~[b,c]~~[*2,3*]	CAPMIC Maximum Sorbed on Microbes~~[cd]~~[*4*]	Proportion Sorbed on Humics~~[b]~~[*2*]		CAPHUM Maximum Sorbed on Humics~~[a]~~[*1*]
					PHUMSIM Salado	PHUMCIM Castile	
Th(IV)	2.6×10^{-8}	0.0	3.1	0.0019	6.3	6.3	1.1×10^{-5}
U(IV)	2.6×10^{-8}	0.0	0.0021	0.0021	6.3	6.3	1.1×10^{-5}
U(VI)	2.6×10^{-8}	0.0	0.0021	0.0023	0.12	0.51	1.1×10^{-5}
Np(IV)	2.6×10^{-8}	0.0	12.0	0.0027	6.3	6.3	1.1×10^{-5}
Np(V)	2.6×10^{-8}	0.0	12.0	0.0027	9.1×10^{-4}	7.4×10^{-3}	1.1×10^{-5}
Pu(III)	2.6×10^{-8}	0.0	0.3	6.8×10^{-5}	0.19	1.37~~[d,]~~[e]	1.1×10^{-5}
Pu(IV)	2.6×10^{-8}	1.0×10^{-9}	0.3	6.8×10^{-5}	6.3	6.3	1.1×10^{-5}
Am(III)	2.6×10^{-8}	0.0	3.6	NA	0.19	1.37[d]	1.1×10^{-5}

~~[a]~~[*1*] In units of -moles colloidal actinide per liter

~~[b]~~[*2*] In units of moles colloidal actinide per mole dissolved actinide

~~[c]~~[*3*] ***For the CRA-2004 PA, there were no microbial colloids in nonmicrobial vectors***

~~[c d]~~[*4*] In units of moles total mobile actinide per liter

~~[d e]~~[*5*] A cumulative distribution from 0.065 to 1.60 with a mean value of 1.1 was used

NOTE: The colloidal source term is added to the dissolved source term to arrive at a total source term. Mineral fragments were provided with distributions, but the maximum was used as described in SOTERM-~~-~~7.1.3. Humic proportionality constants for III, IV, and V were provided with distributions, but only the Castile Am(III) and Pu(III) were sampled.

SOTERM-7.***0*** USE OF THE ACTINIDE SOURCE TERM IN PERFORMANCE ASSESSMENT

As described in the preceding sections, the ~~actinide source term program~~ ***ASTP*** provided the parameters that were needed to construct maximum dissolved and suspended colloidal actinide concentrations for use in modeling the mobilization and transport of actinides in the disposal system, as modeled by NUTS and PANEL. Prior to these transport calculations, however, some simplifications and manipulations (using ~~ALGEBRA~~ ***PANEL***) were required as discussed in the following sections.

SOTERM-7.1 Simplifications

The DOE has concentrated on those processes ~~that are~~ most likely to have a significant impact on system performance. Therefore, several simplifications were used in the modeling of radionuclide mobilization in ~~performance assessment~~ ***the CRA-2004 PA, the CCA PA, and the 1997 PAVT*** calculations. These include

- using constant solubility and colloid parameters throughout the repository and regulatory period for a given realization ~~as described in Section SOTERM.2.2~~,
- limiting the number of isotopes modeled to the ones most important to compliance ~~(see Appendix WCA, Section WCA.3)~~,
- using the chemistries of Castile and Salado brines — the end member brines — to bracket the behavior of ~~mixed~~ ***mixtures of these*** brines within the repository,
- sampling only the uncertain parameters having the most significant effect on repository performance***,***
- combining dissolved and colloidal species for transport within the disposal system, as modeled by NUTS and PANEL.

SOTERM-7.1.1 Elements and Isotopes Modeled

Selection of isotopes for modeling transport in the disposal system with NUTS and PANEL is described in Appendix ~~WCA, Section WCA.3~~ ***TRU WASTE, Section TRU WASTE-2.0***. PANEL ~~model~~ runs included nearly all isotopes of the ~~6~~ ***six*** actinides studied in the AST***P*** ~~program~~: ~~Am, Cm, Np, Pu, Th, and U~~ ***Th, U, Np, Pu, Am, and Cm***. NUTS ~~model~~ runs included ~~5~~ ***five*** isotopes: ~~^{238}Pu, ^{239}Pu, ^{241}Am, ^{234}U, and ^{230}Th~~ ***Th, ^{234}U, ^{238}Pu, ^{239}Pu, and ^{241}Am***. ~~The rationale for use of these isotopes is also reported by Garner (1996).~~

SOTERM-7.1.2 Use of Brine End Members

Brine from three sources may enter the repository, depending on the nature of future human intrusion. The general scenarios described in Chapter 6.0 (Section 6.3), and considered in the ~~source~~ ***source-***term calculations may be categorized into three groups: (1) undisturbed performance (UP), (2) intrusion through the repository and into the Castile intersecting a pressurized brine reservoir (E1 and E1E2); and (3) intrusion through the repository but not into a pressurized brine reservoir (E2).

Under all scenarios, brine may flow from the surrounding Salado through the disturbed rock zone (DRZ)~~,~~ and into the repository in response to the ***difference between the*** hydraulic head ~~difference between~~ ***in*** the repository and the surrounding formation. ***For*** scenarios ~~where~~ ***in which*** a borehole is drilled into the repository, brine may flow down the borehole from the Rustler and***/or the*** Dewey Lake. ***For*** scenarios ~~where~~ ***in which*** a pressurized Castile brine reservoir is intercepted, brine from the Castile may flow up the borehole into the repository. As mentioned in Section ~~SOTERM.~~2.2.1, the brines in these three formations have ~~considerably~~ different compositions and the solubilit~~y~~***ies*** of actinides are ~~significantly~~ ***somewhat*** different in each of these ~~end~~ ***end-***member compositions. The composition of the more dilute ~~brines~~ ***groundwaters*** ~~of~~ ***from*** the Rustler and Dewey Lake, however, are expected to change rapidly upon entering the repository due to fast dissolution of host Salado minerals***,*** ~~(~~about ~~93.2~~ ***90-95*** percent halite and about ~~1.7~~ ***1-2*** percent each of polyhalite, gypsum, anhydrite, and magnesite~~;~~ ***(***Brush 1990) from the walls and floor of the repository. ~~EQ3/6 c~~***C***alculations titrating Salado rock into dilute brines ***with the geochemical software package EQ3/6 (Wolery 1992; Wolery and Daveler 1992)*** show that gypsum, anhydrite and magnesite saturate before halite. When halite saturates, the brine composition is very similar to that of Castile brine. One hundred times as much polyhalite must be added to the system before the resulting brine has a composition similar to Salado brines. These calculations indicate that if dilute brines dissolve away only the surfaces of the repository, they will obtain Castile-like compositions, but if they circulate through the Salado after saturating with halite, they may obtain compositions similar to Salado brine. Similarly, if Castile brine circulates through enough host rock, it may also approach ~~Salado~~ ***Salado*** brine composition. In either case, the actual brine within the repository may be described as a mixture of the two ~~concentrated~~ ***concentrated-***brine end members — Salado and Castile. This mixture, however, is very hard to quantify, because it is both temporally and spatially variable. Only in the undisturbed scenario is the mixture well defined as 100 percent Salado brine over the 10,000-year regulatory period.

For a panel intersected by a borehole, the BRAGFLO calculations show that in the 10 percent of the repository represented by the BRAGFLO panel computational cells, the ratio of brine inflow that enters by the borehole versus inflow from the repository walls varies through time and depends on the sampled parameter values and scenario being considered. This ratio was the only measure of brine mixing available to the ~~source~~ ***source-***term ~~ALGEBRA~~ runs in the ~~performance assessment~~ ***CRA-2004 PA, CCA PA, and 1997 PAVT*** calculations. This ratio was quite crude because it (1) did not account for ~~brine~~ composition***al*** changes that occur when ~~water~~ ***H_2O*** was consumed by corrosion reactions, -(2) did not resolve the details of flow, diffusion and brine interaction with internal pillars and the ~~disturbed rock zone (~~DRZ~~)~~, and (3) was an average over one tenth of the repository. It is expected that the fraction of Salado brine will be quite high in areas of the repository distant from the borehole and the fraction will be much lower near the borehole. Because radionuclide travel up the borehole is required for significant release, it is the solubility of radionuclides near the borehole that is most important. Given these uncertainties, the DOE decided to calculate radionuclide solubilities using the Castile ~~end~~ ***end-***member composition for scenarios in which a borehole penetrates a brine reservoir and Salado end-member composition for scenarios where it does not.

*SOTERM-7.1.3 Sampl~~e~~**ing of** Uncertain Parameters*

Distributions of parameter values for up to 30 source-term parameters are available, but many of these are expected to have very limited impact on disposal-system performance. The most important parameters are expected to be the oxidation-state parameter and the solubilities of Pu(III), Pu(IV), and Am(III) in the two brine end members.

A single distribution (Figures SOTERM-~~6~~***1*** and SOTERM-~~7~~***2***) was provided for modeling the solubilit~~y~~***ies*** of all oxidation states of all actinides in both brines. However, the amount of correlation between the solubilities of the actinides was uncertain. Some factors that cause uncertainty in the solubilit~~y~~***ies*** affect all oxidation states of all actinides similarly and some factors will affect only some actinides or some oxidation states. For example, uncertainties in the ~~sulfate~~ SO_4^{2-} concentrations will have more effect in the uncertainty of the solubility of the actinides in the +IV oxidation state, while uncertainties in the ionic strength ha~~s~~***ve*** a more generalized effect of increasing the uncertainty in the stability of any highly charged species. In nature, solubilities show correlation due to ~~reduction-oxidation~~ ***redox*** effects as well as compositional effects. It is therefore expected that solubilities within the WIPP should show some correlation, but not 100 percent correlation.

The use of the ~~end~~ ***end-***member brines in the calculations results in a correlation of solubilities due to ionic strength and ~~major~~ ***major-***ion effects, and the use of the ~~oxidation~~ ***oxidation-***state parameter results in a correlation due to ~~reduction-oxidation~~ ***redox*** effects. The DOE assumes these effects (that is, ionic strength, major ions, and ~~reduction-oxidation~~ ***redox*** state) encompass the major correlations and therefore impose***s*** no further correlations. A better estimate of this correlation would be necessary for more detailed chemical modeling, but for use in ~~performance assessment~~ ***PA***, this ~~decision is not very important~~ ***is unnecessary***. ~~With nine possible element-oxidation state combinations (Am(III), Cm(III), Np(IV), Np(V), Pu(III), Pu(IV), Th(IV), U(IV), and U(VI)), and two brines, a 0 percent correlation implies 18 independent samples of the distribution.~~

The parameters to be sampled were selected based on expectations of their significance of effect on disposal-system performance.

- A 100 percent correlation was made between Am and Cm ~~dissolved~~ solubilities. Only the parameters for Am were sampled, and these were copied for Cm.

- Np solubilities were not sampled because Np does not have a very large EPA unit during the 10,000-year regulatory period (see Appendix ~~WCA, Section.WCA.3~~ ***TRU WASTE, Section TRU WASTE-2.0*** for ***a*** discussion of EPA unit*s* and the relative importance of Np).

- ~~The solubilities of U(IV) and Th(IV) in Castile brine were not sampled because (1) the EPA units of U and Th are only a little larger than the EPA unit of Np during the regulatory period (Garner 1996), and (2) the solubility of the IV oxidation state in Castile brine is low enough that it cannot adversely affect system performance.~~

- The ***parameter for*** actinide concentration on mineral fragment***s*** ~~parameters~~ was not sampled because the concentrations of actinides that may be mobilized on mineral fragments were in most cases much lower that the possible concentrations of dissolved actinides.

- Of the humic-acid proportionality constants, only the one for the +III oxidation state in Castile brine was sampled because it was high and it applied to significant elements (Pu and Am).

Parameters not sampled were fixed at a maximum reasonable value during the calculations.

~~Twelve~~***Fourteen*** parameters were sampled in ~~performance assessment~~ ***the CRA-2004 PA*** for the source term (see Appendix PAR):

Material Name	Parameter Name
SOLAM3	SOLSIM, SOLCIM
SOLPU3	SOLSIM, SOLCIM
SOLPU4	SOLSIM, SOLCIM
SOLU4	SOLSIM***, SOLCIM***
SOLU6	SOLSIM, SOLCIM
SOLTH4	SOLSIM***, SOLCIM***
GLOBAL	OXSTAT
PHUMOX3	PHUMCIM

where

SOLAM3 = distribution parameter for SOLubility of AM(III),
SOLSIM = ~~SOLubility in Salado brine, Inorganic only, $Mg(OH)_2$/$MgCO_3$ *buffer*~~ ***solubility variability in Salado brine***,
SOLCIM = ~~SOLubility in Castile brine, Inorganic only, $Mg(OH)_2$/$MgCO_3$ buffer~~ ***solubility variability in Castile brine***,
OXSTAT = OXidation-STATe parameter,
PHUMOX3 = the Proportionality constant for HUMic colloids and actinides in the +3 OXidation state,
PHUMCIM = the Proportionality constant for HUMic colloids in Castile brine.~~, Inorganic only, $Mg(OH)_2$/$MgCO_3$ buffer.~~

In the CCA PA and the 1997 PAVT, 12 parameters were sampled (all of the 14 parameters listed above except SOLU4, SOLCIM; and SOLTH4, SOLCIM).

SOTERM-7.1.4 Combining the Transport of Dissolved and Colloidal Species in the Salado

Dissolved and colloidal species may transport differently because of different diffusion rates, sorption onto stationary materials, and size exclusion effects (filtration and hydrodynamic chromatography). With maximum molecular diffusion coefficients of about 4 ~~x~~ × 10^{-10} m~~eters~~^{2} ~~squared~~ per s~~econd~~, actinides are estimated to diffuse about 10 m~~eters~~ in 10,000 years, a negligible distance. Sorption and filtration have beneficial but unquantifiable effects on performance. Hydrodynamic chromatography may increase colloid transport over dissolved transport by at most a factor of ~~2~~ ***two*** for theoretically perfect colloid***al*** transport conditions. In real situations, the increase is much less. Given the small or beneficial nature of these effects, ~~the DOE did not model them~~ ***they were not included*** in ~~performance assessment~~ ***the CRA-2004 PA, the CCA PA and the 1997 PAVT*** calculations of radionuclide transport ***in the repository***.

Because there was no modeled mechanism to differentiate dissolved from colloidal species, the DOE combined them for transport within the Salado. In the modeling of transport within the Culebra, however, these simplifications were ~~not~~ ***in***appropriate. While transport within the repository is through at most hundreds of meters of poorly defined waste that is undergoing decomposition, transport through the Culebra is over kilometers in a relatively homogeneous (as compared to waste) fractured dolomite. ~~Diffusion of radionuclides into, and sorption on, a dolomite matrix have been shown by sensitivity analysis (WIPP Performance Assessment Department 1992) to be processes important in performance assessment.~~ ***Dissolved and colloidal species could be transported differently through the Culebra.*** Therefore, the mobilized actinide**s** delivered to the Culebra by Salado transport codes ~~was~~ **are** separated into ~~its~~ five ~~species~~ ***components*** (dissolved, humic, microb~~e~~***ial***, ~~mineral~~ ***mineral-***fragment, ***and*** intrinsic colloid***s***).

SOTERM-7.2 Construction of Source Term

The parameters required for constructing the source term were (1) ~~modeled~~ solubilities for four oxidation states in each brine end member, (2) a***n uncertainty*** distribution to be ~~used around the~~ ***applied to the*** ~~modeled~~ solubilit~~y~~***ies*** ~~values~~, (3) a scheme for assigning sampled ~~dominant~~ oxidation states, (4) colloidal concentrations or proportionality constants for the ~~5~~ ***five*** actinides or the ~~4~~ ***four*** oxidation states for each of four ~~colloid~~ types ***of colloids***, and (5) caps on the actinide concentrations that may be ~~carried on~~ ***applied to*** two ~~colloid~~ types ***of colloids***. Use of these parameters in the ~~performance assessment~~ ***CRA-2004 PA, the CCA PA, and the 1997 PAVT*** calculations required combining the~~se~~***m*** into a single ~~effective solubility or~~ maximum concentration for each modeled actinide. The term ~~effective solubility~~ ***"total mobilized concentration"*** is used for the ~~maximum~~ combined ~~mobilized actinide~~ concentration***s*** due to dissolved and colloidal species~~, because the NUTS and PANEL codes use these numbers for each actinide as if they were solubilities~~. The ~~maximum~~ ***combined concentrations*** ~~is~~ ***are*** not ***necessarily*** the ~~maximum of the distribution~~ ***actual concentrations***, ~~but is called the maximum~~ because the concentration may be lower due to inventory limits. Both NUTS and PANEL assume that the ***concentrations of*** actinides ***specified by the total mobilized concentration*** ~~instantly~~ ***are attained instantaneously*** ~~mobilize up to this effective solubility limit~~ as long as sufficient inventory is available~~ in the computational cell for this to occur~~. When the inventory is ~~not~~ ***in***sufficient, the actual mobilized concentration will be lower and is said to be inventory limited. The calculation of the ~~effective solubilities~~ ***total mobilized concentration*** ~~was~~ ***is*** performed ~~prior to NUTS and~~ **by** PANEL ~~using ALGEBRA~~, for each of 100 sampled ~~realizations~~ ***vectors in a replicate***,~~. as shown in Figure SOTERM-9.~~

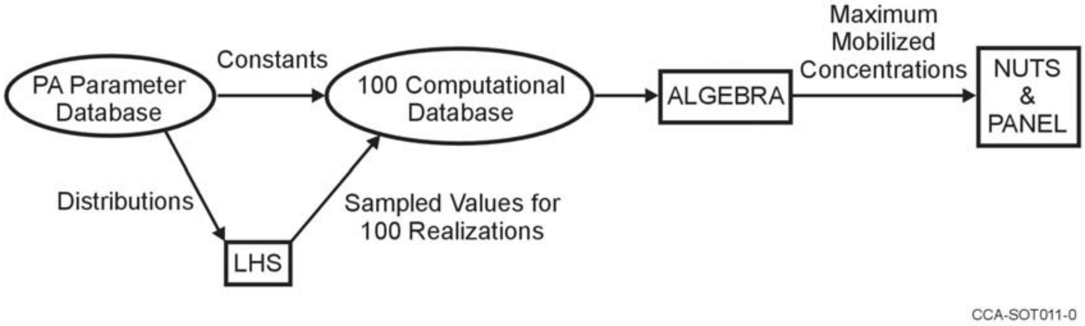

~~**Figure SOTERM-9. Calculations Performed by ALGEBRA for Each Replicate of 100 Realizations to Produce Effective Solubilities for Each Modeled Actinide.**~~

All ***of*** the ~~source~~ ***source-***term parameter***s*** ~~rvalues~~ and their distributions were entered into the ~~performance assessment~~ ***PA*** parameter database. For ~~the~~ ***each*** sampled parameter~~s~~, the LHS code ~~read~~ ***uses*** the distribution ~~information~~ from the ~~performance assessment~~***PA*** parameter database ~~and~~ ***to*** create~~d~~ 100 sampled values ~~for each~~. These values ~~were~~ ***are*** combined with the ~~constant value~~ parameters ***with constant values*** and stored in computational databases for each of the 100 ~~realizations~~ ***vectors***, which ~~comprised~~ ***constitute*** one replicate. For each realization, ~~ALGEBRA~~ ***PANEL*** ~~read~~ ***uses*** both the constant and sampled values for all ***of*** the ~~source~~ ***source-***term parameters, and construct~~ed~~***s*** ~~effective solubilities~~***the source term*** for NUTS and PANEL, as shown below. This process ~~was~~ ***is*** repeated for scenarios using ***the*** Salado end-member ~~effective solubilities~~ ***total mobilized concentration*** and for scenarios using ***the*** Castile end-member ~~effective solubilities~~ ***total mobilized concentration***. (Parameters that are sampled and values derived from them are indicated by italics. Parameters ~~read~~ ***used*** by ~~ALGEBRA~~ ***PANEL*** are in bold.)

Dissolved = **Model Solubility** * $10^{\textbf{\textit{Sampled from Solubility Distribution}}}$ ***(73)***

Humic = *Dissolved* * ***Proportionality Constant*** ***(74)***
if *Dissolved* * ***Prop. Const***. < **Humic Cap**, otherwise

Humic = **Humic Cap** ***(75)***

Microbe ***(microbial vectors only)*** = *Dissolved* * **Proportionality Constant** ***(76)***

if the *Total Mobile* < **Microbe Cap**, otherwise

Microbe = **Microbe Cap** ***(77)***

Mineral = **Database Concentration** ***(78)***

Intrinsic = **Database Concentration** ***(79)***

Total Mobile = *Dissolved* + *Humic* + *Microbe* + Mineral + Intrinsic ***(80)***

For actinides with more than one oxidation state, the ~~above procedure is performed for each~~ oxidation state ***is specified by the oxidation-state parameter***~~, and the final total mobile concentration is set based on the oxidation state parameter~~:

~~Total Mobile = Total Mobile (~~***L***ower ~~o~~***O***xidation ~~s~~***S***tate~~)~~ if -OXSTAT ≤ 0.5
~~= Total Mobile (h~~***H***igher ~~o~~***O***xidation ~~s~~***S***tate~~)~~ if OXSTAT > 0.5,

where OXSTAT is the oxidation-state parameter that is sampled uniformly from 0 to 1.

For example, for one realization, in Salado brine, the sampled value for OXSTAT was 0.9 so Pu would be present in the +IV state. The sample of the solubility distribution was 0.8 for the modeled solubility for the +IV state, which has a model solubility of ~~4.4 x 10^{-6}~~ ***1.19×10^{-8} M***. The humic proportionality constant for the +IV oxidation state in Salado brine is 6.3, the microbe proportionality constant for Pu is 0.3, the humic cap is 1.1 ~~x~~ $\times 10^{-5}$ M, the microbe cap for Pu is 2.1 ~~x~~ $\times 10^{-3}$ ***M***, the ***concentration of the*** actinide on mineral fragment***s*** ~~concentration~~ is 2.6 ~~x~~ $\times 10^{-8}$ ***M***, and the Pu ~~intrinsic~~ ***intrinsic-***colloid concentration is 1 ~~x~~ $\times 10^{-9}$ ***M***.

For this realization, the maximum ***mobilized*** concentration of ~~dissolved plutonium~~ ***Pu*** used by ~~performance assessment~~ ***PA*** would be:

Maximum concentration of dissolved Pu:

C_{Pu} = (~~4.4 x 10^{-6}~~ ***1.19×10^{-8}***)~~-~~ $\times (10^{0.8})$ = 2.8 ~~x~~ $\times 10^{-5}$ ~~mole/liter~~ ***M*** ***(81)***

(This example has been rounded to two significant figures, although ~~performance assessment~~ ***PA*** would not round at this intermediate point.) C_{Pu} is the maximum concentration of all combined isotopes of Pu.

The maximum humic complexed ~~plutonium~~ ***Pu*** would be:

(2.8 ~~x~~ $\times 10^{-5}$ ~~mole/liter~~***M***)(6.3 mole~~s~~ adsorbed per mole~~)~~ = 1.8 ~~x~~ $\times 10^{-4}$ ~~moles/liter~~ ***M*** ***(82)***

This value, however, exceeds the cap for humic-mobilized ~~plutonium~~ ***Pu***, 1.1 ~~x~~ $\times 10^{-5}$ ~~mole/liter~~ ***M***. Therefore, in this case, the cap would be used for the maximum humic mobilized actinide concentration.

The maximum microbial mobilized ~~plutonium~~ ***Pu*** would be:

(2.8 ~~x~~ $\times 10^{-5}$ ~~mole/liter~~ ***M***)(0.3 mole~~s~~ bioaccumulated per mole~~)~~ = 8.3 ~~x~~ $\times 10^{-6}$ ~~moles/liter~~ ***M*** ***(83)***

which is less than the cap.

The total maximum ~~plutonium~~ ***Pu*** concentration or ~~effective solubility~~***total mobilized concentration*** for this realization would then be the sum of the dissolved and colloidal actinides:

Dissolved + Humic + Microbe + Mineral + Intrinsic

2.8 ~~x~~ $\times 10^{-5}$ + 1.1 ~~x~~ $\times 10^{-5}$ + 8.3 ~~x~~ $\times 10^{-6}$ + 2.6 ~~x~~ $\times 10^{-8}$ + 1.0 ~~x~~ $\times 10^{-9}$ = 4.7 ~~x~~ $\times 10^{-5}$ ~~moles/liter~~ ***M*** ***(84)***

~~ALGEBRA~~ ***PANEL*** also calculates the fraction of each actinide ~~that is~~ mobilized by ~~the~~ ~~5~~ ***five*** different mechanisms***,*** as follows:

Fraction dissolved = Dissolved/Total Mobil~~e~~***ized Conc.*** ***(85)***

Fraction on humics = Humic/Total Mobile ***(86)***

Fraction in/on microbes = Microbe/Total Mobile ***(87)***

Fraction on mineral fragments = Mineral/Total Mobile ***(88)***

Fraction as intrinsic colloid = Intrinsic/Total Mobile ***(89)***

The total mobil~~e~~***ized*** concentration and mobile fractions are then copied from Am to Cm. In addition, ~~the ALGEBRA run~~ ***PA*** also combines isotopes (Appendix ~~WCA, Section WCA.3.2~~ ***TRU WASTE, Section TRU WASTE-2.0***~~; Garner 1996~~) for the NUTS and SECOTP2D transport codes. For example, ~~the curies of ^{233}U are added to the curies of ^{234}U and~~ the ~~uranium~~ ***U*** solubility is decreased ~~by a factor of 100~~ to account for the shared solubility with the ~~low~~ ***low-*** activity ^{238}U, which is not modeled, enabling NUTS to properly model the effect of the ~~uranium~~ ***U*** isotopes on compliance using the single “lumped” isotope ^{234}U.

The output of the ~~ALGEBRA~~ ***PANEL*** calculations are computational databases that contain the ~~effective solubilities~~ ***source term*** and effective inventories. NUTS and PANEL both assume instantaneous dissolution and colloidal mobilization up to the ~~effective~~ solubility limit when sufficient inventory is present, as discussed in Chapter 6.0 (Section 6.4.13.***5***). Table SOTERM-~~15~~***12*** shows the ~~total effective solubilities~~ ***dissolved and colloidal components of the source term and the total mobile actinide concentrations*** obtained when median parameter values are used.

~~Table SOTERM-15. Log Molar Total Maximum Mobilized Concentrations Using Median Parameter Values~~

~~Brine~~	~~Am(III)~~	~~Pu(III)~~	~~Pu(IV)~~	~~U(IV)~~	~~U(VI)~~	~~Th(IV)~~	~~Np(IV)~~	~~NP(V)~~
~~Salado~~	~~-5.64~~	~~-6.14~~	~~-4.80~~	~~-4.84~~	~~-5.10~~	~~-4.59~~	~~-4.17~~	~~-4.52~~
~~Castile~~	~~-6.47~~	~~-6.77~~	~~-7.19~~	~~-7.16~~	~~-4.96~~	~~-7.05~~	~~-6.85~~	~~-4.54~~

Table SOTERM-12. Concentrations (M) of Dissolved, Colloidal, and Total Mobile Actinides Obtained Using Median Parameter Values~~.~~

Actinide Oxidation State, and Brine	*CRA, Microbial Vectors*[1]	*CRA, Nonmicrobial Vectors*	*PAVT*	*CCA*
Pu(III), dissolved, Salado brine	2.50×10^{-7}	2.50×10^{-7}	9.75×10^{-8}	4.73×10^{-7}
Pu(III), colloidal, Salado brine	1.49×10^{-7}	7.44×10^{-8}	7.48×10^{-8}	2.59×10^{-7}
Pu(III), total mobile, Salado brine	3.99×10^{-7}	3.24×10^{-7}	1.72×10^{-7}	7.32×10^{-7}
Pu(III), dissolved, Castile brine	1.37×10^{-7}	1.44×10^{-7}	1.06×10^{-8}	1.06×10^{-8}
Pu(III), colloidal, Castile brine	2.56×10^{-7}	2.24×10^{-7}	4.46×10^{-8}	4.46×10^{-8}
Pu(III), total mobile, Castile brine	3.94×10^{-7}	3.68×10^{-7}	5.52×10^{-8}	5.52×10^{-8}
Am(III), dissolved, Salado brine	2.50×10^{-7}	2.50×10^{-7}	9.75×10^{-8}	4.73×10^{-7}
Am(III), colloidal, Salado brine	9.72×10^{-7}	7.34×10^{-8}	3.96×10^{-7}	1.82×10^{-6}
Am(III), total mobile, Salado brine	1.22×10^{-6}	3.23×10^{-7}	4.93×10^{-7}	2.29×10^{-6}
Am(III), dissolved, Castile brine	1.37×10^{-7}	1.44×10^{-7}	1.06×10^{-8}	1.06×10^{-8}
Am(III), colloidal, Castile brine	6.99×10^{-7}	2.13×10^{-7}	7.78×10^{-8}	7.78×10^{-8}
Am(III), total mobile, Castile brine	8.36×10^{-7}	3.57×10^{-7}	8.83×10^{-8}	8.83×10^{-8}
Th(IV), dissolved, Salado brine	9.67×10^{-9}	1.01×10^{-8}	1.06×10^{-8}	3.58×10^{-6}
Th(IV), colloidal, Salado brine	1.17×10^{-7}	8.95×10^{-8}	1.25×10^{-7}	2.21×10^{-5}
Th(IV), total mobile, Salado brine	1.27×10^{-7}	9.96×10^{-8}	1.36×10^{-7}	2.57×10^{-5}
Th(IV), dissolved, Castile brine	2.01×10^{-8}	4.75×10^{-9}	3.33×10^{-8}	4.88×10^{-9}
Th(IV), colloidal, Castile brine	2.15×10^{-7}	5.59×10^{-8}	3.39×10^{-7}	7.18×10^{-8}
Th(IV), total mobile, Castile brine	2.35×10^{-7}	6.07×10^{-8}	3.73×10^{-7}	7.67×10^{-8}
U(IV), dissolved, Salado brine	9.67×10^{-9}	1.01×10^{-8}	1.06×10^{-8}	3.58×10^{-6}

Table SOTERM-12. Concentrations (M) of Dissolved, Colloidal, and Total Mobile Actinides Obtained Using Median Parameter Values — Continued

Actinide Oxidation State, and Brine	CRA, Microbial Vectors[1]	CRA, Nonmicrobial Vectors	PAVT	CCA
U(IV), colloidal, Salado brine	8.70×10^{-8}	8.95×10^{-8}	9.26×10^{-8}	1.10×10^{-5}
U(IV), total mobile, Salado brine	9.66×10^{-8}	9.96×10^{-8}	1.03×10^{-7}	1.46×10^{-5}
U(IV), dissolved, Castile brine	2.01×10^{-8}	4.75×10^{-9}	3.33×10^{-8}	4.88×10^{-9}
U(IV), colloidal, Castile brine	1.53×10^{-7}	5.59×10^{-8}	2.36×10^{-7}	5.67×10^{-8}
U(IV), total mobile, Castile brine	1.73×10^{-7}	6.07×10^{-8}	2.69×10^{-7}	6.16×10^{-8}
Pu(IV), dissolved, Salado brine	9.67×10^{-9}	1.01×10^{-8}	1.06×10^{-8}	3.58×10^{-6}
Pu(IV), colloidal, Salado brine	9.08×10^{-8}	9.05×10^{-8}	9.67×10^{-8}	1.21×10^{-5}
Pu(IV), total mobile, Salado brine	1.01×10^{-7}	1.01×10^{-7}	1.07×10^{-7}	1.57×10^{-5}
Pu(IV), dissolved, Castile brine	2.01×10^{-8}	4.75×10^{-9}	3.33×10^{-8}	4.88×10^{-9}
Pu(IV), colloidal, Castile brine	1.60×10^{-7}	5.69×10^{-8}	2.47×10^{-7}	5.92×10^{-8}
Pu(IV), total mobile, Castile brine	1.80×10^{-7}	6.17×10^{-8}	2.80×10^{-7}	6.41×10^{-8}
U(VI), dissolved, Salado brine	7.07×10^{-6}	7.07×10^{-6}	7.07×10^{-6}	7.07×10^{-6}
U(VI), colloidal, Salado brine	8.89×10^{-7}	8.75×10^{-7}	8.89×10^{-7}	8.89×10^{-7}
U(VI), total mobile, Salado brine	7.96×10^{-6}	7.95×10^{-6}	7.96×10^{-6}	7.96×10^{-6}
U(VI), dissolved, Castile brine	7.15×10^{-6}	7.15×10^{-6}	7.15×10^{-6}	7.15×10^{-6}
U(VI), colloidal, Castile brine	3.69×10^{-6}	3.67×10^{-6}	3.69×10^{-6}	3.69×10^{-6}
U(VI), total mobile, Castile brine	1.08×10^{-5}	1.08×10^{-5}	1.08×10^{-5}	1.08×10^{-5}

REFERENCES

Alexander, A.E., and P. Johnson. 1949. *Colloid Science*. New York, NY: Oxford University Press. Vol. 1.

Allard, B., H. Kipatsi, and J. O. Liljenzin. 1980. "Expected Species of Uranium, Neptunium and Plutonium in Neutral Aqueous Solutions," *Journal of Inorganic Nuclear Chemistry*. Vol. 42, no. 7, 1015-1027.

Avogadro, A., and G. de Marsily. 1984. "The Role of Colloids in Nuclear Waste Disposal," *Scientific Basis for Nuclear Waste Management VII, Materials Research Society Symposia Proceedings, Boston, MA, November 14-17, 1983.* Ed. G.L. McVay. New York, NY: North-Holland. Vol. 26, 495-505.

Baes, C.F., Jr., and R.E. Mesmer. 1976. *The Hydrolysis of Cations.* New York, NY: Wiley Interscience.

Baskaran, M., P. H. Santschi, G. Benoit, and B. D. Honeyman. 1992. "Scavenging of Thorium Isotopes by Colloids in Seawater of the Gulf of Mexico," *Geochimica et Cosmochimica Acta*. Vol. 56, no. 9, 3375-3388.

Bates, J.K., J.P. Bradley, A. Teetsov, C.R. Bradley, and M. Buchholtz. 1992. "Colloid Formation During Waste Form Reaction: Implications for Nuclear Waste Disposal," *Science.* Vol. 256, no. 5057, 649-561.

Brush, L.H. 1990. *Test Plan for Laboratory and Modeling Studies of Repository and Radionuclide Chemistry for the Waste Isolation Pilot Plant.* SAND90-0266. Albuquerque, NM: Sandia National Laboratories. WPO 26015.

Brush, L.H. 1995. Systems Prioritization Method - Iteration 2 Baseline Position Paper: Gas Generation in the Waste Isolation Pilot Plant. Unpublished report, March 17, 1995. Albuquerque, NM: Sandia National Laboratories. ERMS 228740.

Brush, L.H., and Y. Xiong. 2003a. Calculation of Actinide Solubilities for the WIPP Compliance Recertification Application, Analysis Plan AP-098, Rev 1. Unpublished analysis plan. Carlsbad, NM: Sandia National Laboratories. ERMS 527714.

Brush, L.H., and Y. Xiong. 2003b. Calculation of Organic Ligand Concentrations for the WIPP Compliance Recertification Application. Unpublished analysis report. Carlsbad, NM: Sandia National Laboratories. ERMS 527567.

Brush, L.H., and Y. Xiong. 2003c. Calculation of Actinide Solubilities for the WIPP Compliance Recertification Application. Unpublished analysis report, May 8, 2003. Carlsbad, NM: Sandia National Laboratories. ERMS 529131.

Brush, L.H., and Y. Xiong. 2003d. Calculation of Organic Ligand Concentrations for the WIPP Compliance Recertification Application and for Evaluating Assumptions of

Homogeneity in WIPP PA. Unpublished analysis report. Carlsbad, NM: Sandia National Laboratories. ERMS 531488.

Buckau, G., R. Stumpe, and J.I. Kim. 1986. "Americium Colloid Generation in Groundwaters and Its Speciation by Laser-Induced Photoacoustic Spectroscopy," *Journal of the Less-Common Metals*. Vol. 122, 555-562.

Buddemeier, R.W., and J.R. Hunt. 1988. "Transport of Colloidal Contaminants in Groundwater: Radionuclide Migration at the Nevada Test Site," *Applied Geochemistry*. Vol. 3, no. 5, 535-548.

Bynum, R. V. May 23, 1996. Memo to M. S. Tierney and C. Stockman. "Update of Uncertainty Range and Distribution for Actinide Solubilities to be Used in CCA NUTS Calculation." WPO 35835.

Choppin, G.R. 1983. "Solution Chemistry of the Actinides," *Radiochimica Acta*. Vol. 32, no. 1-3, 43-53.

Choppin, G. R. 1988. Unpublished Letter to L. H. Brush, December 29, 1988, Tallahassee, FL. (Copy on file at Sandia WIPP Central Files.)

Choppin, G.R., A.H. Bond, M. Borkowski, M.G. Bronikowski, J.F. Chen, S. Lis, J. Mizera, O. Pokrovsky, N.A. Wall, Y.X. Xia, and R.C. Moore. 2001. Waste Isolation Pilot Plant Actinide Source Term Test Program: Solubility Studies and Development of Modeling Parameters. SAND99-0943. Albuquerque, NM: Sandia National Laboratories.

Choppin, G. R., and P. M. Shanbhag. 1981. "Binding of Calcium by Humic Acid," *Journal of Inorganic and Nuclear Chemistry*. Vol. 43, no. 5, 921–922.

Clark, D. L. and Tait, C. D. 1996. Monthly Reports Under SNL Contract AP2274, Sandia WIPP Central File A:WBS 1.1.10.1.1. These data are qualified under LANL QAPjP CST-OSD-QAP1-001/0. WPO 31106.

Clark, D.L., D.E. Hobart, and M.P. Neu. 1995. "Actinide Carbonate Complexes and Their Importance in Actinide Environmental Chemistry," *Chemical Reviews.* Vol. 95, no. 1, 25-48.

Cleveland, J.M. 1979a. *The Chemistry of Plutonium.* La Grange Park, IL: American Nuclear Society.

Cleveland, J.M. 1979b. "Critical Review of Plutonium Equilibria of Environmental Concern," *Chemical Modeling in Aqueous Systems: Speciation, Sorption, Solubility, and Kinetics, 176th Meeting of the American Chemical Society, Miami Beach, FL, September 11-13, 1978.* Ed. E.A. Jenne. Washington, DC: American Chemical Society. 321-338.

Comans, R.N.J., and J.J. Middelburg. 1987. "Sorption of Trace Metals on Calcite: Applicability of the Surface Precipitation Model," *Geochimica et Cosmochimica Acta.* Vol. 51, no. 9, 2587-2591.

Cotton, F.A., and G. Wilkinson. 1988. *Advanced Inorganic Chemistry*. 5th ed. New York, NY: John Wiley & Sons.

Crawford, B.A. 2003. "Updated Estimate of Complexing Agents in Transuranic Solidified Waste Forms Scheduled for Disposal and Emplaced at WIPP." Unpublished letter to C.D. Leigh, April 8, 2003. Carlsbad, NM: Los Alamos National Laboratory. ERMS 527409.

~~U.S. DOE (U.S. Department of Energy). 1996~~**a**~~. *Transuranic Waste Baseline Inventory Report (Revision 3)*. DOE/CAO-95-1121. Carlsbad, NM: U.S. Department of Energy.~~

Downes, P.S. 2003a. "Spreadsheet Calculations of Actinide Solubilities for the WIPP Compliance Recertification Application." Unpublished memorandum to L.H. Brush, April 21, 2003. Carlsbad, NM: Sandia National Laboratories. ERMS 528395.

Downes, P.S. 2003b. "Spreadsheet Calculations of Actinide Solubilities for the WIPP Compliance Recertification Application in Support of AP-098, 'Calculation of Actinide Solubilities for the WIPP Compliance Recertification Application, Analysis Plan AP-098, Rev. 1.'" Unpublished analysis report. Carlsbad, NM: Sandia National Laboratories. ERMS 530441.

Drez, P.E. 1991. "Preliminary Nonradionuclide Inventory of CH-TRU Waste,"*Preliminary Comparison with 40 CFR Part 191, Subpart B for the Waste Isolation Pilot Plant, December 1991. Volume 3: Reference Data.* WIPP Performance Assessment Division Eds. R.P. Rechard, A.C. Peterson, J.D. Schreiber, H.J. Iuzzolino, M.S. Tierney, and J.S. Sandha. SAND91-0893/3. Albuquerque, NM: Sandia National Laboratories, A-43 through A-53.

~~Duan, Z., N. Møller, J. Greenberg, and J.H. Weare. 1992. "The Prediction of Methane Solubility in Natural Waters to High Ionic Strengths from 0 to 250°C and from 0 to 1600 bar," *Geochimica et Cosmochimica Acta*. Vol. 56, no. 4, 1451-1460.~~

Ephraim, J. H., C. Petersson, M. Norden, and B. Allard. 1995. "Potentiometric Titrations of Humic Substances: Do Ionic Strength Effects Depend on the Molecular Weight?" *Environmental Science and Technology*. Vol. 29, no. 3, 622-628.

Eugster, H.P., C.E. Harvie, and J.H. Weare. 1980. "Mineral Equilibria in the Six-component Seawater System, Na-K-Mg-Ca-SO_4-Cl-H_2O, at 25°C," *Geochimica et Cosmochimica Acta.* Vol. 44, no. 9, 1335-1347. WPO 30424.

Fanghänel, Th., V. Neck, and J.I. Kim. 1995. "Thermodynamics of Neptunium(V) in Concentrated Salt Solutions: II. Ion Interaction (Pitzer) Parameters for Np(V) Hydrolysis Species and Carbonate Complexes," *Radiochimica Acta.* Vol. 69, no. 3, 169-176. WPO 40233.

Felmy, A.R., and J.H. Weare. 1986. "The Prediction of Borate Mineral Equilibria in Natural Waters, Application to Searles Lake, California," *Geochimica et Cosmochimica Acta.* Vol. 50, no. 12, 2771-2783. WPO 30421.

~~Felmy, A.R., and D. Rai. 1992. "An Aqueous Thermodynamic Model for a High Valence 4:2 Electrolyte Th4+-SO in the System Na+-K+-Li+-NH-SO-HSO-H2O to High Concentration," Journal of Solution Chemistry. Vol. 21, no. 5, 407-423. WPO 40224.~~

Felmy, A. R., D. Rai, J. A. Schramke, and J. L. Ryan. 1989. "The Solubility of Plutonium Hydroxide in Dilute Solution and in High-Ionic-Strength Chloride Brines," *Radiochimica Acta.* Vol. 48, no. 112, 29-35.

Felmy, A. R., D. Rai, and R. W. Fulton. 1990. "The Solubility of AmOHCO$_3$(c) and the Aqueous Thermodynamics of the System Na$^+$-H CO $_3$--(CO $_3$)$^{2-}$-OH-H$_2$ O," *Radiochimica Acta.* Vol. 50, no. 4, 193-204.

~~Felmy, A.R., D. Rai, and M.J. Mason. 1991. "The Solubility of Hydrous Thorium(IV) Oxide in Chloride Media: Development of an Aqueous Ion-Interaction Model," Radiochimica Acta. Vol. 55, no. 4, 177-185. WPO 40225.~~

Felmy, A.R., D. Rai, S.M. Sterner, M.J. Mason, N.J. Hess, and S.D. Conradson. 1996. "Thermodynamic Models for Highly Charged Aqueous Species: The Solubility of Th(IV) Hydrous Oxide in Concentrated NaHCO$_3$ and Na$_2$CO$_3$ Solutions." In preparation. (Copy on file in the Sandia WIPP Central Files. A:1.1.10.1.1: TO: QA: Inorganic (IV) Actinide Thermodynamic Data, WPO 40226, 8/14/96).

Francis, A.J., and J.B. Gillow. 1994. *Effects of Microbial Processes on Gas Generation Under Expected Waste Isolation Pilot Plant Repository Conditions. Progress Report through 1992.* SAND93-7036. Albuquerque, NM: Sandia National Laboratories. WPO 26555.

Francis A.J., J.B. Gillow, and M.R. Giles. 1997. Microbial Gas Generation under Expected Waste Isolation Pilot Plant Repository Conditions. SAND96-2582. Albuquerque, NM: Sandia National Laboratories.

Garner, J. March 15, 1996. "Radioisotopes to Be Used in the 1996 CCA Calculations." Memorandum to Christine Stockman. WPO 35202.

Giambalvo, E.R. 2002a. "Recommended Parameter Values for Modeling An(III) Solubility in WIPP Brines." Unpublished memorandum to L.H. Brush, July 25, 2002. Carlsbad, NM: Sandia National Laboratories. ERMS 522982.

Giambalvo, E.R. 2002b. "Recommended Parameter Values for Modeling Organic Ligands in WIPP Brines." Unpublished memorandum to L.H. Brush, July 25, 2002. Carlsbad, NM: Sandia National Laboratories. ERMS 522981.

Giambalvo, E.R. 2002c. "Recommended Parameter Values for Modeling An(IV) Solubility in WIPP Brines." Unpublished memorandum to L.H. Brush, July 26, 2002. Carlsbad, NM: Sandia National Laboratories. ERMS 522986.

Giambalvo, E.R. 2002d. "Recommended Parameter Values for Modeling An(V) Solubility in WIPP Brines." Unpublished memorandum to L.H. Brush, July 26, 2002. Carlsbad, NM: Sandia National Laboratories. ERMS 522990.

Giambalvo, E.R. 2002e. "Recommended μ^0***/RT Values for Modeling the Solubility of Oxalate Solids in WIPP Brines." Unpublished memorandum to L.H. Brush, July 31, 2002. Carlsbad, NM: Sandia National Laboratories. ERMS 523057.***

Giambalvo, E.R. 2003. "Release of FMT Database FMT_021120.CHEMDAT." Unpublished memorandum to L.H. Brush, March 10, 2003. Carlsbad, NM: Sandia National Laboratories. ERMS 526372.

Grenthe, I., and H. Wanner. 1992. *Guidelines for the Extrapolation to Zero Ionic Strength.* NEA-TBD-2, Revision 2, Gif-sur-Yvette, France: OECD Nuclear Energy Agency, Data Bank. WPO 21109.

Harvie, C.E., N. Møller, and J.H. Weare. 1980a. "The Prediction of Mineral Solubilities in Natural Waters, The Na-K-Mg-Ca-Cl-SO_4-H_2O System from Zero to High Concentration at 25°C," *Geochimica et Cosmochimica Acta.* Vol. 44, no. 7, 981-997. WPO 30423.

Harvie, C.E., J.H. Weare, L.A. Hardie, and H.P. Eugster. 1980b. "Evaporation of Seawater: Calculated Mineral Sequences," *Science.* Vol. 208, no. 4443, 498-500.

Harvie, C.E., N. Møller, and J.H. Weare. 1984. "The Prediction of Mineral Solubilities in Natural Waters, The Na-K-Mg-Ca-H-Cl-SO_4-OH-HCO_3-CO_2-H_2O System to High Ionic Strengths at 25°C," *Geochimica et Cosmochimica Acta.* Vol. 48, no. 4, 723-751. WPO 30422.

Helton, J.S., J.E. Bean, J.W. Berglund, F.J. Davis, K. Economy, J.W. Garner, J.D. Johnson, R.J. MacKinnon, J. Miller, D.G. O'Brien, J.L. Ramsey, J.D. Schreiber, A. Shinta, L.N. Smith, D.M. Stoelzel, C.W. Stockman, and P. Vaughn. 1998. Uncertainty and Sensitivity Analysis Results Obtained in the 1996 Performance Assessment for the Waste Isolation Pilot Plant. SAND98-0365. Albuquerque, NM: Sandia National Laboratories.

Hiemenz, P.C. 1986. *Principles of Colloid and Surface Chemistry*. 2nd ed. New York, NY: Marcel Dekker, Inc.

Hirtzel, C.S., and R. Rajagopalan. 1985. *Colloidal Phenomena. Advanced Topics*. Park Ridge, NJ: Noyes Publications.

Hobart, D.E. 1990. "Actinides in the Environment," *Proceedings of the Robert A. Welch Foundation Conference on Chemical Research, No., XXXIV: 50 Years With Transuranium Elements, Houston, TX, October 22-23, 1990*. Vol. 34, 378-436.

Hobart, D.E., and R. Moore. 1996. "Analysis of Uranium (VI) Solubility Data for WIPP Performance Assessment: Implementation of Analysis Plan AP-028." Copy on file in Sandia WIPP Central File. WPO 39856 (5/28/96).

Hobart, D. E., K. Samhoun, and J. R. Peterson. 1982. "Spectroelectrochemical Studies of the Actinides: Stabilization of Americium (IV) in Aqueous Carbonate Solution," *Radiochimica Acta.* Vol. 31, no. 3/4, 139-145.

Hobart, D.E., C.J. Bruton, F.J. Millero, I-Ming Chou, K.M. Trauth, and D.R. Anderson. 1996. *Estimates of the Solubilities of Waste Element Radionuclides in Waste Isolation Pilot Plant Brines: A Report by the Expert Panel on the Source Term.* SAND96-0098. Albuquerque, NM: Sandia National Laboratories.

Horita, J., T. J. Friedman, B. Lazar, and H.D. Holland. 1991. "The Composition of Permian Seawater," *Geochimica et Cosmochimica Acta.* Vol. 55, no. 2, 417-432.

Hunter, R.J. 1991-1992. *Foundations of Colloid Science.* Reprinted. New York, NY: Oxford University Press. Vols. I-II.

Johnson, G.L., and L.M. Toth. 1978. *Plutonium(IV) and Thorium(IV) Hydrous Polymer Chemistry.* ORNL/TM-6365. Oak Ridge, TN: Oak Ridge National Laboratory, Chemistry Division.

Katz, J.J., G.T. Seaborg, and L.R. Morss, eds. 1986. *The Chemistry of the Actinide Elements.* 2nd ed. New York, NY: Chapman and Hall. Vols. 1-2.

Keller, C. 1971. *The Chemistry of the Transuranium Elements.* Weinheim, Germany: Verlag Chemie, GmbH.

Kim, J.I. 1992. "Actinide Colloid Generation in Groundwater," *Radiochimica Acta*. Vol. 52/53, pt. 1, 71-81.

Kim, J.I. 1994. "Actinide Colloids in Natural Aquifer Systems," *MRS Bulletin, A Publication of the Materials Research Society.* Vol. 19, no. 12, 47-53.

Kim, J.-I., and T. Sekine. 1991. "Complexation of Neptunium(V) with Humic Acid," *Radiochimica Acta.* Vol. 55, no. 4, 187-192.

Kim, J.I., M. Bernkopf, Ch. Lierse, and F. Koppold. 1984a. "Hydrolysis Reactions of Am(III) and Pu(VI) Ions in Near-Neutral Solutions," *Geochemical Behavior of Disposed Radioactive Waste*. Eds. G.S. Barney, J.D. Navratil, and W.W. Schulz. ACS Symposium Series 246. Washington, DC: American Chemical Society. 115-134.

Kim, J.I., G. Buckau, F. Baumgärtner, H.C. Moon, and D. Lux. 1984b. "Colloid Generation and the Actinide Migration in Gorleben Groundwaters," Scientific Basis for Nuclear Waste Management VII, Materials Research Society Symposia Proceedings, Boston, MA, November 14-17, 1983. Ed. G.L. McVay. New York, NY: North-Holland. Vol. 26, 31-40.

Kim, J.I., Ch. Apostolidis, G. Buckau, K. Bueppelmann, B. Kanellakopulos, Ch. Lierse, S. Magirius, R. Stumpe, I. Hedler, Ch. Rahner, and W. Stoewer. 1985. *Chemisches Verhalten von Np, Pu und Am in verschiedenen knozentrierten Salzloesunger = Chemical Behaviour of Np, Pu, and Am in Various Brine Solutions.* RCM 01085. Munich, Germany: Institut für Radiochemie der Technische Universitaet Muenchen. (Available from National Technical Information Service, 555 Port Royal Road, Springfield, VA 22161, 703/487-4650 as DE857 2334.)

Korpusov, G.V., E.N. Patrusheva, and M.S. Dolidze. 1975. “The Study of Extraction Systems and the Method of Separation of Trivalent Transuranium Elements Cm, Bk, and Cf,” *Soviet Radiochemistry.* Vol 17, no. 1-6, 230-236.

Kraus, K.A. 1956. “Hydrolytic Behavior of the Heavy Elements,” *Proceedings of the International Conference on the Peaceful Uses of Atomic Energy, Geneva, August 8-20, 1955.* New York, NY: United Nations. Vol. 7, 245-257.

Larson, K.L., March 13, 1996. “Brine Waste Contact Volumes for Scoping Analysis of Organic Ligand Concentration.” Memorandum to R. V. Bynum. ~~WPO 30644~~ ***ERMS 236044*****.**

Laul, J.C., M.R. Smith, and N. Hubbard. 1985. “Behavior of Natural Uranium, Thorium and Radium Isotopes in the Wolfcamp Brine Aquifers, Palo Duro Basin, Texas,” *Scientific Basis for Nuclear Waste Management, Materials Research Society Symposia Proceedings, Boston, MA, November 26-29, 1984.* Eds. C.M. Jantzen, J.A. Stone, and R.C. Ewing. Pittsburgh, PA: Materials Research Society. Vol. 44, 475-482.

Lieser, K., B. Gleitsmann, S. Peschke, and T. Steinkopff. 1986a. “Colloid Formation and Sorption of Radionuclides in Natural Systems,” *Radiochimica Acta*. Vol. 40, no. 1, 39-47.

Lieser, K., B. Gleitsmann, and T. Steinkopff. 1986b. “Sorption of Trace Elements or Radionculides in Natural Systems Containing Groundwater and Sediments,” *Radiochimica Acta*. Vol. 40, no. 1, 33-37.

Lieser, K.H., A. Ament, R. Hill, R.N. Singh, U. Stingl, and B. Thybusch. 1990. “Colloids in Groundwater and Their Influence on Migration of Trace Elements and Radionuclides,” *Radiochimica Acta*. Vol. 49, no. 2, 83-100.

Lieser, K.H., R. Hill, U. Mühlenweg, R.N. Singh, T. Shu-De, and Th. Steinkopff. 1991. “Actinides in the Environment,” *Journal of Radioanalytical and Nuclear Chemistry, Articles.* Vol. 147, no. 1, 117-131.

Lyklema, J. 1978. “Surface Chemistry of Colloids in Connection with Stability,” T*he Scientific Basis of Flocculation.* Ed. K.J. Ives. NATO Advanced Study Institute Series, Series E, Volume E27. Alphen aan den Rijn: Sijthoff & Noordhoff. 3-36.

Maiti, T.C., M.R. Smith, and J.C. Laul. 1989. “Colloid Formation Study of U, Th, Ra, Pb, Po, Sr, Rb, and Cs in Briny (High Ionic Strength) Groundwaters: Analog Study for Waste Disposal,” *Nuclear Technology*. Vol. 84, no. 1, 82-87.

~~Martell, A.E., and R.M. Smith. 1982. *Critical Stability Constants, Volume 5: First Supplement.* New York, NY: Plenum Press.~~

Martinot, L. and J. Fuger. 1985. “The Actinides,” *Standard Potentials in Aqueous Solution.* Eds. A.J. Bard, R. Parsons, and J. Jordan. New York, NY: Marcel Dekker. 631-674.

McCarthy, J.F., and J.M. Zachara. 1989. “Subsurface Transport of Contaminants,” *Environmental Science & Technology*. Vol. 23, no. 5, 496-502.

Molecke, M.A. 1983. A Comparison of Brines Relevant to Nuclear Waste Experimentation. SAND83-0516. Albuquerque, NM: Sandia National Laboratories.

~~Moore, R.C. Feburary 22, 1996. “Model Parameters for Deprotonation of Lactic Acid, Citric Acid, Oxalic Acid, and EDTA and Complexation of Acetate, Lactate, Citrate, Oxalate, and EDTA with Mg2+, NpO2+, Am3+, Th4+, and UO22+ in NaCl Media.” Memorandum to C.F. Novak. (Copy on file in the Sandia WIPP Central Files A:1.1.1.1.4: TD:QA; WPO 35307).~~

Munson, D.E., R.L. Jones, D.L. Hoag, and J.R. Ball. 1987. Heated Axisymmetric Pillar Test (Room H): In Situ Data Report (February, 1985 - April, 1987), Waste Isolation Pilot Plant (WIPP) Thermal/Structural Interactions Program. SAND87-2488. Albuquerque, NM: Sandia National Laboratories.

Nash, K.L., and G.R. Choppin. 1980. “Interaction of Humic and Fulvic Acids with T~~H~~***h***(IV),” *Journal of Inorganic and Nuclear Chemistry.* Vol. 42, no. 7, 1045–1050.

~~National Institute of Standards and Technology. 1995. *NIST Standard Reference Materials Catalog, 1995-1996.* Washington, DC: Commerce Department, Technology Administration, National Institute of Standards and Technology. 25-38.~~

Neck, V., J.I. Kim, and B. Kanellakopulos. 1992. “Solubility and Hydrolysis Behavior of Neptunium (V),” *Radiochimica Acta.* Vol. 56, no. 1, 25-30.

Neck, V., W. Runde, and J.I. Kim. 1995. “Solid-Liquid Equilibria of Np(V) in Carbonate Solutions at Different Ionic Strengths: II,” *Journal of Alloys and Compounds.* Vol. 225, 295-302.

Neretnieks, I. 1982. *The Movement of a Redox Front Downstream From a Repository for Nuclear Waste.* KBS Report TR 82-16. Stockholm: Svensk Kärnbränsleforsorjning AB.

Nitsche, H. 1987. “Effects of Temperature on the Solubility and Speciation of Selected Actinides in Near-Neutral Solution,” *Inorganica Chimica Acta.* Vol. 127, no. 1, 121-128.

Nitsche, H., and N.M. Edelstein. 1985. “Solubilities and Speciation of Selected Transuranium Ions. A Comparison of a Non-complexing Solution with a Groundwater from the Nevada Tuff Site,” *Radiochimica Acta.* Vol. 39, no. 1, 23-33.

Nitsche, H., K. Roberts, R.C. Gatti, T. Prussin, K. Becraft, S.C. Leung, S.A. Carpenter, and C.F. Novak. 1992. *Plutonium Solubility and Speciation Studies in a Simulant of Air Intake Shaft Water from the Culebra Dolomite at the Waste Isolation Pilot Plant.* SAND92-0659. Albuquerque, NM: Sandia National Laboratories. WPO 23480.

Nitsche, H., K. Roberts, R. Xi, T. Prussin, K. Becraft, I. Al Mahamid, H.B. Silber, S.A. Carpenter, R.C. Gatti, and C.F. Novak. 1994. “Long Term Plutonium Solubility and Speciation Studies in a Synthetic Brine,” *Radiochimica Acta, Special Issue: Chemistry and Migration Behaviour of Actinides and Fission Products in the Geosphere, Proceedings of the Fourth*

International Conference, Charleston, SC, December 12-17, 1993. Munich: R. Oldenbourg Verlag. Vol. 66/67, 3-8. WPO 21107.

Novak, C.F. 1995. *The WIPP Actinide Source Term: Test Plan for the Conceptual Model and the Dissolved Concentration Submodel.* SAND95-1985. Albuquerque, NM: Sandia National Laboratories. WPO 27860.

Novak, C.F., and R.C. Moore, March 28, 1996. "Estimates of Dissolved Concentrations for III, IV, V, and VI Actinides in Salado and Castile Brine Under Anticipated Repository Conditions." SNL Tech Memo. (Copy on file in the Sandia WIPP Central File A: WBS 1.2.0.7.1; WBS 1.1.10.1.1: WPO 36207.)

Novak, C.F., R.C. Moore, and R.V. Bynum. 1996. "Prediction of Dissolved Actinide Concentrations in Concentrated Electrolyte Solutions: A Conceptual Model and Model Results for the Waste Isolation Pilot Plant (WIPP)," *Proceedings of the International Conference on Deep Geological Disposal of Radioactive Waste, Winnipeg, Manitoba, Canada, September 16-19, 1996.*

Papenguth, H.W. 1996a: H.W. Papenguth to Christine T. Stockman: "Parameter Record Package for Colloidal Actinide Source Term Parameters" May 7, 1996: Attachment A: Rationale for Definition of Parameter Values for Actinide Intrinsic Colloids." WPO 35852.

Papenguth, H.W. 1996b: H.W. Papenguth to Christine T. Stockman: "Parameter Record Package for Colloidal Actinide Source Term Parameters" May 7, 1996: Attachment A: Rationale for Definition of Parameter Values for Microbes." WPO 35856.

Papenguth, H.W. 1996c: H.W. Papenguth to Christine T. Stockman: "Parameter Record Package for Colloidal Actinide Source Term Parameters" May 7, 1996: Attachment A: Rationale for Definition of Parameter Values for Humic Substances." WPO 35855.

Papenguth, H.W. 1996d: H.W. Papenguth to Christine T. Stockman: "Parameter Record Package for Colloidal Actinide Source Term Parameters" May 7, 1996: Attachment A: Rationale for Definition of Parameter Values for Mineral Fragment Type Colloids." WPO 35850.

Papenguth, H.W., and Y.K. Behl. 1996. "Test Plan for Evaluation of Colloid-Facilitated Actinide Transport at the Waste Isolation Pilot Plant." SNL Test Plan TP 96-01. (Copy on file in the Sandia WIPP Central File A:1.1.10.2.1. PUB:QA; WPO 31337.)

Pearson, R.G. 1963. "Hard and Soft Acids and Bases," Journal of the American Chemical Society, Vol. 85, no. 22, 3533-3539.

Pitzer, K.S., ed. 1991. *Activity Coefficients in Electrolyte Solutions.* 2nd ed. Boca Raton, FL: CRC Press.

Popielak, R.S., R.L. Beauheim, S.R. Black, W.E. Coons, C.T. Ellingson and R.L. Olsen. 1983. Brine Reservoirs in the Castile Formation, Waste Isolation Pilot Plant Project, Southeastern New Mexico. TME 3153. Carlsbad, NM: U.S. Department of Energy WIPP Project Office.

Pryke, D.C., and J.H. Rees. 1986. “Understanding the Behaviour of the Actinides Under Disposal Conditions: A Comparison between Calculated and Experimental Solubilities,” *Radiochimica Acta.* Vol. 40, no. 1, 27-32.

Rai, D., and R.G. Strickert. 1980. “Chemical Aspects of Medium- and Long-Term Radioactive Waste Disposal,” *Transactions of the American Nuclear Society and the European Nuclear Society.* Vol. 35, 185-186.

Rai, D., and J.L. Swanson. 1981. “Properties of Plutonium(IV) Polymer of Environmental Importance,” *Nuclear Technology*. Vol. 54, no. 1, 107-111. WPO 30420.

Rai, D., R.J. Serne, and D.A. Moore. 1980. “Solubility of Plutonium Compounds and Their Behavior in Soils,” *Soil Science Society of America Journal.* Vol. 44, no. 3, 490-495.

Rai, D., R.G. Strickert, and G.L. McVay. 1982. “Neptunium Concentrations in Solutions Contacting Actinide-Doped Glass,” *Nuclear Technology.* Vol. 58, no. 1, 69-76.

Rai, D., A.R. Felmy, and R.W. Fulton. 1995. “Nd^{3+} and Am^{3+} Ion Interactions with Sulfate Ion,” *Journal of Solution Chemistry.* Vol 24, no. 9, 879-895.

Rao, L., and G.R. Choppin. 1995. “Thermodynamic Study of the Complexation of Neptunium(V) with Humic Acids,” *Radiochimica Acta*. Vol. 69, no. 2, 87-95.

Rao, L., D. Rai, A.R. Felmy, R.W. Fulton, and C.F. Novak. 1996. “Solubility of $NaNd(CO_3)_2{\cdot}6H_2O$ in Concentrated Sodium Carbonate and Sodium Bicarbonate Solutions.” *Radiochimica Acta.* In press. WPO 36484.

Reed, D.T., D.G. Wygmans, and M.K. Richman. 1996. “Actinide Stability/Solubility in Simulated WIPP Brines.” Interim Report under SNL WIPP Contract AP-2267. (Copy on file in the Sandia WIPP Central files.)

Refait, Ph. and J.-M.R. Génin. 1994. “The Transformation of Chloride-Containing Green Rust One Into Sulphated Green Rust Two by Oxidation in Mixed Cl^- and SO_4^{2-} Aqueous Media,” *Corrosion Science.* Vol. 36, no. 1, 55-65.

Robinson, R.A., and R.H. Stokes. 1959. *Electrolyte Solutions, The Measurement and Interpretation of Conductance, Chemical Potential, and Diffusion in Solutions of Simple Electrolytes.* 2nd ed. (revised). London, England: Butterworths.

Ross, S., and I.D. Morrison. 1988. *Colloidal Systems and Interfaces.* New York, NY: John Wiley & Sons.

Runde, W. and J.I. Kim. 1994. Untersuchungen der Übertragbarkeit von Labordaten natürliche Verhältnisse. Chemisches Verhalten von drei- und fünfwertigem Americium in salinen NaCl-Lösungen. Report RCM-01094, Munich: Institut für Radiochemie, Technische Universität München. (Available from National Technical Information Service, 555 Port Royal Road, Springfield, VA, 22161, 703/487-4650 as DE 95752244.)

Sagoe-Crentsil, K.K., and F.P. Glasser. 1993. “ ‘Green Rust**,**’~~,~~ Iron Solubility and the Role of Chloride in the Corrosion of Steel at High pH,” *Cement and Concrete Research.* Vol. 23, no. 4, 785-791.

Sanchez, L.C., and H.R. Trellue. January 17, 1996. “Estimation of Maximum RH-TRU Thermal Heat Load for WIPP.” WPO 31165.

Scherer, C.P., I. Archuleta, and R. Villarreal. 2001a. Los Alamos National Laboratory STTP Data Historical Compilation, September 2000 (Revised July 2001), Volume I. LA-UR-01-5278. Los Alamos, NM: Los Alamos National Laboratory.

Scherer, C.P., I. Archuleta, and R. Villarreal. 2001b. Los Alamos National Laboratory STTP Data Historical Compilation, November 2000 (Revised July 2001), Volume II. LA-UR-01-6911. Los Alamos, NM: Los Alamos National Laboratory.

Scherer, C.P., I. Archuleta, and R. Villarreal. 2001c. Los Alamos National Laboratory STTP Data Historical Compilation (July 2001), Volume III. LA-UR-01-4245. Los Alamos, NM: Los Alamos National Laboratory.

Scherer, C.P., and R. Villarreal. 2000. A Study of Actinide and pcH Trends from Brine Analyses of the Liter-Scale Containers in the STTP Program. LA-UR-01-376. Los Alamos, NM: Los Alamos National Laboratory.

Scherer, C.P., and R. Villarreal. 2001. Phosphate Addition to Drums 7. 8, and 9 and Its Effect on Soluble Actinide Species. LA-UR-01-3081. Los Alamos, NM: Los Alamos National Laboratory.

Schnitzer, M., and S. I. M. Skinner. 1967. “Organo-Metallic Interactions in Soils: 7 Stability Constants of Pb^{++}, Ni^{++}, Mn^{++}, Co^{++}, Ca^{++}, and Mg^{++} - Fulvic Acid Complexes,” *Soil Science*. Vol. 103, no. 4, 247-252.

Siegel, M.D. 1996. “Solubility Parameters for Use in the CCA NUTS and GRIDFLOW Calculations.” SNL Technical memorandum dated 29 March 1996 to Martin S. Tierney. (Copy on file in the Sandia WIPP Central File A:WBS 1.2.0.7.1; WBS 1.1.10.61: WPO 35835.) Also WPO 37314.

Snider, A.C. 2003a. Verification of the Definition of Generic Weep Brine and the Development of a Recipe for This Brine. Unpublished report. Carlsbad, NM: Sandia National Laboratories. ERMS 527505.

Snider, A.C. 2003b. Calculation of MgO Safety Factors for the WIPP Compliance Recertification Application and for Evaluating Assumptions of Homogeneity in WIPP PA. Unpublished analysis report. Carlsbad, NM: Sandia National Laboratories. ERMS 531508.

~~Storz, L. June 24, 1996. “Estimate of the Amount of $Ca(OH)_2$ Contained in the Portland Cement Fraction of the Waste for Disposal in the WIPP,” Memorandum to Yifeng Wang. (Copy on file in Sandia WIPP Central File A: WBS 1.1.09.1.1.~~

Stumm, W. 1992. *Chemistry of the Solid-Water Interface.* New York, NY: John Wiley & Sons, Inc.

Stumm, W. 1993. "Aquatic Colloids as Chemical Reactants: Surface Structure and Reactivity," *Colloids in the Aquatic Environment.* Ed. T.F. Tadros and J. Gregory. New York, NY: Elsevier Applied Science. (Reprinted from Colloids and Surfaces. Vol. 73, 1-18.)

Trauth, K.M., S.C. Hora, R.P. Rechard, and D.R. Anderson. 1992. *The Use of Expert Judgment to Quantify Uncertainty in Solubility and Sorption Parameters for Waste Isolation Pilot Plant Performance Assessment.* SAND92-0479. Albuquerque, NM: Sandia National Laboratories. WPO 23526

Trovato, E.R. 1997. Untitled letter from E.R. Trovato to G. Dials, April 25, 1997. Washington, DC: U.S. Environmental Protection Agency Office of Radiation and Indoor Air.

U.S. Department of Energy (DOE). 1996a. Transuranic Waste Baseline Inventory Report, Rev. 3. DOE/CAO-95-1121. Carlsbad, NM: U.S. Department of Energy Carlsbad Area Office.

U.S. Department of Energy (DOE). 1996b. Title 40 CFR Part 191 Compliance Certification Application for the Waste Isolation Pilot Plant, Vol. 1-21. Carlsbad, NM: U.S. Department of Energy Carlsbad Area Office.

U.S. Environmental Protection Agency (EPA). 1998a. Compliance Application Review Documents for the Criteria for the Certification and Recertification of the Waste Isolation Pilot Plant's Compliance with the 40 CFR Part 191 Disposal Regulations: Final Certification Decision. CARD 23: Models and Computer Codes. EPA Air Docket A93-02-V-B-2. Washington, DC: U.S. Environmental Protection Agency Office of Radiation and Indoor Air.

U.S. Environmental Protection Agency (EPA). 1998b. Technical Support Document for Section 194.23 – Models and Computer Codes. EPA Air Docket A93-02-V-B-6. Washington, DC: U.S. Environmental Protection Agency Office of Radiation and Indoor Air.

~~U.S. EPA. 1988c. "Technical Support Document for Section 194.23: Parameter Justification Report." EPA Air Docket A93-02-V-B-14. Washington, DC: U.S. Environmental Protection Agency Office of Radiation and Indoor Air.~~

Villareal, R., J.M. Bergquist, and S.L. Leonard. 2001a. The Actinide Source-Term Waste Test Program (STTP) Final Report, Volume I. LA-UR-01-6822. Los Alamos, NM: Los Alamos National Laboratory.

Villareal, R., J.M. Bergquist, and S.L. Leonard. 2001b. The Actinide Source-Term Waste Test Program (STTP) Final Report, Volume II. LA-UR-01-6912. Los Alamos, NM: Los Alamos National Laboratory.

Villareal, R., M. King, and S.L. Leonard. 2001. The Actinide Source-Term Waste Test Program (STTP) Final Report, Volume IV. LA-UR-01-6914. Los Alamos, NM: Los Alamos National Laboratory.

Villareal, R., A.C. Morzinski, J.M. Bergquist, and S.L. Leonard. 2001. The Actinide Source-Term Waste Test Program (STTP) Final Report, Volume III. LA-UR-01-6913. Los Alamos, NM: Los Alamos National Laboratory.

Villarreal, R., M. Neu, L. Field, S. Reilly, E. Medina, and M. King. Undated. The Actinide Source-Term Waste Test Program (STTP) Final Report, Volume III. LA-UR-02162. Los Alamos, NM: Los Alamos National Laboratory.

Villarreal, R., A. Trujillo, C. Scherer, M. Neu, S. Reilly, and A.C Morzinski. 2000. A Study of STTP Pyrochemical Salt Tests and Results Featuring Pu(VI). LA-UR-00-1606. Los Alamos, NM: Los Alamos National Laboratory.

Vold, R.D., and M.J. Vold. 1983. *Colloid and Interface Chemistry.* Reading, MA: Addison-Wesley.

~~Wang, Y. March 18, 1996a. "Define Chemical Conditions for FMT Actinide Solubility Calculations," Memorandum to Malcolm D. Siegel, Sandia WIPP Central File A:WBS 1.1.09.1.1. WPO 37038.~~

~~Wang, Y. July 19, 1996b. "Evaluation of the Thermal Effect of Exothermal Chemical Reactions for WIPP Performance Assessment," memorandum to Richard Vann Bynum and Laurence H. Brush. (Copy on file in the Sandia WIPP Central File A:1.1.0.9.1.1.CO/COM:QA; WPO 39871.)~~

Wang, Y. and L. Brush. January 26, 1996***a***. "Estimates of Gas-Generation Parameters for the Long-Term WIPP Performance Assessment." WPO 31943.

Wang, Y. and L.H. Brush. 1996b. "Modify the Stoichiometric Factor y in the BRAGFLO to Include the Effect of MgO Added to WIPP Repository as a Backfill." Unpublished memorandum to M.S. Tierney, February 23, 1996. Albuquerque, NM: Sandia National Laboratories. ERMS 232286.

Weiner, R. 1996. "Documentation Package For: Oxidation State Distribution of Actinides in the Repository." SNL Technical memorandum dated 27 March 1996 to SWCF-A: Records Center, SWCF-A: WBS 12.1.10.1.1:PDD: QA: Dissolved Species: Oxidation State Distribution: Actinides: OX3: OX4: OX5: OX6 (WPO 35194).

~~WIPP Performance Assessment Department. 1992. Preliminary Performance Assessment for the Waste Isolation Pilot Plant, December 1992. Volume 2: Technical Basis. SAND92-0700/2. Albuquerque, NM: Sandia National Laboratories. WPO 20805.~~

~~WIPP Performance Assessment Department. 1995. User's Manual for FMT, Version 2.0, WPO 28119.~~

WIPP Performance Assessment Department. 1996. *User's Manual for NONLIN, Version 2.0*, ~~WPO 30740~~ ***ERMS 230740***.

Wolery, T.J. 1992. EQ3/6, *A Software Package for Geochemical Modeling of Aqueous Systems: Package Overview and Installation Guide (Version 7.0)*. UCRL-MA-110662 PT 1. Livermore, CA: Lawrence, CA: Lawrence Livermore National Laboratory.

Wolery, T.J., and S.A. Daveler. 1992. *EQ6, A Computer Program for Reaction Path Modeling of Aqueous Geochemical Systems: Theoretical Manual, User's Guide, and Related Documentation (Version 7.0).* UCRL-MA-110662-Pt. 4. Livermore, CA: Lawrence Livermore National Laboratory.

Wood, J.R. 1975. "Thermodynamics of Brine-Salt Equilibria. I. The Systems NaCl-KCl-$MgCl_2$-$CaCl_2$-H_2O and NaCl-$MgSO_4$-H_2O at 25°C," *Geochimica et Cosmochimica Acta.* Vol. 39, no. 8, 1147-1163.